A methodology for the performance characterisation of a variable speed CO2 compressor

JP Bester
23461357

orcid.org 0000-0002-1758-2743

Dissertation submitted in partial fulfilment of the requirements for the degree *Master* in Mechanical Engineering at the Potchefstroom Campus of the North-West University

Supervisor: Mr PVZ Venter
Dr Martin van Eldik

Graduation May 2018

Student Number: 23461357

Acknowledgements

This study was only possible due to the continued and unconditional support received from various sources. I want to use this opportunity to express my deepest gratitude to the following individuals;

- Mr. PvZ Venter and Dr. M van Eldik for their advice, guidance and sacrifices. The effort and persistence they showed regularly extended past normal office hours and standards.
- My colleagues, both in the post-graduate group and ArcelorMittal, who were always willing to listen, discuss and advise without a second thought.
- My family and close friends who supported and encouraged me beyond measure, accompanied by an endless amount of prayers.
- God, for not only blessing me with potential but also granting me countless opportunities to develop and grow into my potential. The blessing of the groups and individuals mentioned above should also not be overlooked.

Keywords

R-744

Compressor Characterisation

Heat pump

Variable speed control

Variable speed drive

Numerical Characterisation

Universal Methodology

Abbreviations

CFC	Chlorofluorocarbons
COP_H	Heating Coefficient of Performance
GWP	Global warming potential
HCFC	Hydrochlorofluorocarbons
HFC	Hydrofluorocarbons
HFO	Hydrofluro-Olefins
ODP	Ozone depletion potential
R-744	Refrigerant reference for CO_2
R^2	Coefficient of Determination
VSD	Variable speed drive

Abstract

Heat pump cycles have a vast range of industrial applications. A refrigerant withdraws heat from a reservoir, transferring it to another fluid. In order to design and sufficiently size these cycles, accurate operating predictions of all the components are crucial. Amongst these components are the compressor.

Some analytical formulations exist to predict the working parameters of a single speed compressor. However, in most cases measurements and specifications known only by the manufacturer, or are difficult to obtain, are needed. The addition of variable speed compressors widened the range in which predictions are made.

This study defines a numerical methodology that allows empirical derivation of operating equations for a variable speed reciprocating compressor. Operational equations are derived for a reciprocating carbon dioxide multi-hertz compressor at between 40 and 60 Hz after applying the methodology to a specific compressor. Four out of the six operating parameters must be known to calculate the remaining two. These parameters are;

Refrigerant mass flow rate	Refrigerant compressor outlet pressure
Refrigerant compressor inlet temperatures	Refrigerant inlet pressure
Refrigerant compressor outlet temperatures	Compressor operating frequency

During the methodology description, the adaptability, versatility and applicability of the methodology is evaluated and discussed. The methodology has internal decisions that can affect the accuracy and complexity of the end result.

Due to the amount of data required and time constraints, experimental data with acceptable accuracies were used instead of actual test-bench values.

From the comparison table and the accompanying plots it can be observed that the discharge temperature equation tends to predict values that are on average 0.43% above the experimental values. The absolute error average of 0.99% shows a low measure of inaccuracy.

The mass flow equation tends to predict 0.06 % on average above the experimental value. The absolute error value of 0.43% is combined with the plain average to state that over a large sample group, the mass flow prediction equation will be the more accurate equation since the tendency of over- and under-predicted value are minimal.

As discussed, these accuracies are between the experimental and predicted values. Comparison with the actual test-bench values for mass flow and discharge temperature will contribute a further around 3% and 5% inaccuracy respectively.

Table of Contents

List of Tables

List of Figures

1. Introduction

1.1 Background

Thermodynamic cycles are critical to everyday life in the modern age. Ranging from power generation to heating and cooling, the applications and necessity of thermodynamic cycles cannot be ignored. The vapour-compression cycle in particular is used for air-conditioning, refrigeration and heat pumps.

Since no major deviations have been made to the mechanisms of the cycle; basic cycle breakdown still consists of compression, heat exchanging and expansion, some changes had to be made to continually improve thermodynamic cycles (Calm & A, 1998). No aspect of these cycles are more researched and experimented on than the refrigerant being used. There seems to be no refrigerant that satisfies all of the modern day requirements. Modern day requirements include but are not limited to efficiency, adaptability and environmental friendliness. At the early stages of refrigeration, the requirements and available range of refrigerants were not as extensive as they are today.

In the first 25 years from the first refrigeration cycle in the 1800's, 5 refrigerants have been identified. These 5 are ethyl-ether, carbon dioxide (R-744), ammonia (R-717), sulphur dioxide and methyl chloride (Pearson, 2005). All of these refrigerants, and their accompanying cycle designs, satisfied factors taken into account in that era, which merely consisted of ease of use, followed by reliability, space required and cost of installation. All of them were, however, in some way hazardous, either due to flammability, being noxious or the need for high pressure equipment.

A phone-call to Thomas Midgley in 1928 sparked the discovery and use of chlorofluorocarbons (CFCs) as refrigerants, with the caller merely stating that for the refrigeration industry to have any future, a new refrigerant is needed. R-12 was the first CFC refrigerant produced in 1931 followed by R-11 in 1932 (Calm & A, 1998). This initiated the phase out of almost all of the early, natural refrigerants, except for Ammonia (R-717).

With the discovery of damages to the ozone and environment, came new selection criteria for refrigerants. Note that at this stage, between the 1970's and 80's, various refrigerants were in use. All known substances, refrigerants and numerous other industrial gasses included, were given ratings on their Ozone Depletion Potential (ODP) and Global Warming Potential (GWP) (Calm & A, 1998). Ozone depletion potential is a relative measure of the depletion effect of a given gas to that of R-11 with the same mass. The global warming potential is a relative measure of the heat trapping effect of a gas to that of an equal mass of CO_2.

This lead to the second generation of fluorine-based gases, called hydro-chlorofluorocarbons (HCFC's) being developed which was relatively more environmentally friendly. These gases also provided a quick retrofit of the existing systems (Linde-gas, 2018).

The signing of the Montreal Protocol caused the global phase-out of high ODP refrigerants in 1987, with all production of CFC's ending in 1995 (Calm & A, 1998).

This lead to hydro-fluorocarbons (HFCs) gases being produced like R-410A and R-134A to identify but a few. These refrigerants are less dangerous to the ozone but still have a profound effect on climate change. R-134a has a GWP = 1300 (Ma, et al., 2013).

Climatologists have called for a worldwide phase-out of high GWP refrigerants, referred to as the Kyoto Protocol (Calm, 2008). This will have the same result as with the signing of the Montreal Protocol. This leads to a new phase of refrigerant upgrading. Substitutes for a few have already been found like R-1234yf, which is a hydrofluoro-olefin or a HFO gas for short. It has all of the same properties for R-134a except for its ODP and GWP which is 0 and 4 respectively. The protocol also renewed interest in natural refrigerants.

The use of CO_2 is highly debated. Carbon dioxide can be recovered from industrial processes and its non-toxic, non-flammable and non-corrosive. It also has no impact on the ozone layer. The performance of CO_2 in heat pumps is also competitive with that of currently used refrigerants. Carbon dioxide, also known as R-744, was first utilised as a refrigerant in 1866 (Ma, et al., 2013). The use of R-744 in air-conditioning grew drastically, and at the start of the 1930's it has reached industries, commercial offices and even residences. Due to poor technology, these cycles where sub-critical and thus extremely inefficient, this ultimately caused it to be replaced in majority by synthetic refrigerants. During the 1990's, interest in R-744 was renewed due to the phase-out of ozone depleting refrigerants. The use of heat pumps running with R-744 has been extensively researched. It has been found that water can be heated with up to 75% less electrical energy when compared to conventional element heaters (Ma, et al., 2013).

The environmental considerations are not only applicable to the working fluid in the system, but to the components within it as well. The compressor is the only component within the primary fluid system to utilise electrical energy. The reciprocating hermetic compressor has been in existence since the 19th century, and due to its simplicity and ability to operate in a wide range of applications, are still in use today (Navarro, et al., 2007)

With the advancement of technology, compressors have become more efficient than it was in the 19th century. However, with the alterations such as increased accuracy when it comes to fabrication or a change of materials, the increased economical investment for the increased energy efficiency can often seem financially illogical.

The addition of a variable speed drive (VSD) has increased the ways in which a compressor can be made to run more efficient. Typically, compressors are designed to run efficiently for one specific operating condition, but in reality, these conditions will vary along with the temperatures of the

secondary medium flowing through the heat exchangers. The VSD enables the compressor to alter the amount of work inserted, to still reach the desired temperatures with the least amount of electrical energy. The inverter type air-conditioners on the market today are fine examples of a VSD inspired system.

Through experimental studies, it has been determined that the employment of heat pump systems result in less than half of the conventional methods' total CO_2 emissions, making this an indispensable technology (Chua, et al., 2010). Much has already been done to integrate this technology into modern day lives, but more is required in terms of energy efficiency to enhance the viability thereof. To evaluate and understand the energy efficiency of these systems, a basic understanding of the cycle is required.

A basic vapour compression cycle setup is used in the heat pump applicable to the problem addressed in this paper. The cycle and its mechanisms are described in the figures to follow.

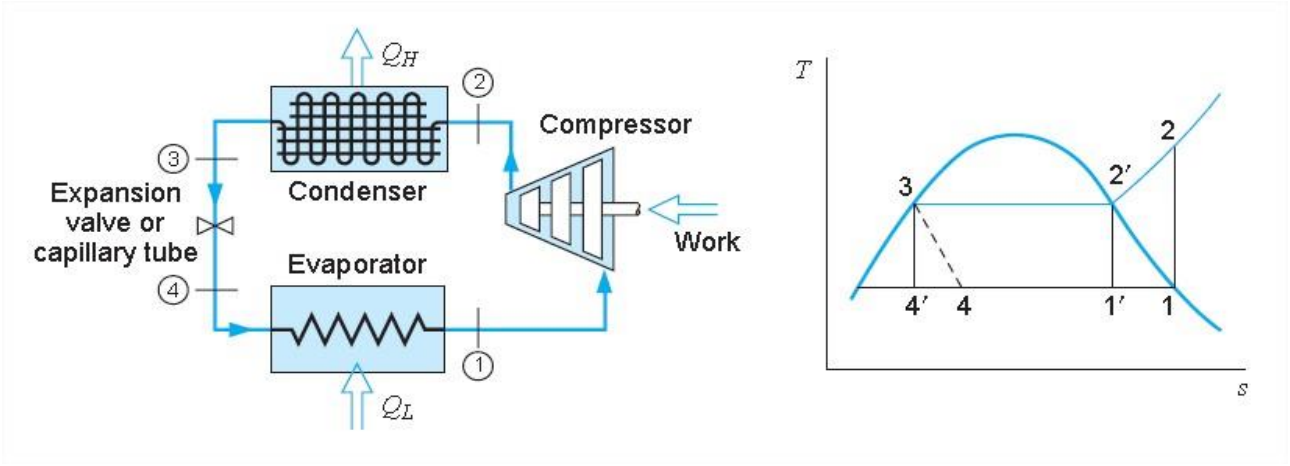

Figure 1: Schematic of a Refrigeration Cycle along with its ideal T-s Diagram (Borgnakke & Sonntag, 2009).

On the right hand side of Figure 1, the cycle depicted by 1'-2'-3-4' is known as the ideal Carnot cycle, and is compared to a typical vapour-compression cycle (1-2-3-4). A typical vapour-compression cycle operates as follows (Borgnakke & Sonntag, 2009):

1. Vapour enters the compressor and undergoes compression.
2. Heat is rejected at the heat exchanger known as the condenser, or in super- and trans-critical cases, a gas-cooler. The cooled fluid leaves the heat exchanger, typically either as a saturated or sub-cooled liquid.
3. The fluid is adiabatically throttled over the expansion valve to a lower pressure and leaves as a two-phase mixture.
4. The two-phase mixture enters the evaporator where heat is transferred from the surroundings, resulting in a saturated or super-heated vapour that enters the compressor at point 1. The Degree Of Superheat (DOS) is the difference between the compressor inlet vapour and the vapour saturation temperature.

The difference between the cycle in figure 1 and the super-critical cycle is shown in Figure 2. The refrigerant is compressed beyond the critical pressure, causing the fluid to be cooled without crossing the saturation lines.

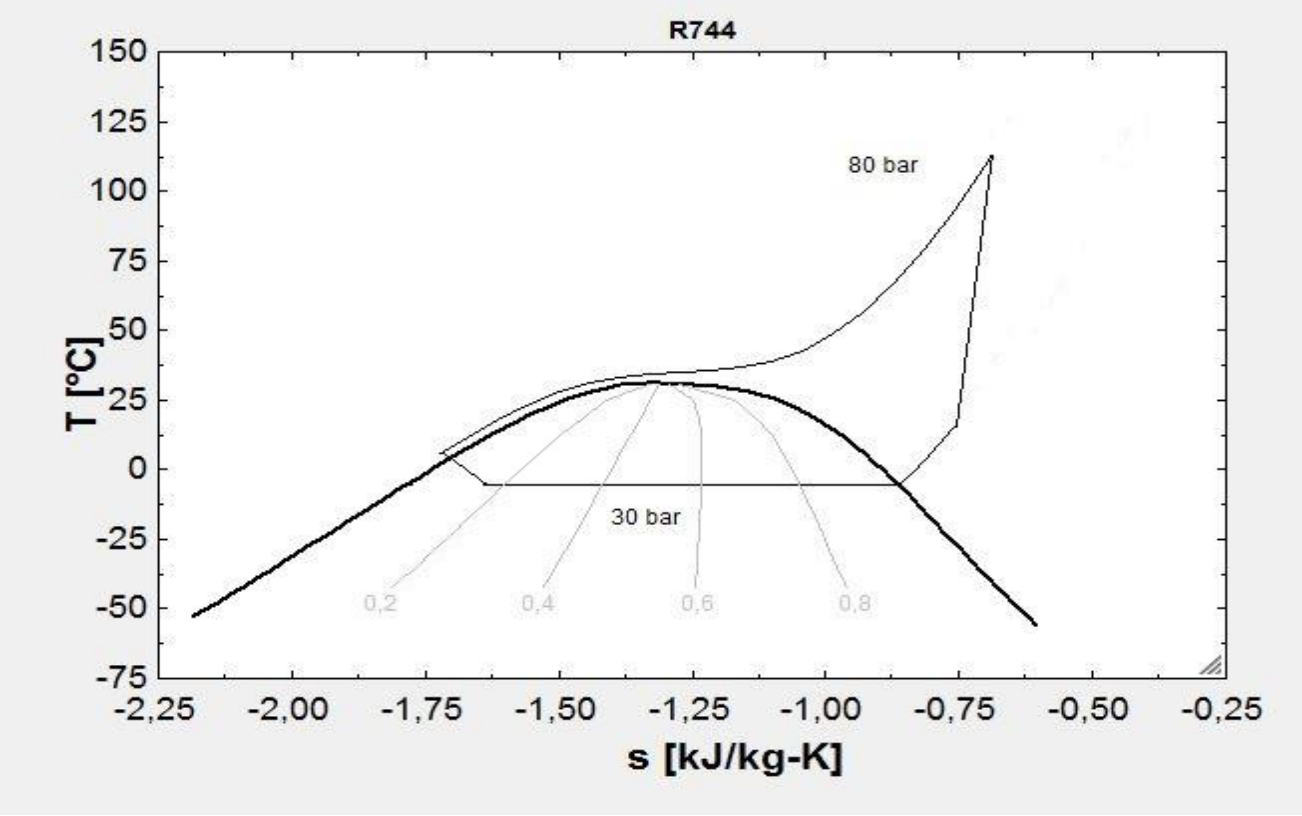

Figure 2: Super-Critical Cycle T-s Diagram for R744

The compressor in these cycles, noted as [1] in the cycle description, is the only component where work is inserted. The work is inserted in the form of electrical energy. The actual work inserted, efficiencies, mass flows and suction and discharge temperatures and pressures are all inter-related. Since the addition of a VSD to the system, frequency also has an influence on all of the variables and vice versa.

To predict any of these properties, performance charts of the compressor are required that show suction and discharge conditions alongside the varying frequencies and/or mass flows. These charts are specific to working fluids and compressors.

Performance charts for some common refrigerants with their applicable compressors are already generated. Carbon dioxide does not form part of these common refrigerants. These charts are normally produced following a set methodology. The methodology would use known data and parameters to generate predictive models such as graphs or equations.

1.2 Problem Statement

No universal characterisation methodology has been applied to generate performance charts or equations that can be used to predict the conditions for any set of in-range conditions for the specific reciprocating compressor when utilising carbon dioxide and a VSD.

1.3 Objectives

To address this problem, the following objectives must be met:

Investigate and evaluate existing compressor characterisation methodologies, both analytical and numerical. Identify the advantages and disadvantages of using these methodologies.

Achieve an understanding of compressor charts/equations and their elements. Identify variables in these charts/equations and determine their influence with the use of the fundamental and/or governing laws of thermodynamics and physics.

Formulate a universal, numerical methodology that can be applied to a specific compressor to produce characterisation equations. The final characterisation equations/charts needs to be evaluated and validated to ensure accuracy and applicability within the operational limits of the specific compressor.

1.4 Method of Investigation

To fulfil the objectives, a certain approach or method of investigation is identified and set.

A list of methodologies is grouped and investigated. The researched methodologies are evaluated on complexity, applicability and accuracy. The applicability needs to be addressed since the type of compressor or fluid can contribute an unknown, but required variable that can render the specific methodology invalid for a reciprocating compressor with the properties as discussed above.

A brief revision on the fundamental, governing laws of physics and thermodynamics with its applicability to the vapour-compression cycle components will be made. This will identify the major contributors to compressor performance and its properties in a cycle.

This approach will also aid in encouraging certain approaches in formulating the numerical methodology. The methodology is also formulated in a logical, universal manner. The representation of the methodology with the use of a logic diagram will aid in understanding it.

Since it is a numerical methodology, compressor data will be generated in an experimental study after which the formulated methodology will be applied to deliver predictive equations.

The obtaining of experimental data from a specific compressor will be done whilst considering the formulated methodology and the operational limits of the compressor. The characteristic equations formulated will then be compared and evaluated using independent, experimental data.

2. Literature Review

This chapter serves to provide information on studies relevant to compressor characterisation and the approaches that was followed. Firstly, a basic overview of refrigerant purpose and the use of R-744 specifically will be given. After this the relevancy of characterisation is declared followed by a thorough discussion on previous methodologies investigated.

2.1 R-744 as a Refrigerant

Thermodynamics are governed by laws, like any other physical science. The 1st and 2nd laws of thermodynamics must be satisfied for to ensure that a cycle occurs (Borgnakke & Sonntag, 2009). To summarise these 2 laws:

1. Energy cannot be destroyed or created, but can only be transformed/transferred.
2. Entropy will always increase over time in a closed isolated system if no cooling takes place.

Whereas the 1st law ensures that energy is flowing, the 2nd law ensures that the energy is flowing only in a certain direction (Borgnakke & Sonntag, 2009). These 2 laws can also be applied to the components within the cycle. It is the changes in energy and entropy over and within the compressor that interests the researcher, as they are the fundamental entities upon which the resulting data of this project is based. The fluid used in these cycles, known as the refrigerant, transfers these properties as the cycle progresses.

As mentioned, R744 was one of the first 5 natural refrigerants used in refrigerant cycles. Due to low technological advancement relative to modern day, only sub-critical cycles were used (Ma, et al., 2013). This had a negative effect on R744 cycles, since the efficiencies were low. However, modern day manufacturing technologies has eliminated a huge part of the volume and weight penalties once connected with high-pressure refrigerants such as R744 (Kim, et al., 2004). Cycles where the refrigerant is compressed beyond the critical point, but the evaporator operates sub-critical, is known as super-critical cycles.

The relatively low critical temperature of R744, which is 31.10℃, makes it ideal for use in super- or trans-critical cycles if the critical pressure of 73.9 *bar* is surpassed (Lorentzen, 1995).

2.2 Justification and Relevancy of Characterisation

The vapour-compression cycle is used for both the cooling and heating of ambient fluids, typically water or air. When heating is the purpose of the cycle it is referred to as a heat pump, where they compete mostly with electrical heating (Chua, et al., 2010).

The entire cycle efficiency is represented as the COP value. “COP” is an abbreviation for *Coefficient of Performance* and in standard, unmodified cycles, the COP value is specific for the refrigerant used

(Kim, et al., 2004). The COP value for heat pump cycles is determined through the following formula (Borgnakke & Sonntag, 2009) :

$$COP_H = \frac{\dot{Q}_{condenser}}{\dot{\boldsymbol{W}}_{\boldsymbol{compressor}}} \quad (1)$$

Where $\dot{Q}_{condenser}$ is the amount of work energy delivered to the medium being heated at the condenser part of the cycle, $\dot{W}_{compressor}$ is the amount of electrical work energy consumed by the compressor, and COP_H is the heating coefficient of performance.

Therefore, one way to increase the specific COP value of a cycle is to reduce the compressor work, while keeping the heating energy at the condenser constant. These values are mostly dependent on the type of refrigerant in use, and for this reason better refrigerants are being researched. With the phasing out of CFC, HCFC and HFC refrigerants, refrigerants are also evaluated on their environmental safety traits and compatibility when it comes to cycle modifications (Kim, et al., 2004).

Cechinnato *et al.* (2005) concluded that, as a whole, the trans-critical cycle of R744 is more energy efficient only if its peculiar characteristics are exploited through a proper design of the entire system. The trans-critical cycles will take advantage over old-fashioned cycles during warmer seasons when the higher evaporation temperature reduces the throttling exergy losses which are the main disadvantage of reverse cycles (heat pump cycles) that run on refrigerants with a low critical temperature (Cecchinato, et al., 2005).

Both R134a and R-744 compressors, for the specific cycle set-up used in their research, delivered similar isentropic efficiencies with the R134a scroll compressor getting the slight upper hand (Cecchinato, et al., 2005). The R744 compressor used in the referenced study and accompanying experiment was a semi-hermetic reciprocating compressor.

Heat pump systems are generally designed to satisfy maximum load, however, due to wide variations in load conditions, these systems operate at part load for the bigger margin of their lifetime (Tassou & Quresh, 1998). Conventional part load conditions are normally controlled through on/off switches and to an extent, result in lower efficiencies, larger losses, poor temperature control and reduced reliability resulting in higher maintenance costs (Tassou & Quresh, 1998). Theoretically, the most efficient capacity control method is a variable speed control of the compressor that can continuously match the compressor capacity to the load required (Tassou & Quresh, 1998).

The importance of minimising primary energy consumption is also noted by (Duprez, et al., 2007). For the application of heat pumps, a calculation tool should be used to predict behavioural aspects

so that the heat pump can adapt in such a way that environmental impact is minimised (Duprez, et al., 2007). The tool mentioned should remain as mathematically simple as possible (Duprez, et al., 2007).

2.3 Methodologies to Map Compressors

The isentropic efficiency along with outlet pressures and temperatures are the desired outputs of any compressor map. Tassou and Quresh (1998) have done an experimental study to determine exactly what would happen to the isentropic efficiencies if only the frequency were changed. The basic setup they used are shown in the figure below:

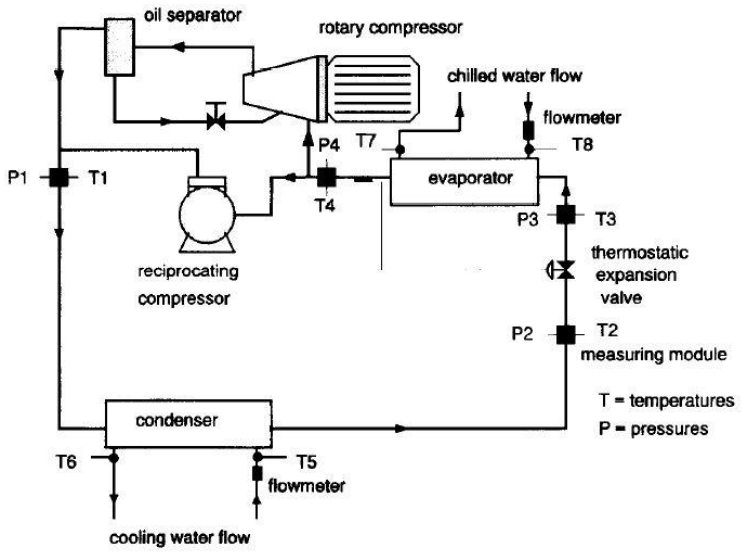

Figure 3: Compressor Test Bench Setup (Tassou & Quresh, 1998)

In this study, two types of compressors where tested; a rotary type and reciprocating (open and semi-hermetic type) compressor type were used. Other results noted were the volumetric efficiency and the degree of superheat. The conclusion was that as the frequency was reduced, the isentropic efficiency increased, this is due to a lower degree of discharge superheat (Tassou & Quresh, 1998). The semi-hermetic compressor showed no improvement in system COP if the inlet pressure is held constant while the frequency is reduced (Tassou & Quresh, 1998).

Perez-Segarra *et al.* (2005) researched the thermodynamic characterisation of hermetic reciprocating compressors. Three approaches to compressor modelling were mentioned and discussed (Perez-Segarra, et al., 2005)

- An exergy analysis method used with the purpose of identifying and measuring shaft power, discussed by (McGovern & Harte, 1995)
- A method using dimensionless compressor parameters presented by (Stouffs, et al., 2001)
- A method detaching the volumetric and isentropic efficiencies (Perez-Segarra *et al., 2005*).

In summary, Perez-Segarra *et al.* (2005) inserted three types of work, actual and isentropic, in specific areas of the compressor instead of just the actual work over the entire compressor. These three areas of work are:

I. The work over the inlet and outlet mean pressures.
II. The work due to under-pressure needed at suction
III. The work due to over-pressure at discharge.

The isentropic work for the 2 areas mentioned last, are equal to 0, resulting in the following 2 equations for isentropic and actual work respectively:

$$W_s = W_s^I \tag{2}$$

$$W_c = W_c^I + W_c^{II} + W_c^{III} \tag{3}$$

W_s is the isentropic work and W_c is the actual work over the area identified by the superscript.

(Lei & Zaheeruddin, 2005) performed tests on a variable speed compressor. The results were displayed using the degree of superheat instead of actual in/outlet temperatures, this may lower the amount of variables needed to plot since the degree of superheat is a function of both temperature and pressure.

The modelling of reciprocating compressors was researched by (Duprez, et al., 2007). The models were summarised into 2 basic groups. The first group is where the compressor is divided into a number of volumes like compression, valves etc., but these models require extensive information, many only known to the manufacturer. The other type is where thermodynamic assumptions are made, requires only in/outlet data and details such as clearance volumes and frequency.

The compressor model they ultimately used needed 6 input values (Duprez, et al., 2007):

1. Swept volume, given in data sheets.
2. Frequency of the motor.
3. Temperature of the inside wall.
4. The global heat transfer coefficient at suction.
5. Diameter of the suction pipe.
6. The ratio between the dead space and swept volume.

The above model delivered inaccuracies not exceeding 2% (Duprez, et al., 2007). This specific model only delivered needed power input as well as required mass flow rate, so to determine the efficiency and performance of the compressors from the results of these models would require intensive mathematical manipulation.

(Navarro, et al., 2007) proposed a model that use 10 parameters, which mainly represent the losses inside the compressor that can predict the compressors' isentropic and volumetric efficiencies. A statistical fitting procedure was built based on the Monte Carlo method for further adjustment in this model (Navarro, et al., 2007). The model predicted performance with sufficient accuracy; a maximum deviation of 3% was obtained (Navarro, et al., 2007). As will be observed further on, this method is complex and time consuming, with information required that only manufacturers have.

Distinguishable groups of compressor models were also created. The first group relies on a magnitude of compressor design data (Navarro, et al., 2007). However, if the main aim is to predict performance, the second group is recommended where the compressor is described globally. In this group there are 3 main approaches to the problem (Navarro, et al., 2007):

- Correlations from experimental data for some of the significant variables such as COP and cooling capacity. This is most common but it does not really give any valuable physical information of the internal workings of the compressor. There is also a limited range in which these correlations can be used.
- Numerical methods to solve differential equations implied in conservation laws of the processes in the compressor. These models generally require an intensive amount of variables, some known only to the manufacturer. It is only fitting that these models are then mainly used in optimisation of compressor design.
- Semi-empirical models produce performance variables like COP and cooling capacity using empirically adjusted, simple models that include a small amount of the physical background of the compressor.

The model aimed to produce efficiency values by using a set of parameters that can be obtained by correlations of standard characterisation performance data (Navarro, et al., 2007). Once correlated, the model should predict performance data for operating conditions not tested, for example extreme temperatures or adjusted speeds. The correlated model can very well be used to predict performance for other refrigerants with little or no data (Navarro, et al., 2007).

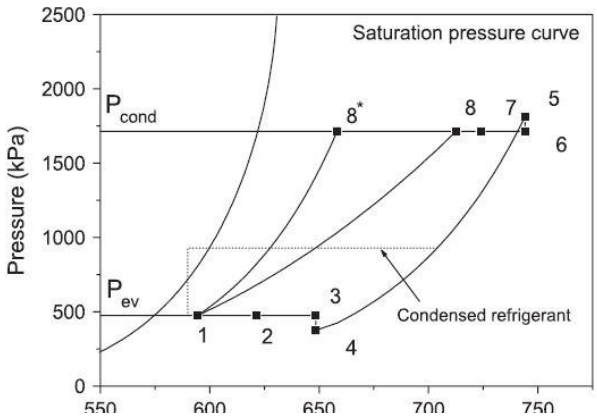

Figure 4: Process Breakdown within Compressor (Navarro, et al., 2007)

To generate their model, they broke down the compressor into 6 basic processes, as shown in figure 4 with the description to follow (Navarro, et al., 2007).

The refrigerant enters at point 1 and leaves at point 8. 8* is the isentropic outlet point.

- 1-2. Vapour is heated due to motor cooling effects and mechanical loss dissipation (friction).
- 2-3. Vapour is heated due to heat transfer from the discharge side.
- 3-4. Isenthalpic pressure loss at the suction valve.
- 4-5. Isentropic compression from actual intake conditions. Leakages and condensation may also be existent.
- 5-6. Isenthalpic pressure loss at discharge valve.
- 6-7. Vapour cooling due to heat transferred to the suction side.

Thermodynamic equations were set-up for each of the processes based on both physical dimensions and fluid properties (Navarro, et al., 2007). These equations deliver a set of variables that are still incomplete. In order to complete the entire set, other design and flow parameters are used in a Monte Carlo based algorithm to determine the last unknown value. The algorithm used to complete the sets of parameters is given in Figure 5:

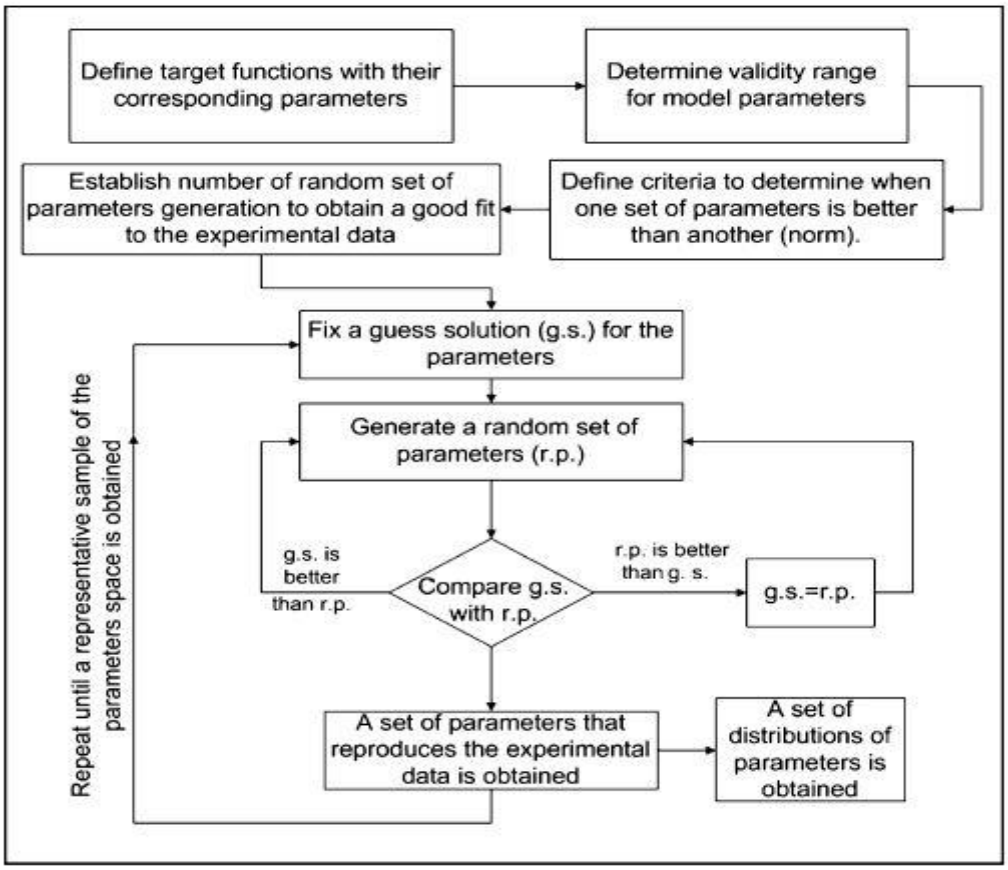

Figure 5: The Monte Carlo Based Fitting Procedure (Navarro, et al., 2007)

The values generated are in essence the effective parameters within the compressor. It can then be used in the functions produced after combining the processes to determine the efficiencies.

The previous methods and models are mostly of an analytical approach. Numerical models are not so easy to find, sources like Koury *et al.* (2001) generated these models for entire variable speed refrigeration systems. Further investigation showed that they assumed the efficiency of the compressor to be at 70% for all operating speeds within the operational range (Koury, et al., 2001). A more focused numerical study on the compressor is therefore not only needed for compressor analysis, but also for more accurate systems modelling.

(Barskii, et al., 2011) generated an empirical model on a reciprocating compressor at off design conditions. No declaration on the background of the system setup was given but they generated performance models for the compressor using the quality of the refrigerant at the inlet of the evaporator.

(Winandy, et al., 2002) proposed a simpler modelling technique to that of (Navarro, et al., 2007). The compressor stage was setup in exactly the same phases as in the last mentioned paper. The compressor is equipped with internal sensors to measure the values of these phases previously analytically determined, as explained earlier. Figure 6 displays one of the results obtained after the experimental study was concluded:

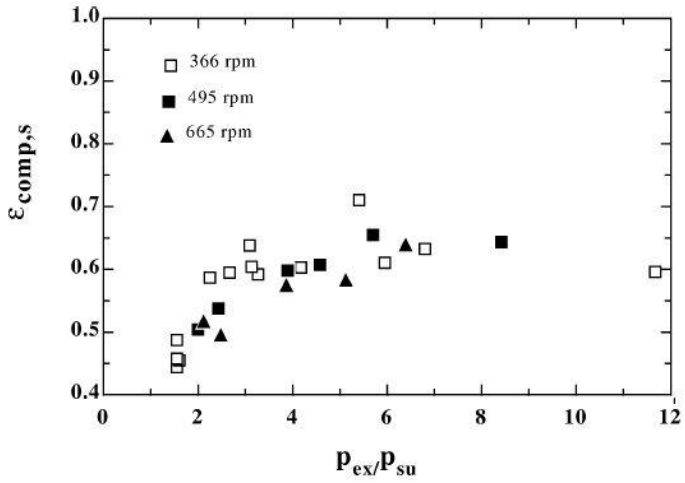

Figure 6: Efficiency vs Compression Ratio for different Frequencies (Winandy, et al., 2002)

A few indications on the workings of the compressor can be identified. Firstly, as the compression ratio of the specific compressor is increased, the efficiency also tend to increase. This increase is also elevated further with a decrease in frequency.

The models further generated and discussed in the mentioned source still need values that are difficult to determine. These values include the volumes and clearance factor, along with throttling parameters, heat transfer coefficients, parameters for shaft power and a losses term (Winandy, et

al., 2002). Mass flows, power consumption and exhaust temperatures are the delivered variables (Winandy, et al., 2002).

A map-based method is used for the modelling of the inverter compressor by Shao *et al.* (2004) where conditions and frequencies were varied in the simulations of inverter air conditioners (Shao, et al., 2004). Performance curves, delivered by manufacturers, deliver power input, mass flow rates and cooling/heating capacities. The model is based upon the rationale that a variable speed compressor at a certain frequency will perform the same as a similar, but constant speed compressor at that frequency (Shao, et al., 2004).

The data obtained through the performance curves was then interpolated and extrapolated to deliver sensible data at other frequencies. The problem with this is that the relation between performance and frequency is not easily distinguishable (Shao, et al., 2004).

The power input and mass flow rate equations used in the map condition, for a constant speed compressor, was in this case a second order function of the condensation and evaporation temperatures:

$$M_0 = a_1 T_c^2 + a_2 T_c + a_3 T_c T_e + a_4 T_e^2 + a_5 T_e + a_6 \quad (4)$$

$$P_0 = b_1 T_c^2 + b_2 T_c + b_3 T_c T_e + b_4 T_e^2 + b_5 T_5 + b_6 \quad (5)$$

The mass flow and power input is defined by M_0 and P_0 respectively, while T_c is the condensing temperature and T_e the evaporating temperature. The constants a_1 – a_6 and b_1 – b_6 are dependent on the specific compressor. The methodology to find the performance at different frequencies was as follows:

1. The performance curves for the different frequencies to be displayed and analysed, were given.
2. They generated performance data such as power input and flow rates and tabulated these values.
3. In order to find the relation between frequency and performance, they then compared these values to the base frequency (in this case 60 Hz). This was done by generating the ratio of delivered power input to that at the base frequency.
4. They determined correction factors that is stored in matrix form for ease of access.

The following two figures were some of the deliverables;

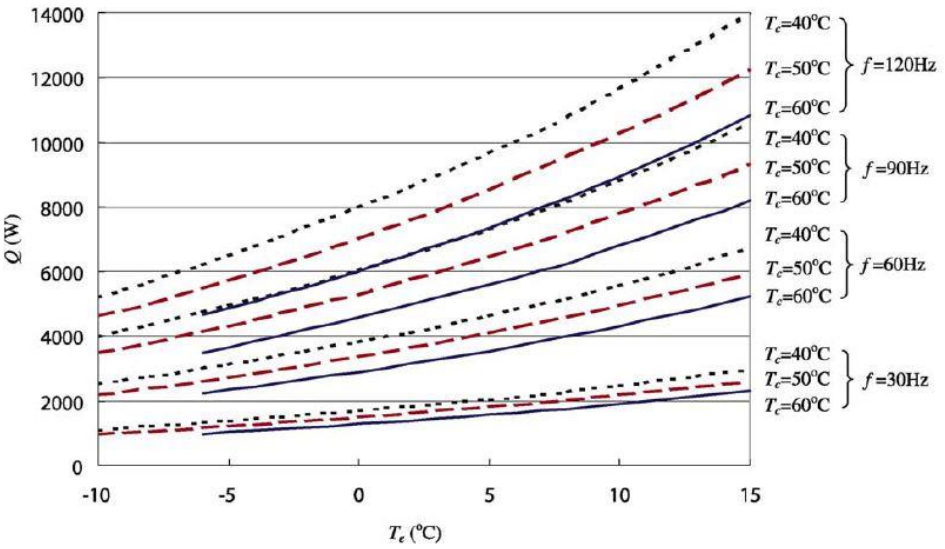

Figure 7: Cooling Capacity vs Temp$_e$ for different Frequencies and Temp$_c$ (Shao, et al., 2004)

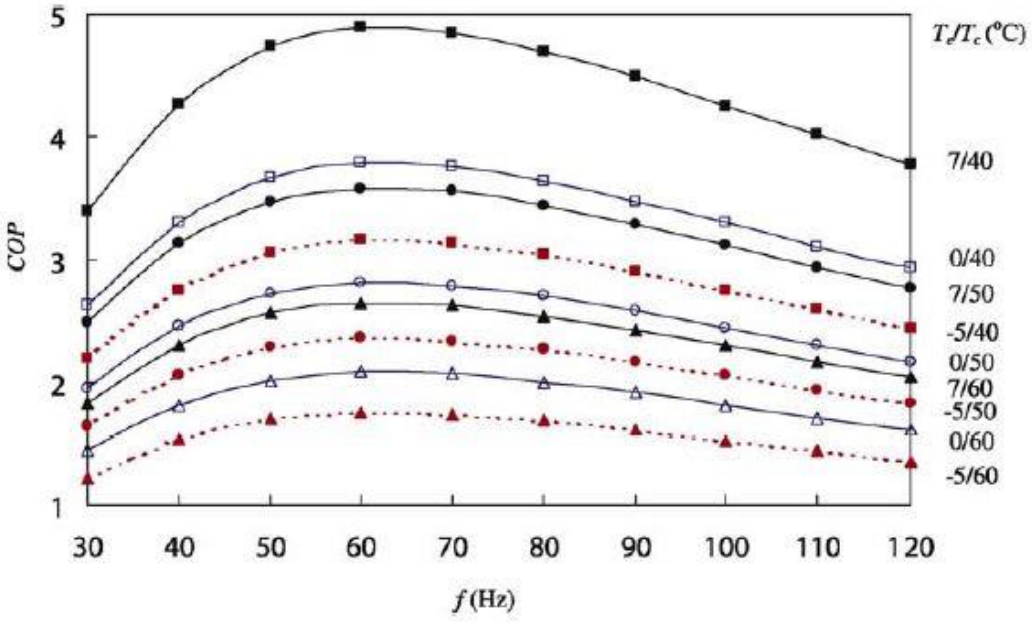

Figure 8: COP vs Frequency vs T$_e$/T$_c$ (Shao, et al., 2004)

These figures show the relation between the performance of the compressor at different frequencies in terms of COP and capacities. Similar maps should therefore be obtainable for efficiencies with the use of more parameters.

Since the last source cited delivered data and charts similar to those needed, the experimental methodology to be discussed next should more or less be the same as used, with the exception that the performance curves will not be delivered by the manufacturer. These curves should therefore be determined in the experimental phase.

2.4 Research Conclusion

A list of modelling approaches was investigated, with both the advantages and disadvantages noted. From these advantages and disadvantages, the approaches and methodologies were evaluated.

The approaches that can be grouped into the analytical type were rendered to have too many unknowns and assumptions. The numerical approach will therefore be considered where actual experimental data is used to compile charts and/or equations.

The next step is to develop a formulation method from existing knowledge that will reach the objectives set in Chapter 1.

3. Methodology

In the previous chapter, an investigation into characterisation methodologies was completed, where the advantages and disadvantages for each method has also been identified. It was stated that a numerical approach is expected to deliver a methodology that will meet all of the desired objectives.

This chapter delivers the basic principles for the formulation of a numerical compressor characterisation method, followed by a case study's numerical equations.

To understand the reasoning behind the methodology formulated, a brief overview of heat pump cycle fundamentals and governing laws will first be discussed.

3.1 Cycle Fundamentals

The methodology development needs to be understood in terms of a mathematical approach to aid in the usage of regression methods already described to formulate equations. The methodology should also be perceived as universal and not only applicable to this study.

Firstly, the compressor cycle has six variables, as was the case in the majority of methodologies examined in Chapter 2. These variables are the suction temperature and pressure, discharge temperature and pressure, operating frequency and mass flow.

The relationship between these variables need to be determined and understood. A basic vapour compression cycle is revised below, along with component specific equations.

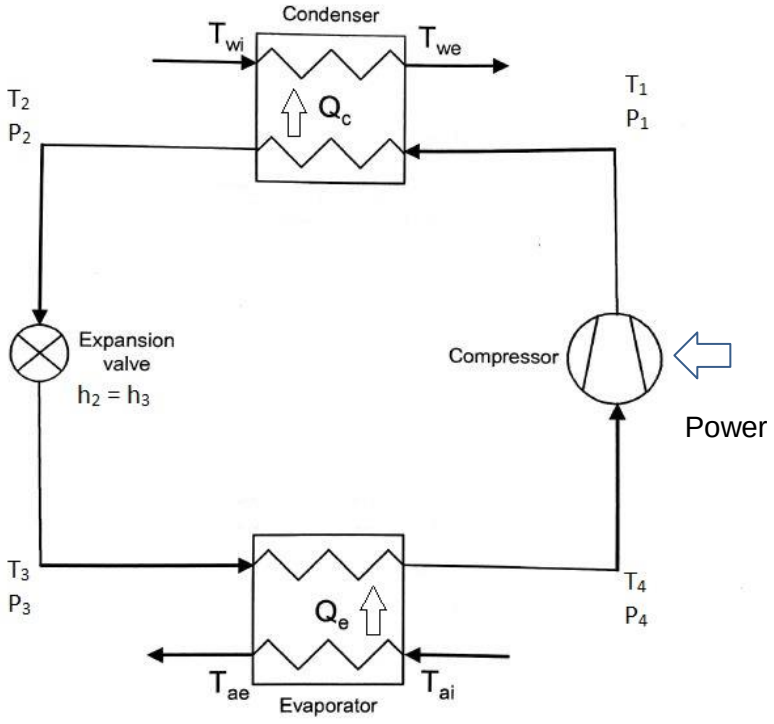

Figure 7: Vapour Compression Cycle Variables

To summarise the diagram above; the compressed fluid moves, at high temperature and pressure, through a condenser where heat energy is transferred to another fluid. The condensed fluid is then expanded over an isenthalpic valve after which it absorbs energy from another fluid in the evaporator to deliver a superheated fluid at the compressor inlet.

The conservation laws always apply to a cycle, as well as to every internal component. These laws and their accompanying equations are used as the fundamentals in formulating and deriving other cycle descriptive equations such as heat transfers or efficiency.

The derivation from integral form for each law and the use of an infinitesimal control volume is discussed in (Rousseau, 2013). These laws and their integrated equations are;

1. **Conservation of Mass**

$$\forall \left(\frac{\partial \rho}{\partial t}\right) + \dot{m}_e - \dot{m}_i = 0 \tag{6}$$

The $\left(\frac{\partial \rho}{\partial t}\right)$ is the change in fluid density over time as it moves through the control volume. The entire term, $\forall \left(\frac{\partial \rho}{\partial t}\right)$ is then the rate of change for mass since $\forall$ is referring to the volume flow through the control volume. The $\dot{m}_e$and $\dot{m}_i$ refer to the mass flow going out and into the control volume respectively.

The units of each term in the conservation of mass is normally in kg/s.

2. **Conservation of Momentum**

$$\rho\left(\frac{\partial V}{\partial t}\right) + \rho V\left(\frac{\partial V}{\partial \ell}\right) + \frac{\partial p}{\partial \ell} + \rho g\left(\frac{\partial z}{\partial \ell}\right) + \frac{\Delta p_{0L}}{L} = 0 \tag{7}$$

The $\rho\left(\frac{\partial V}{\partial t}\right)$ term is the rate of change of momentum over the control volume. The $\rho V\left(\frac{\partial V}{\partial \ell}\right)$ term is the net outflow of momentum from the control volume. The change in momentum due to surface forces, such as frictional losses, is given in the term $\frac{\Delta p_{0L}}{L}$. The $\frac{\partial p}{\partial \ell}$term is the change in momentum due to other surface forces. The last term to mention is the $\rho g\left(\frac{\partial z}{\partial \ell}\right)$ term which shows the change in momentum due to body forces such as gravity.

This equation is then applied to both compressible and incompressible flows (Rousseau, 2013). After using the flow types to establish a final derivative form for each, the equations are then integrated over a control volume with length ℓ and average cross-sectional area A. This then results in;

Compressible Flow:

$$\rho L\left(\frac{\partial V}{\partial t}\right) + \frac{p}{p_0}(p_{0e} - p_{0i}) + \frac{1}{2}\rho V^2\left(\frac{1}{T_0}\right)(T_{0e} - T_{0i}) + \rho g(z_e - z_i) + \Delta p_{0L} = 0 \tag{8}$$

Incompressible Flow:

$$\rho L\left(\frac{\partial V}{\partial t}\right) + (p_{0e} - p_{0i}) + \rho g(z_e - z_i) + \Delta p_{0L} = 0 \tag{9}$$

Since a vapour compression cycle is utilised in this study, only the compressible flow variant is applicable and will be discussed.

The rate of change in momentum is now given in the term $\rho L\left(\frac{\partial V}{\partial t}\right)$, whilst the net outflow of momentum is given by $\frac{p}{p_0}(p_{0e} - p_{0i})$. The momentum change due to frictional and other losses are determined by $\frac{1}{2}\rho V^2\left(\frac{1}{T_0}\right)(T_{0e} - T_{0i})$. The change in momentum due to gravity, is $\rho g(z_e - z_i)$. The change in momentum due to other surface force losses is then finally compensated for in the Δp_{0L} term.

The subscripts "e" and "i' indicate the exit and entering properties respectively. The units of each term in the conservation of momentum equations are normally in Pa.

3. Conservation of Energy

$$\dot{Q} + \dot{W} = \cancel{V}\frac{\partial}{\partial t}(\rho h_0 - p) + (\dot{m}_e h_{0e} - \dot{m}_i h_{0i}) + (\dot{m}_e g z_e - \dot{m}_i g z_i) \tag{10}$$

The total rate of heat transfer **to the fluid** is in the term $\dot{Q}$, whilst the total rate of work done **on the fluid** is in the term $\dot{W}$. The $\cancel{V}\frac{\partial}{\partial t}(\rho h_0 - p)$ term is the rate of change of energy in the control volume. The $(\dot{m}_e h_{0e} - \dot{m}_i h_{0i})$ term is the net outflow of thermal energy whilst the $(\dot{m}_e g z_e - \dot{m}_i g z_i)$ term is the net outflow of energy due to changes in potential energy from an acting body force such as gravity.

The subscripts "e" and "i" indicate the exit and entering properties respectively. The units of every term in the conservation of energy equation is normally in Watt (W). Since the mass flow is in kg/s, the unit of enthalpy, h, is then typically in J/kg. One unit of Watt is therefore similar to one unit of J/s.

Other Thermodynamic Properties

From (10), the use of a thermodynamic property called enthalpy, symbolised by h, is noted. To fully understand the energy equation, a basic understanding of enthalpy is needed. A simple definition of enthalpy is;

$$h = u + \frac{p}{\rho} \tag{11}$$

From (11) it is stated that the enthalpy of a fluid is the internal energy, symbolised by u, combined with the product of pressure and specific volume, since $\frac{1}{\rho} = v$. From this it clear that enthalpy is a measurement of the energy in a system.

Changes in internal energy is typically noted with changes in temperature, indicating that internal energy is a function of temperature. The density ρ is also a function of pressure and temperature and thus;

$$h = f(T, P) \tag{12}$$

Another property not yet mentioned in this chapter but important to understand for future reference, is entropy, denoted by s.

The entropy of a system is a measure of the disorder within that system. Simply put, entropy is a quantity representing the unavailability of a system's thermal energy for conversion into a mechanical work.

The 2nd law of thermodynamics states that an isolated system's entropy will never decrease. For a more in depth discussion on entropy, refer to the start of Chapter 2. It is clear that;

$$s = g(T, P) \tag{13}$$

The use of entropy in cycle calculations are important, especially with the compressor. An indication known as isentropic efficiency is used to define the measure of irreversibility of a process.

If the compressor had an isentropic efficiency of 1, meaning it was reversible process, the conservation equations could have been used to predict the performance since 100% available energy is inserted into the fluid.

This would have eliminated the requirement for studies like this one and other similar characterisation studies since a simple energy conservation equation such as the following would have been sufficient. With the assumption of no heat transfer to the surrounding environment;

$$\dot{W_{isen}} = \dot{m}(h_{0e_s} - h_{0i}) \tag{14}$$

With $\dot{W}_{isen}$ the reversible work inserted and h_{0e_s} the isentropic enthalpy value at the higher pressure.

However, this is not the case. Not all of the energy inserted into a compressor in the form of work is available. The isentropic efficiency of compressors are given by the following equation;

$$\eta_c = \frac{\dot{W}_{isen}}{\dot{W}} \tag{15}$$

With $\dot{W}_{isen}$ as shown in (14), and $\dot{W}$ the actual work inserted. A more in-depth discussion on isentropic efficiencies will be given when the fundamental equations are applied to the compression process.

3.2 Application of Fundamental Equations

To apply these fundamental equations to the vapour-compression cycle components, certain assumptions are made to further simplify the equations.

For all of the components, the body force term is rendered insignificant since the vertical distance between the in- and outlets are negligible with each component.

The rates of change in mass, momentum and energy in the control volume is also eliminated since the assumption is made that these fundamentals do not vary as a function of time.

By making these two assumptions, the fundamental equations simplify to the following;

Conservation of Mass

$$\dot{m}_e - \dot{m}_i = 0 \tag{16}$$

Conservation of Momentum

$$\frac{p}{p_0}(p_{0e} - p_{0i}) + \frac{1}{2}\rho V^2 \left(\frac{1}{T_0}\right)(T_{0e} - T_{0i}) + \Delta p_{0L} = 0 \tag{17}$$

Conservation of Energy

$$\dot{Q} + \dot{W} = \dot{m}_e h_{0e} - \dot{m}_i h_{0i} \tag{18}$$

From (16) it can be argued that the mass flow subscripts can be eliminated, simply referring to mass flow as $\dot{m}$ since;

$$\dot{m}_e = \dot{m}_i \tag{19}$$

The equations in (15) – (18) are now applied to every component in the cycle after which further simplifications can be made to better describe the internal operations of a vapour compression cycle.

The condenser and evaporator are discussed together since they are both heat exchangers. The isenthalpic valve and compressor are then also discussed in terms of these fundamental equations.

Applied to Heat Exchangers:

Firstly, the assumption is made that the pressure loss through the heat exchangers are negligible, eliminating the need for the momentum conservation equation. This leaves the mass conversation equation, (15), which merely states that the mass flow into the heat exchanger are equal to the mass flow out of the heat exchanger and the conservation of energy equation.

Since no work is done to the fluid, the work term in (17) is removed. Using (18), the energy equation then simplifies to;

$$\dot{Q} = \dot{m}(h_{0e} - h_{0i}) \tag{20}$$

Applying (18) to the schematic of the vapour compression cycle, the subscripts of the enthalpy values change. Using Figure 7, the energy transfers in the condenser and evaporator are then in the form;

$$-\dot{Q}_c = \dot{m}(h_2 - h_1) \quad (21)$$

$$\dot{Q}_e = \dot{m}(h_4 - h_3) \quad (22)$$

The $\dot{Q}_c$ and $\dot{Q}_e$ terms refer to the heat transfer in the condenser and the evaporator respectively. The $\dot{Q}_c$ term in (21) is negative since heat is extracted **from the fluid**.

The equations in (21) and (22) are normally used in conjunction with other equations to determine design and operational parameters such as sizes and secondary fluid mass flows.

Applied to Expansion Valve:

During this process fluid is throttled over a restriction that causes a local pressure loss in the fluid. A better understanding of this process will be discussed after the conservation equations have been applied.

The following two properties are considered when applying the conservation equations to the expansion valve.

1. No work is done by or on the control volume.
2. No heat is transferred from or to the control volume.

Taking these two properties into account when considering the energy and mass conservation equations, simplifies (17) to;

$$h_i = h_e \quad (23)$$

From Figure 7; $h_2 = h_3$

From the definition of enthalpy in (15), it is clear that if pressure decreases then specific volume must increase if the enthalpy is to remain constant (under the assumption that internal energy also remains constant). Due to the mass conservation equation stating that mass flow is constant, the change in specific volume equates to an increase in velocity.

If a change in the internal energy is obtained, then a temperature change is expected. Normally, the temperature will drop, but in some cases it can remain constant or even increase.

Applied to Compressor:

During compression, mechanical work is transferred to the fluid. This results in an increase in pressure as well as temperature. The assumption is generally made that the process happens isolated, with no heat transfer to or from the fluid.

By taking this assumption into consideration whilst evaluating the energy conservation equation, the following equation is obtained;

$$\dot{W} = \dot{m}(h_{0e} - h_{0i})$$

$$\dot{W} = \dot{m}(h_1 - h_4) \tag{24}$$

As mentioned in the previous section, the compression process is not reversible. This is indicated by a value known as the isentropic efficiency. The equation for isentropic work and efficiency is recalled below.

$$\dot{W_{isen}} = \dot{m}(h_{0e_s} - h_{0i}) \tag{14}$$

$$\eta_c = \frac{\dot{W}_{isen}}{\dot{W}} \tag{15}$$

Combining (14), (15) and (24) with subscripts referring to the respective points in the process schematic given in Figure 7, results in the following;

$$\eta_c = \frac{\dot{m}(h_{1_s} - h_4)}{\dot{m}(h_1 - h_4)} \tag{25}$$

The enthalpy values of h_1 and h_4 can be determined from the respective pressure and temperatures, refer to (12). The enthalpy value of h_{1s} can be determined as follows;

Due to isentropic property;

$$s_4 = g(P_4, T_4) \tag{26}$$

$$s_1 = s_4 \tag{27}$$

$$h_{1_s} = h(P_1, s_1) \tag{28}$$

The isentropic efficiency value of a process is rarely constant, with losses varying as the operating parameters and environment changes. As can be seen from (25) – (28), the isentropic efficiency is a function of both the suction and discharge temperatures and pressures. Other influences on the isentropic efficiency can also be identified.

As mentioned, losses and leakages will be a major influence on the isentropic efficiencies since it results in the unavailability of energy through the mechanical work applied.

By considering friction losses, the equation of friction force (F_f) is first evaluated;

$$F_f = \mu_k F_n \tag{29}$$

With μ_k the kinetic friction coefficient and F_n the normal force between two objects. The energy loss due to the kinetic friction in (29) can then be determined by obtaining the work done by the friction force (E_f). Since the assumption is made that the reciprocating compressor has a constant displacement, the friction force is therefore multiplied by this distance (d);

$$E_f = F_f d \tag{30}$$

The energy loss, (E_f), is then measured in Joules (J). In the case of a reciprocating compressor with a set number of rotations per second, an energy loss rate with a J/s unit can be established.

The addition of a variable speed drive (VSD) enables the compressor to operate at other frequencies (Hz). The VSD can therefore indirectly alter the energy loss obtained throughout the process. This may lead to variations in frictional losses and thus the isentropic efficiency.

The addition of the VSD may also lead to variations in other parameters for the compressor. As already mentioned, the compressor is assumed to have constant displacement. By altering the frequency, or number of rotations per second, the volume flow through the compressor is changed.

$$\dot{V} = V_R \cdot Hz \tag{31}$$

With V_R the volume displaced per rotation $\left(\frac{m^3}{rotation}\right)$ and Hz the rotations per second $\left(\frac{rotation}{s}\right)$. This results in the volume displaced per second, $\dot{V}$ $\left(\frac{m^3}{s}\right)$.

Since density, ρ, is a function of temperature and pressure, the variation in volume flow may lead to changes in mass flow as well;

$$\dot{m} = \rho\dot{V} \tag{32}$$

Another way in which mass flow can alter compressor operating parameters is by changing the heat transferred in the heat exchangers, as seen in (22) and (23). Since it is a closed cycle, with the outlet of one component being the inlet of another, the properties at the inlet of te compressor will vary, influencing the performance.

To summarise, all of the discussed properties have either a direct or an indirect influence on the compressor performance. These properties are the discharge and suction temperatures and pressures, the mass flow and the operating frequency

The internal relationships and dependencies between these variables are yet to be established. The fundamental purpose of a characterisation study is to find and quantify these relationships. This will enable the prediction of changes in performance when one or more of these variables are altered.

It has been mentioned that a numerical approach will be followed to find these relationships and therefore characterise the performance of the compressor. By using this approach, a number of reliable experimental data points will need to be used.

However, to find the relationship between these variables, certain methods and theories can be applied. These methods and theories will typically lead to either charts, tables or equations that have a predictive quality for determining changes in the variables.

3.3 The Validity of Using Statistics

As discussed in the previous section, a number of variables have an influence on compressor performance. It was also mentioned that a numerical approach will be followed, leading to the use of experimental data for the characterisation.

The use of data alone is not enough to formulate the desired variable relationships. The data needs to be grouped and evaluated. The use of statistics to predict future variables from already existing sample groups will be beneficial. A number of statistical methods exist, one of which is the regression theory.

3.3.1 The Concept of Regression

To fully understand this concept, first visualise a scatter plot with a number of points depicted. Both axis' of the plot is named after a variable with each point having its own set of coordinates in terms of these two axis', as in Figure 9 (Swanepoel, et al., 2015).

The main aim of regression is to fit a line unto this plot. The accuracy of the fitted line can be improved and evaluated which will be discussed in paragraphs to come. Since a line is fitted unto this plot, an equation can be determined that will aid in the prediction of other points if one of the coordinates are known.

The figure below shows some fitted lines to an example scatter plot of weight versus height;

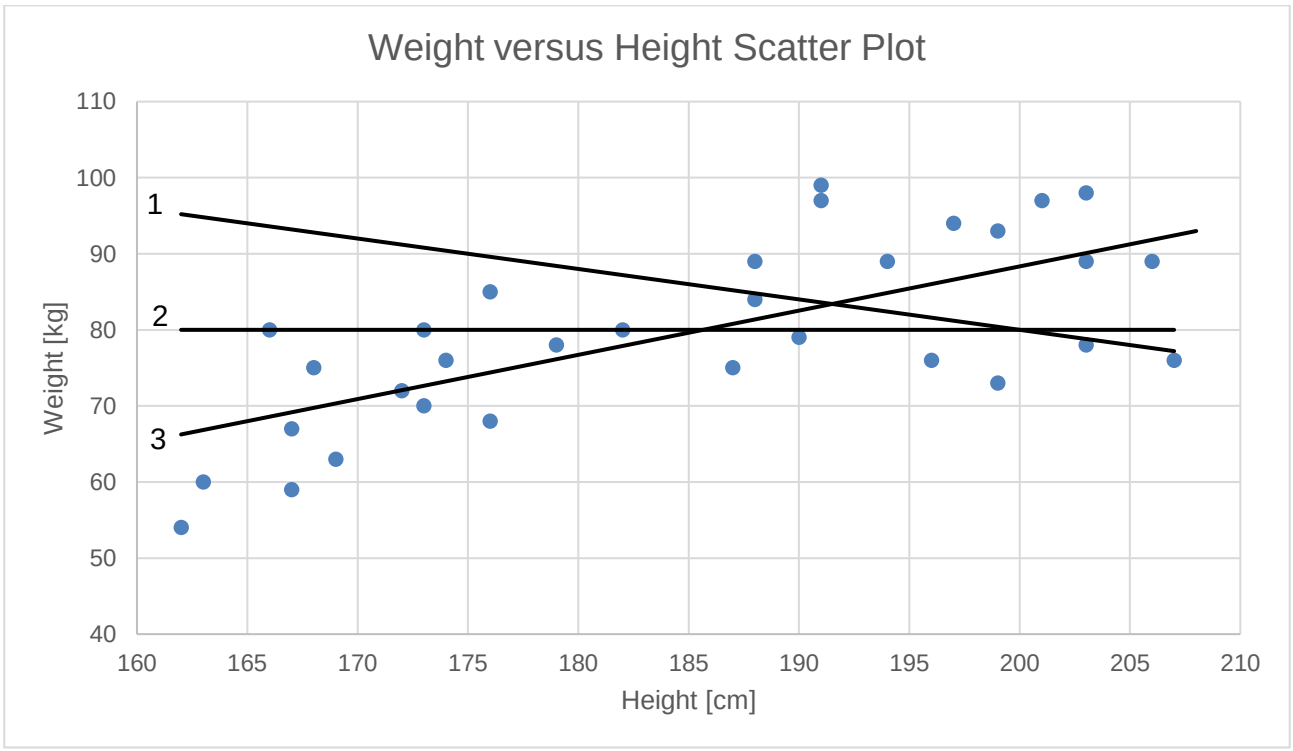

Figure 8: Example Scatter Plot with Fitted Line

The three fitted lines are all linear for illustrative purposes. Since these lines each have their own equations, it can be used to determine predictive weight values when a height value is known and vice versa.

It is important to grasp that correlation curves try to explain the relationship between a dependent variable and other variables, regardless of the accuracy. Essentially, the accuracy of the curves are important for formulating reliable relationships between the variables. It is therefore critical to use a method of determining the line equation that will deliver maximum accuracy.

To find such a method, a linear line is viewed that is fitted arbitrarily. A linear line is normally in the following form;

$$y = bx + a \tag{33}$$

Where a is the y-axis intercept and b the slope of the straight line.

The linear regression line must thus be fitted in such a way as to reduce the vertical distance between the line and data points. The vertical distance is known as the residual. In other words, the residual is known as the difference between the observed (y) and estimated value $(\hat{y}_i)$, as shown in the figure to follow.

$$Residual = y_i - \hat{y}_i \tag{34}$$

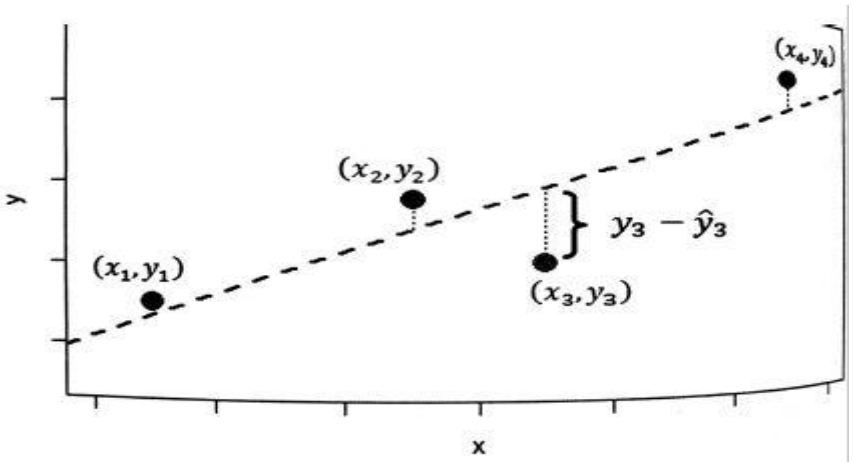

Figure 9: Definition of Residuals (Swanepoel, et al., 2015)

The aim of an accurate regression line is to lower the residual value to a minimum (Swanepoel, et al., 2015). The most common way to achieve this, is the application of the least squares method. The desired end result of the method of least squares is to find the values of a and b so that the following equation will be minimised;

$$\sum_{i=1}^{n}(y_i - \hat{y}_i)^2 = \sum_{i=1}^{n}\left(y_i - (a + bx_i)\right)^2 \quad (35)$$

Where the data consists of n data points (Swanepoel, et al., 2015) when the scatter plot in Figure 9 is expanded. Through partial differentiations of the above equation, the values of a and b can be found through the following equations;

$$b = \frac{\sum_{i=1}^{n} x_i y_i - \frac{1}{n}\sum_{i=1}^{n} x_i \sum_{i=1}^{n} y_i}{\sum_{i=1}^{n} x_i^2 - \frac{1}{n}[\sum_{i=1}^{n} x_i]\text{^}2} \quad (36)$$

$$a = \frac{\sum_{i=1}^{n} y_i}{n} - \left(\frac{\sum_{i=1}^{n} x_i y_i - \frac{1}{n}\sum_{i=1}^{n} x_i \sum_{i=1}^{n} y_i}{\sum_{i=1}^{n} x_i^2 - \frac{1}{n}[\sum_{i=1}^{n} x_i]\text{^}2}\right)\left(\frac{\sum_{i=1}^{n} x_i}{n}\right) \quad (37)$$

$$a = \bar{y} - b\bar{x} \quad (38)$$

With $\bar{y}$ and $\bar{x}$ the average of the y and x respectively. For a full derivation, see Appendix A.

The equations above are mathematically derived so it can be used to determine a linear fit based on the least squared errors for any set of observed data. It does not, however, give an indication on the accuracy or relevancy of the fit or relationship identified.

The coefficient of determination(R^2) is an indication of how well the least-squares line fit the observed data (Swanepoel, et al., 2015). It is defined as;

$$R^2 = 1 - \frac{\sum_{i=1}^{n}(y_i - \hat{y}_i)}{\sum_{i=1}^{n}(y_i - \bar{y}_i)} \quad (39)$$

The characteristics of the coefficient of determination include (Swanepoel, et al., 2015):

- $0 \leq R^2 \leq 1$; The coefficient is always between 0 and 1.
- $R^2 = 1$; Perfect fit between least-squares curve and observed data.

In some cases it can be sufficiently accurate to use other statistical methods, such as basic averages to determine relationships. This can be used, for example, when the dependent variable values change in small increments from one independent variable to another.

Instead of determining an equation, a constant value will then be determined;

$$\bar{y} = \frac{\sum_{i=1}^{n} y_i}{n} \quad (40)$$

With $\bar{y}$ being the average values for a n number of y values.

By using the averages on a specific variable, the variable will not be user-defined in the resulting equations, since it's values are already embedded into the coefficients. This not only removes possible complexity, but also accuracy. A discussion around which method to use under what circumstances will be given when the methodology is applied in the next chapter.

The methods described in this section is used to formulate and evaluate the relationship equations that best fit the observed data. Understanding this section is critical to establish the process used to convert mathematical reasoning to a fixed, universal methodology.

3.4 Methodology Development

In section 3.2 Application of Fundamental Equations a total of six variables was identified to have an influence on the performance of the compressor. It was concluded that dependencies between these variables are to be determined since a numerical approach, using experimental data, will be followed. These dependencies can then be used to characterise the compressor.

In section 3.3 The Validity of Using Statistics the methods of determining regression equations and their respective characteristics where discussed. The least-squares method was identified and a brief description of the method was given.

The use of the least-squares method enables the establishing of a relationship between only two variables at a time. Iteratively using this method to include all of the variables are therefore considered

To do this whilst ensuring maximum accuracy and simplicity, a fixed method needs to be followed. The method needs to be universal, thus the method must be applicable to other studies of similar nature. After following the method, the resulting characterisation must include all of the variables and be able to predict performance properties with sufficient accuracy.

3.4.1 Methodology Walkthrough

It is important to note that this section will only discuss the methodology, the application thereof to create characterisation equations for an actual compressor will follow in the next chapter.

The methodology formulation is done from the perspective of one of the six variables identified. To evaluate the methodology's capability to be applied on different sets of variables, the methodology will be applied twice.

In this case; the variables are discharge temperature and mass flow. The resulting characterisation equations will therefore be in the following forms;

$$T_{out} = f(T_{in}, P_{out}, P_{in}, Hz) \quad (41)$$

$$\dot{m} = g(T_{in}, P_{out}, P_{in}, Hz) \quad (42)$$

As already mentioned, the methodology will focus on finding accurate correlations between different variables. It is therefore imperative that a logic is followed that is both simplistic and universal.

Given below is a logic-diagram summarising the methodology followed. A walkthrough discussion will be given after the diagram for the formulation of (41).

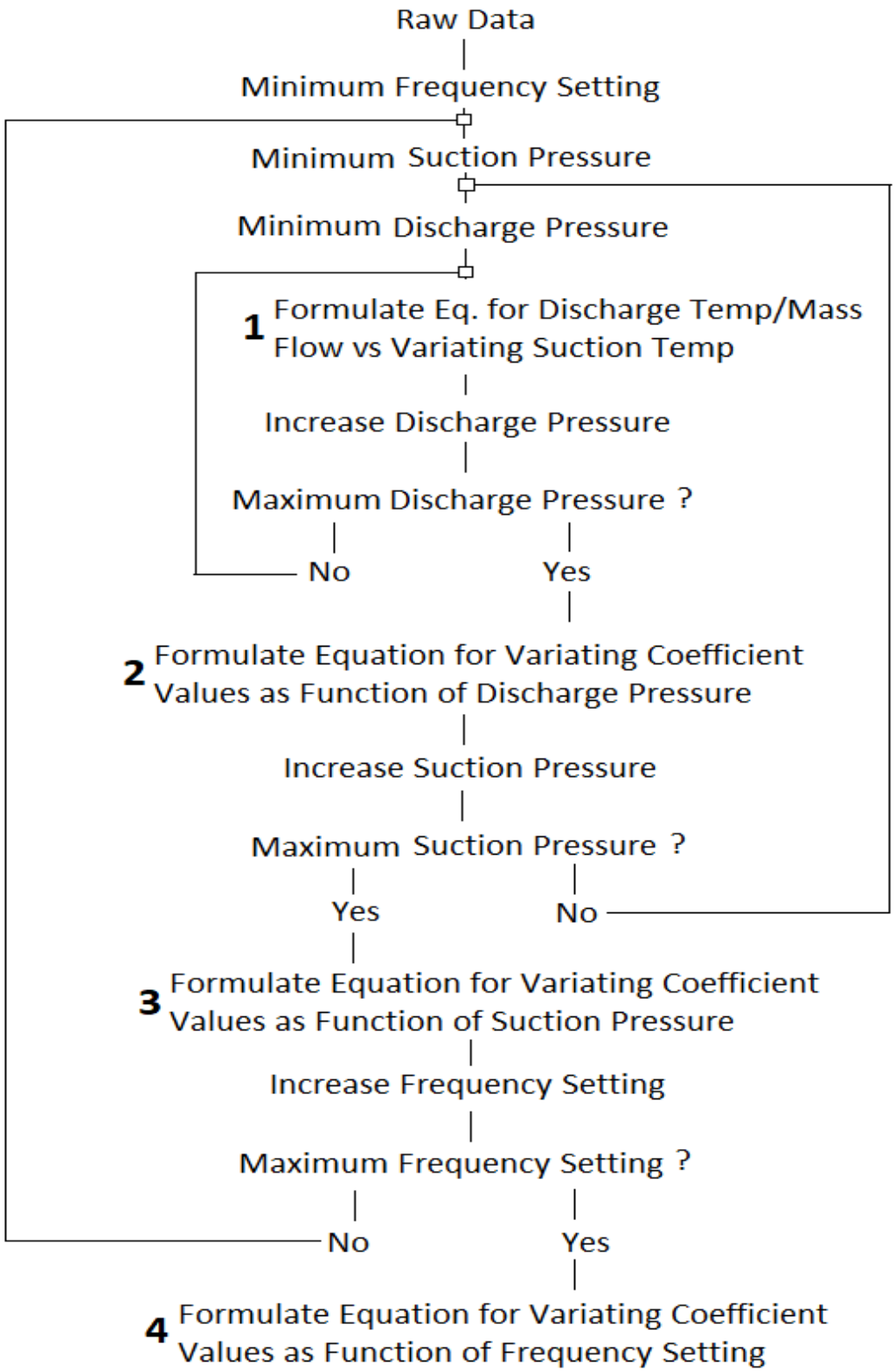

Figure 10: Logic Diagram for Methodology

As shown in Figure 10, equations are formulated for one specific variable before making any adjustments to the other variables. An equation is formulated, one parameter is changed and then another equation is formulated. This process is repeated until all the maximums are reached.

This process is repeated iteratively, as is also shown in Figure 10, until the resulting equations are functions of all the other variables. The logic diagram is also repeated for both the discharge temperature equation and the mass flow variant. These two equations are thus independent of one another and the denotations and subscripts of one should not be confused with those of the other. For discussion, the discharge temperature function is used for the walkthrough to follow.

To build the discharge temperature equation from experimental data, the logic diagram in Figure 10 will be used. The logic diagram shows ranges and variations to be made in settings, which will only be discussed with detail in a latter section when actual experimental data is used. For now, only the numbered items, 1-4, will be discussed with the assumption that all the required data is available.

The formulated equation for T_{out} as a function of all the other variables kept constant with special emphasis on a varying T_{in} can be described;

$$T_{out} = h\big(T_{in}, j(x_1)\big) \tag{43}$$

$$j(x_1) = j(P_{out}, P_{in}, Hz) \tag{44}$$

The function in (44) is shown to emphasise that in the function created in (43), the coefficients formulated is a function of the other variables, with these variables simply denoted by x_1.

If the discharge versus suction temperature plots show a line with no slope, or a marginally small slope it indicates that the discharge temperature will not vary in values with changes in the suction temperature. In simple terms, the discharge temperature is not a function of suction temperature.

If this is the case, the constant value can be maintained, or in the case of marginal differences, an average value can be obtained. This constant value is then viewed as a function for the steps to come.

The assumption is made that the discharge temperature is indeed a function of the suction temperature and that notable differences are observed. This states that the least-squares method is desired, and the resulting polynomial equation of degree n will be in the form;

$$h\big(T_{in}, j(x_1)\big) = j_n(x_1)T_{in}^n + j_{n-1}(x_1)T_{in}^{n-1} + \cdots + j_2(x_1)T_{in}^2 + j_1(x_1)T_{in} + j_0(x_1) \tag{45}$$

In summary;

$$T_{out} = \sum_{i=0}^{n} j_i(x_1)T_{in}^i \tag{46}$$

This is applied in the following chapter, under 4.2.1 The First Correlation.

The next step in Figure 10 is to repeat this process for other discharge pressures until the maximum operational limit of the discharge pressure has been reached. Note that when this maximum discharge pressure has been reached, the equations are still formulated. The break in the loop happens only after the formulation.

The coefficients $j_i(x_1)$ for $i = 0, n$ in the equation would normally be seen as constant values. As mentioned, the x_1 is merely a concise way to indicate that the three other variables still have an influence in the function.

All of the equations formulated in this loop of variations in discharge pressures, can then be evaluated and processed. A difference, whatever the magnitude, is expected for each of these equations' $j_i(x_1)$ values with $i = 0, n$.

If there is no difference in coefficient values, it states that the performance of the compressor is then not a function of the discharge pressure. If there is a relatively small difference, an average value can then be determined. The constant value, or average if the differences are marginal, can then be used for the next process in Figure 10. This is a typical circumstance of where averages can be used instead of regression equations to save on complexity without sacrificing too much accuracy.

With this methodology discussion, the assumption is made that notable differences are observed and that the compressor performance is indeed a function of the discharge pressure. This concludes that the least-squares method is required for this step.

The diagram in Figure 10 shows that the next step is to formulate the equation for variations in coefficient values as a function of discharge pressure.

Since only the discharge pressure was varied from the one formulation to the next, differences between coefficient values from one equation to another can be argued as a direct result from these discharge pressure variations.

The correlation for the coefficient values is considered to be a polynomial function;

For $i = 0 \rightarrow n$;

$$j_i(x_1) = k(P_{out}, l(x_2)) \tag{47}$$

$$l(x_2) = j(P_{in}, Hz) \tag{48}$$

The equation in (48) emphasises that the function in (47) still has coefficient values which are dependent on the remainder of variables. These variables are again denoted by x_2 for concision.

Since the least-squares method is again utilised, the resulting polynomial of degree p will be in the form;

$$k\big(P_{out}, k(x_2)\big) = k_p(x_2)P_{out}^p + k_{p-1}(x_2)P_{out}^{p-1} + \cdots + k_2(x_2)P_{out}^2 + k_1(x_2)P_{out} + k_0(x_2) \tag{49}$$

Thus, for $i = 0, n$

$$j_i(x_1) = \sum_{m=0}^{p} k_m(x_2) P_{out}^m \tag{50}$$

The equations in (49) and (50) can be combined to illustrate the compiled function at this stage;

$$T_{out} = \sum_{i=0}^{n} \left(\sum_{m=0}^{p} k_m(x_2) P_{out}^m \right) T_{in}^i \tag{51}$$

At this stage, the compiled equation (51) is a function by which the discharge temperature can be determined from the discharge pressure and suction temperature.

This is applied in a chapter to follow, under 4.2.2 The Second Correlation.

At this point in Figure 10, the suction pressure is increased and the entire process in the first correlation is repeated. The equations which are in the form of (46) are repeated for the new suction pressure. After the maximum discharge pressure has been obtained with it's final formulation, this step is repeated. Refer to Figure 10.

The second loop is thus broken when the maximum discharge pressure and maximum suction pressure has been achieved.

The coefficients $k_m(x_2)$ for $m = 0, p$ in the equation would under normal circumstances be seen as constant values. Note that x_2 is simply a shorter term to indicate that the two other variables, suction pressure and frequency, still have an influence in the function formulated.

All of the equations in the form of (51) formulated when variations were made in suction pressures, can then be processed. It is expected that a difference in the coefficient values for each equations' $k_m(x_2)$ values with $m = 0, p$ will be achieved.

If there is no difference in coefficient values, it proves that the discharge temperature of the compressor is not a function of suction pressure. If the differences are marginal when compared to one another, an average of these coefficient values can be determined. The constant value, or average in the case of a marginal difference, can then be used for the next step in Figure 10. This method will then save on equation complexity without significantly influencing the accuracy.

During this discussion, the assumption is made that notable differences present and that compressor discharge pressure is in fact a function of suction pressure. This indicates that the least-squares method is required for this correlation step.

The logic in Figure 10 indicates that the next step is to generate equations that will predict the coefficient values in (51) as a function of suction pressure.

The only variation in operational parameters between the equations formulated is the suction pressure. The differences between coefficient values from one function to the next are thus directly influenced by these changes in suction pressure.

The correlation for the coefficient values is considered to be a polynomial function;

For $m = 0 \rightarrow p$; $$k_m(x_2) = q(P_{in}, r(Hz)) \tag{52}$$

If the least-squares method is required, as in this case, the resulting polynomial of degree s will be in the form;

$$q(P_{in}, r(Hz)) = r_s(Hz)P_{in}^s + r_{s-1}(Hz)P_{in}^{s-1} + \cdots + r_2(Hz)P_{in}^2 + r_1(Hz)P_{in} + r_0(Hz) \tag{53}$$

Thus, for $m = 0, p$

$$k_m(x_2) = \sum_{t=0}^{s} r_t(Hz)P_{in}^t \tag{54}$$

The equation in (54) can now be combined with (51) to illustrate the compiled function thus far in the process;

$$T_{out} = \sum_{i=0}^{n}\left(\sum_{m=0}^{p}\left(\sum_{t=0}^{s} r_t(Hz)P_{in}^t\right)P_{out}^m\right)T_{in}^i \tag{55}$$

The function in (55) can be used to determine the discharge temperature from the values of the discharge pressure and suction pressure and temperature.

The step above is applied in a chapter to follow, 4.2.3 The Third Correlation.

With reference to the logic diagram in Figure 10, the upper limit values for all the variables have been reached, with the exception of the frequency setting. After the third correlation, the frequency is increased and the entire process from is repeated with both of the internal loops regarding the discharge and suction pressure.

The final loop is thus broken when the upper limit values have been reached for all of the variables.

The equations created with the third loop are all in the form of (55). These equations can then be used for further formulation after the third loop is completed. The coefficient values in these equations are again expected to have a difference for each equations' $r_t(Hz)$ for $t = 0, s$.

As mentioned before, if there is no difference in coefficient values, it states that the discharge temperature is not a function of the operational frequency. If the differences are marginally small, an average of these coefficient values can be used. The constant value or average, depending on circumstances, can then be used instead of a polynomial. This can aid in reducing the complexity without compromising accuracy.

The assumption is again made that the significant differences are present and that compressor discharge temperature is a function of operational frequency. Thus, the least-squares method will be utilised in this correlation step.

Referencing Figure 10, the last step is identified which states that equations need to be generated that will predict the coefficient values in equation (55) according to the operational frequency.

The only difference in operational parameters between the list of equations formulated is the operational frequency. The differences identified between the specific coefficient values from one function to the next is then concluded to be directly influenced by the operational frequency.

The correlation for the coefficient values is considered to be a polynomial function of degree v since the least-squares method is required, thus it will be in the form;

For $t = 0, s$

$$r_t(Hz) = a_v Hz^v + a_{v-1} Hz^{v-1} + \cdots + a_2 Hz^2 + a_1 Hz + a_0 Hz \tag{56}$$

Thus, for $t = 0, s$

$$r_t(Hz) = \sum_{w=0}^{v} a_w Hz^w \tag{57}$$

The equation in (57) is now combined with (55) to deliver the compiled function at the end of the process in the form;

$$T_{out} = \sum_{i=0}^{n} \left(\sum_{m=0}^{p} \left(\sum_{t=0}^{s} \left(\sum_{w=0}^{v} a_w Hz^w \right) P_{in}^t \right) P_{out}^m \right) T_{in}^i \tag{58}$$

The function in (58) can be used to determine the discharge temperature from the operational frequency, suction and discharge pressures as well as suction temperature.

The step above is applied in a chapter to follow, 4.2.4 The Fourth Correlation

As already mentioned, this methodology can now be used to determine equations similar to the format in (58) for other variables such as the mass flow.

During this chapter, basic cycle fundamentals were discussed to indicate whether a specific variable would have an influence on the performance parameters of a compressor in a vapour compression cycle. Since a numerical approach is followed, experimental data processing is required and some of the methods were discussed. Finally, the methodology developed was discussed via the use of a logic diagram and mathematical formulation.

To evaluate the applicability of the characterisation methodology; it can be applied to an actual compressor for characterisation purposes.

4. Numerical Equations

The previous chapter discussed the design and formulation of the characterisation methodology. This chapter will illustrate the use of the discussed methodology on a specific compressor.

4.1 Experimental Procedure

To test the methodology, it will be applied to a specific compressor. Data in the form of sensor readings at the relevant areas will be used to apply the methodology. The compressor will need to be run in certain conditions for safety and reliability purposes and thus an operational range for various parameters will also be established. This range is applicable only to the specific compressor and cycle used.

The specific compressor is a JTC-15K Bitzer compressor. This compressor is part of an existing test bench similar to the vapour compression cycles discussed. The compressor is also fitted with a variable speed drive, adding the capability of a controllable frequency. A schematic of the cycle with the relevant sensors are shown below;

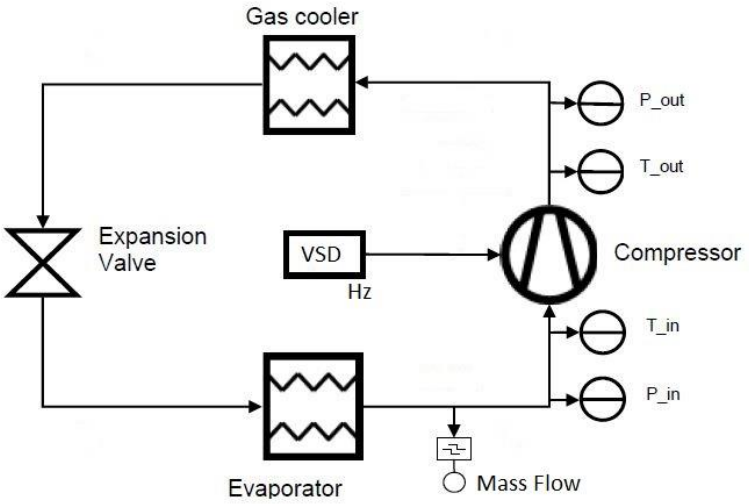

Figure 11: Experimental Test-Bench Setup

The gas cooler, named as such due to a trans-critical cycle, utilises water as secondary medium. The water is pumped from a storage tank, a controllable valve is also fitted into the transport line that can be used to vary the mass flow of water. This will inherently change the heat transfer capabilities of the heat exchanger. This loop of changes in variables from one component to another for a cycle has already been discussed in 3.2 Application of Fundamental Equations.

The evaporator uses air as the secondary fluid. No vanes or VSD are fitted to the fans to enable changes in airflow and thus the heat transferred. The temperature of the air moving through the evaporator is also not controllable.

The only controllable components in this cycle is the water mass flow control valve, the expansion valve and VSD. As already discussed, a change to any one of these components will influence changes on the identified variables.

Initially, the test bench is run at different operating parameters. It is observed that the uncontrollable variables take 10-15 minutes to stabilise after a controllable component is changed such as an increase/decrease in frequency or differing expansion valve settings.

Referring to 3.4.1 Methodology Walkthrough where the methodology is given logically and discussed with an example variable, the discharge temperature, the assumption is made that only 10 different data points are required to determine accurate variable relationships, it is calculated that 10^3 data points, and therefor tests, are required per operating frequency;

1. Referring to the correlation step 1 in the Figure 10, 10 data points are needed to determine the equation of T_{out} vs T_{in}.
2. Referring to the correlation step 2 in the Figure 10, 10 data points are then needed to determine the coefficient values created in the first correlation step as a function of P_{out}. The loop in Figure 10 indicates that the 10 data points mentioned in "1" are therefore repeated for each value of P_{out}.
3. Referring to the correlation step 3 in the Figure 10, 10 more data points are also needed to determine the coefficient values created in the second correlation step as a function of P_{in}. The second loop in Figure 10 shows that steps 1 and 2 above need to be repeated.

From the above outlay, it can be concluded that the number of tests to be done for every **frequency** is $10 \times 10 \times 10$ or 10^3.

The total test time for each frequency is then $10\ minutes\ \times 1000 = 10\,000\ minutes$. The required time does not consider setting op the test bench or extracting data. When the fact is taken into account that the frequency is varied which will multiply this amount with 3 or 4, it can be concluded that an alternative is thus needed to lower the time required to accumulate the necessary data points.

The manufacturer has developed a software that accurately simulates compressor performance from certain inlet variables. The time it takes for the software to determine results is a few seconds and will thus greatly reduce the time required for this study.

Since the objective of the study is to test the methodology developed and not the performance of the specific compressor, the data needed will be generated with the help of the software. To still have a sense of accuracy and applicability, the software data is compared to actual test bench data.

Table I: Verification of Software Values

Setup				Software		Test Bench		$\lvert\%Error\rvert$	
Hz	T_{in} [°C]	P_{in} $[bar]$	$P_{out}[bar]$	$\dot{m}$ $[g/s]$	T_{out}[°C]	$\dot{m}$ $[g/s]$	T_{out}[°C]	$\dot{m}$ [%]	T_{out}[%]
60	-4,1	27,2	95,0	155,8	114,4	162,5	110,2	4,28%	3,67%
60	1,8	32,0	122,3	177,8	131,6	185,2	124,6	4,18%	5,32%
50	2,9	31.4	88.6	173,6	93,3	175,8	88,5	1,26%	5,14%
50	4,8	33,2	122,2	164,2	125,5	167,5	118,2	2,03%	5,82%
40	4,0	32,2	81,8	144,4	84,4	142,5	80,4	1,35%	4,74%
40	6,4	32,7	117,0	114,4	133,1	119,3	127,5	4,24%	4,21%
Absolute Error Value Average								2.89%	4.82%

A series of tests are done on the experimental test bench. After steady-state is obtained in the test bench, all of the variables are noted. These values, except for the mass flow and discharge temperature is then inserted into the software. The results for the mass flow and discharge temperature from the software is then compared to the actual values. The absolute error values are then determined and the accuracy is thus evaluated.

The software values are deemed accurate when considering the resulting errors in each test. The alternative method of obtaining data through the use of software simulations is therefor used in the methodology application.

4.2 Methodology Application

This section will illustrate the application of the methodology by determining the specific compressor characterisation equations within its operational limits.

Firstly, it is required to find and determine the operational limits of the compressor. The range should include the operational conditions as well as the safety limits for the compressor and for the rest of the components within the cycle.

Table II: Applicable Ranges to the Specific Compressor Used

Variable	Range/Limits
Suction Temperature	$DOS > 5$ °C
	-10 °C $< T_{in} < 20$ °C [1]
Suction Pressure	20 bar $< \mathrm{P_{in}} < 40\ bar$
Discharge Temperature	$T_{out} < 160$ °C
Discharge Pressure	$75\ bar < P_{out} < 110\ bar$
Frequency	$40\ Hz < Frequency < 60\ Hz$

The suction temperature limit in terms of DOS is specifically in place to ensure that only vapor enters

[1] Suction pressures have an influence on the *DOS* causing the lower limit to vary from one P_{in} to another.

the compressor. The second limit concerning suction temperature is for applicability purposes. The pressure ranges, both suction and discharge are operational limits of the compressor and due to the thermodynamic properties of the fluid. The discharge temperature is limited for both component safety as well as heat exchanger practicality limits. The particular frequency range is also regarded as a limit due to applicability purposes.

The only variable not mentioned in the table is the mass flow. Mass flow together with discharge temperature are the required outputs for the equations to be formulated, as discussed in 3.4 Methodology Development.

To ensure that adequate data is obtained, Figure 10: Logic Diagram for Methodology is referenced again. Since the generated matrix is too large to display, a concise version is displayed below. For clarity, Figure 10: Logic Diagram for Methodology can be viewed in conjunction with the matrix below;

Table III: Test Matrix for Gathering Experimental Data

Frequency [Hz]	Suction Pressure [bar]	Discharge Pressure [bar]	Suction Temperature [C]	Discharge Temperature [C]	Mass Flow [g/s]
30	20	75	-10 → 20	Output	Output
		80	-10 → 20	Output	Output
		85	-10 → 20	Output	Output
⋮	⋮	⋮	⋮	⋮	⋮
60	40	100	-10 → 20	Output	Output
		105	-10 → 20	Output	Output
		110	-10 → 20	Output	Output

Since the data collection matrix above is built on Figure 10: Logic Diagram for Methodology, the methodology is capable of not only generating the characterisation equations, as discussed below, but also the collection of data for the formulation of equations.

The methodology will be followed and discussed for both the discharge temperature and mass flow equations in conjunction. Their equations are independent of another and any denotation for one should not be confused with the other.

Any variation in decision-making between the two methods with regards to which statistical method to use, as discussed in 3.4.1 Methodology Walkthrough, will be noted. In cases where the same method is used, a short discussion on the mass flow characterisation will be given for clarity purposes.

4.2.1 The First Correlation

The first step of the methodology can be identified as finding a correlation between the discharge temperature or mass flow and the suction temperature.

Start at the lower limits for frequency, suction and discharge pressures, plot the discharge temperature and mass flows versus the suction temperature values.

Whilst obtaining the data for these plots, make sure that the other variables are kept constant. Refer to Figure 10.

The suction temperature axis will start at the minimum allowable value, which depends on the suction pressure, and ends when the upper limit of either the suction or discharge temperature has been reached.

Since this correlation is repetitive for a range of variable values, an example will be illustrated concentrating on a specific set of variables.

Create a least squares regression line from the data points and also determine the correlation coefficient, as shown in the figure to follow.

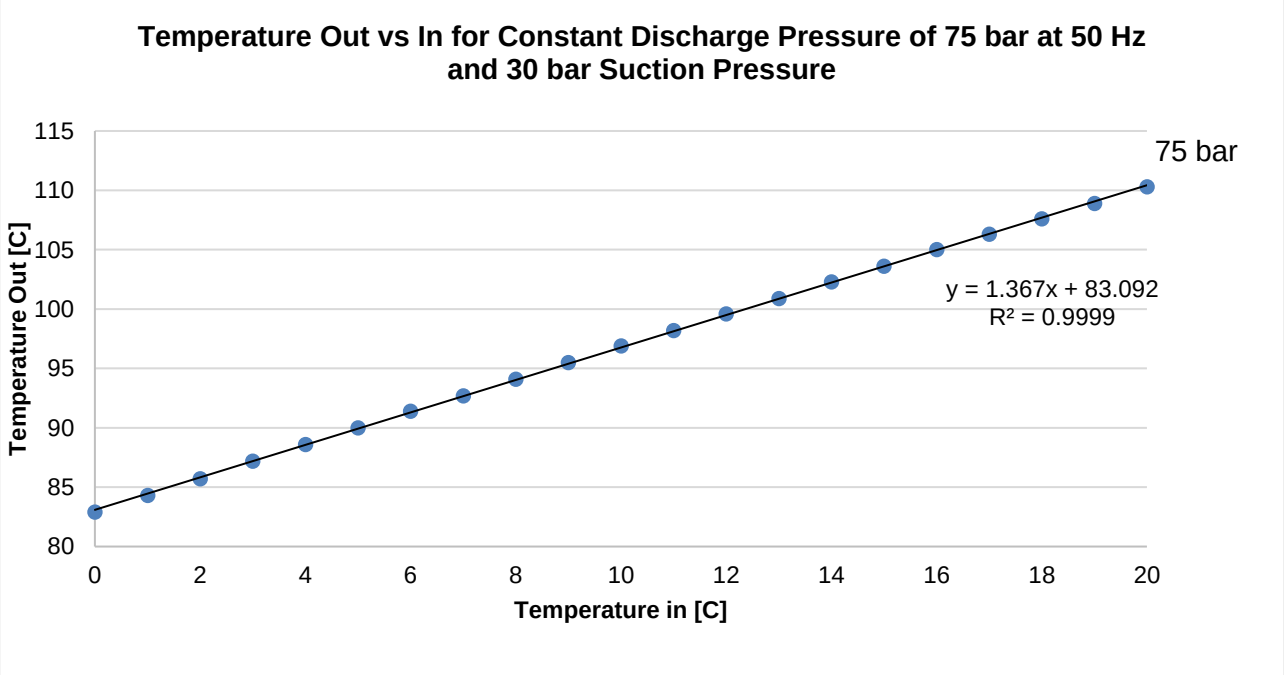

Figure 12: Correlation at Constant Discharge and Suction Pressure (50Hz)

The plot, as described in the graph window, are specific to 50 Hz, 30 bar suction pressure and 75 bar discharge pressure. The temperature out versus in shows a linear correlation. Whilst all other variables are held constant, the discharge temperature increases as the suction temperature is

increased. The correlation coefficient for this particular plot shows that the linear line is 99.99% accurate to the data.

At the current moment, the equation in Figure 12: Correlation at Constant Discharge and Suction Pressure (50Hz) is in the form described by (46) and (47), which is recalled below;

With $n = 1$;

$$T_{out} = \sum_{i=0}^{n} j_i(x_1) T_{in}^{i} \tag{46}$$

$$j_i(x_1) = j_i(P_{Out}, P_{in}, Hz) \tag{47}$$

The above mentioned process is repeated for other values of discharge pressure in the operational range as shown in Table II. After compiling all of these least-squares regression lines, a figure similar to the one below is obtained. Take note that each of these lines has its own regression equation.

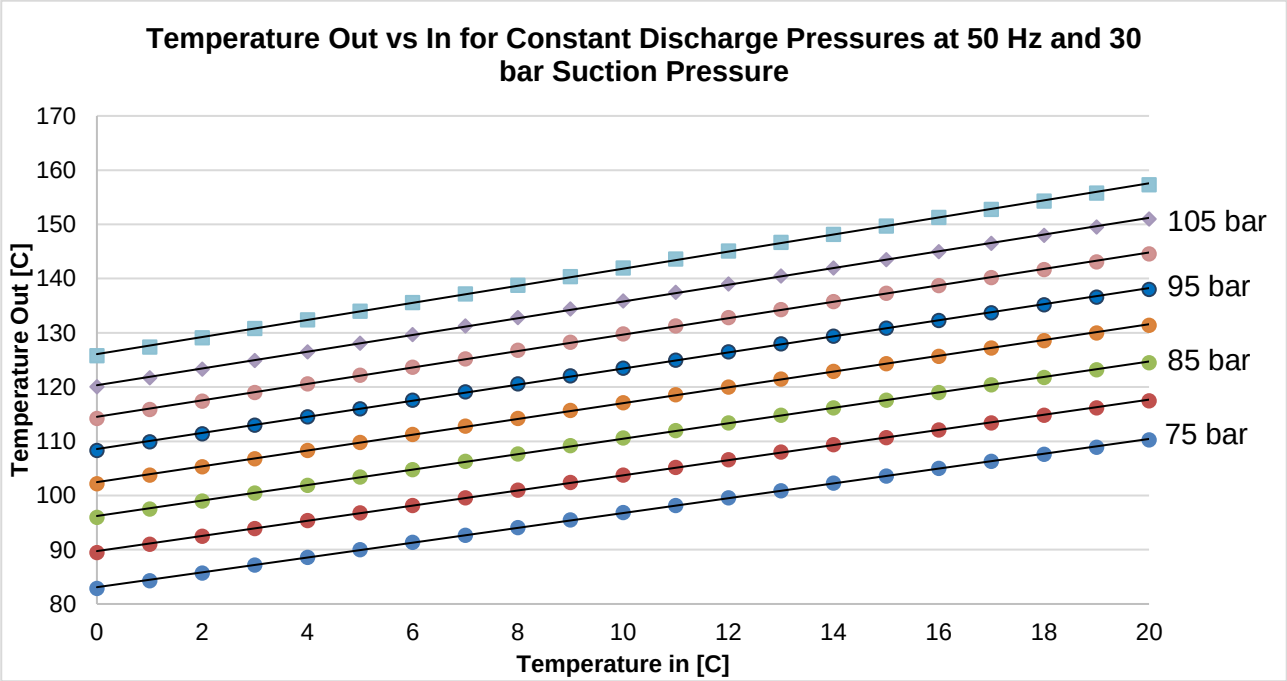

Figure 13: Correlation at Constant Suction Pressure (50Hz)

The linear correlation found for 75 bar discharge pressure is also true for the other discharge pressures. The increase in discharge temperatures as the suction temperature increases is applicable to all constant discharge pressure lines. The increase in discharge temperature due to an increase only in discharge pressure, indicating higher pressure ratio, is also noted.

The same procedure is followed to determine a regression equation between the suction temperature and resulting **mass flow** for varying discharge pressures. The formulated equations indicate that a polynomial of degree 1 delivers sufficient accuracy.

The resulting equations for the entire range of discharge pressures are also in the form shown in (46) and (47) with minor variations;

With $n = 1$;

$$\dot{m} = \sum_{i=0}^{n} j_i(x_1) T_{in}^{i} \tag{59}$$

$$j_i(x_1) = j_i(P_{Out}, P_{in}, Hz) \tag{60}$$

Since the discharge temperature and mass flow equations share the same independent variables, the two plots can be combined for brevity of the illustration of the performance data in this chapter.

Constant mass flows are determined and by using the equations in (48) for each discharge pressure, the corresponding suction temperature can be determined. The basic reasoning in equation terms to follow. From (48);

Assume $n = 1$;

$$\dot{m} = j_1(x_1) T_{in} + j_0(x_1) \tag{61}$$

$$T_{in} = \frac{\dot{m} - j_0(x_1)}{j_1(x_1)} \tag{62}$$

Similar equations to (62) are created for the other discharge pressures.

The resulting suction temperature for each mass flow is then marked on each constant pressure line, after which a correlation line is determined and inserted into the plot. The resulting plot will look similar to the one shown below; the full set of graphs is given in Appendix C.

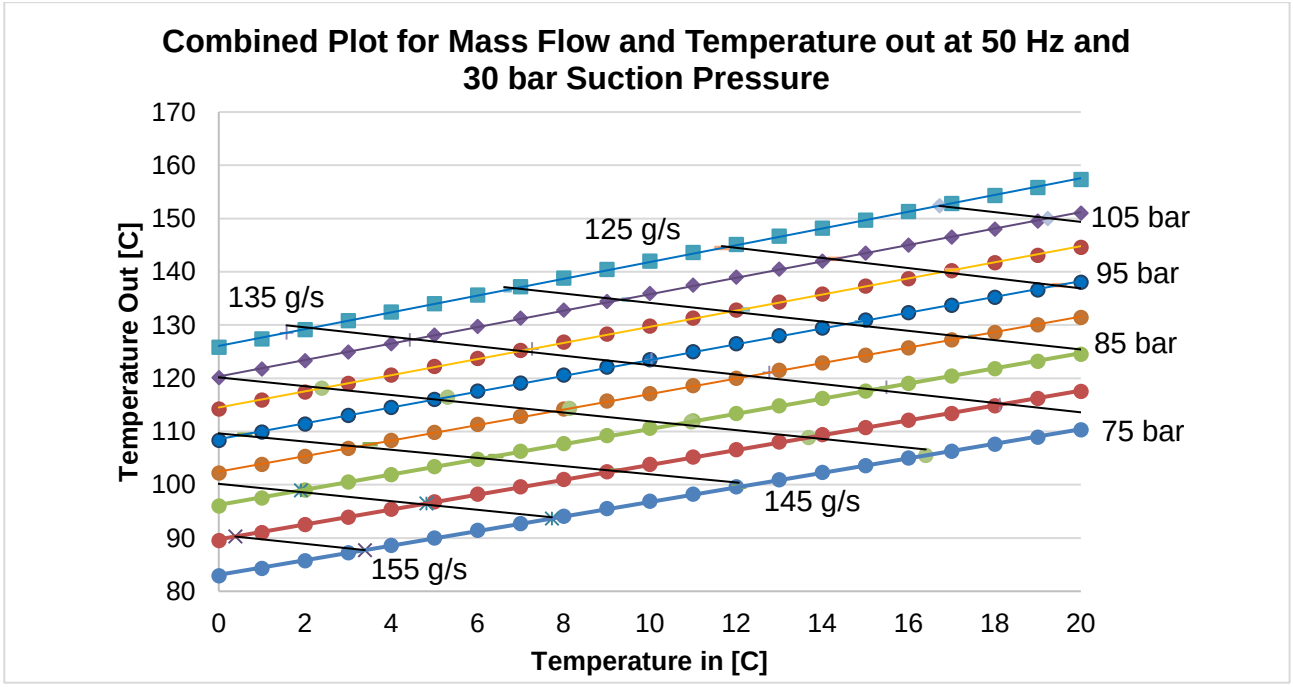

Figure 14: Combined Plot for 30 *bar* Suction Pressure and 50 Hz Operating Frequency

The combination of the two plots show constant mass flow and constant discharge pressure lines. The constant mass flow lines show a decrease in both discharge temperature and pressure as the suction temperature is increased. A decrease in mass flow is noted when the suction temperature is increased at a constant discharge pressure.

To summarise; equations have been formulated that describe the relationship between discharge and suction temperatures at different discharge pressures, as shown in (46) and (47). Constant mass flow lines have also been introduced into the discharge versus suction temperature plot.

4.2.2 The Second Correlation

The next step in the methodology can be identified from the equation formulation and Figure 10 in Chapter 3. The second correlation step commences when the highest discharge pressure has been reached, with a list of internal equations formulated for each discharge pressure.

The relationship between the coefficients in (46) and (47) and their corresponding discharge pressure will need to be established. Thus, the objective with this step is to find a correlation between the coefficient values and the discharge pressure. The complete list of equations is in Appendix B.

As already mentioned, both the discharge temperature and mass flows are discussed simultaneously. Their equations are independent of one another and should not be confused or mixed. To ensure proper reference for the table below, (46) and (47) is recalled;

For $k = 75, 110$ and since $n = 1$;
Thus;

$$T_{out_k} = \sum_{i=0}^{n} j_i(x_1) T_{in}^i \qquad (46)$$

$$T_{out\,k} = j_1(x_1) T_{in} + j_0(x_1)$$

For $k = 75, 110$ and since $n = 1$;
Thus;

$$\dot{m}_k = \sum_{i=0}^{n} j_i(x_1) T_{in}^i \qquad (47)$$

$$\dot{m}_k = j_1(x_1) T_{in} + j_0(x_1)$$

Note that k varies from 75 to 110 since the discharge pressures vary between these limits as discussed in Chapter 4.1. From the first correlation it was concluded that both the polynomials generated are sufficient when in the first degree thus $n = 1$.

Table III: Sample of Data for Plotting Coefficients versus Discharge Pressure

	Discharge Temperature Eq.			Mass Flow Eq.		
P_{out}	k	j_1	j_0	k	j_1	j_0
75 *bar*	75	1.367	83.092	75	−1.148	158.864
80 *bar*	80	1.397	89.748	80	−1.122	155.376
85 *bar*	85	1.425	96.221	85	−1.099	152.050
90 *bar*	90	1.456	102.467	90	−1.075	148.743
95 *bar*	95	1.484	108.572	95	−1.053	145.566
100 *bar*	100	1.515	114.514	100	−1.021	142.401
105 *bar*	105	1.543	120.339	105	−1.009	139.445
110 *bar*	110	1.575	126.073	110	−0.986	136.509

The above table shows the coefficient values from (46) and (47) applicable to a suction pressure of 30 bar and frequency of 30 Hz. As mentioned, the complete list of equations for all frequencies are given in Appendix B.

There are changes in coefficient values, removing the option of just using a constant value. These changes are not negligible, thus removing the option to consider averages. To establish the relationship between these values and the discharge pressure, the least-squares method in the first step is repeated for these values.

The figure below illustrates the values of $j_1$for the mass flow equations in the table with the corresponding discharge pressure. The least squares method again delivers a sufficiently accurate function when the polynomial order is 1. The plot below illustrates this line and the function. Similar plots are created for all of the coefficients in the table above to determine each individual function.

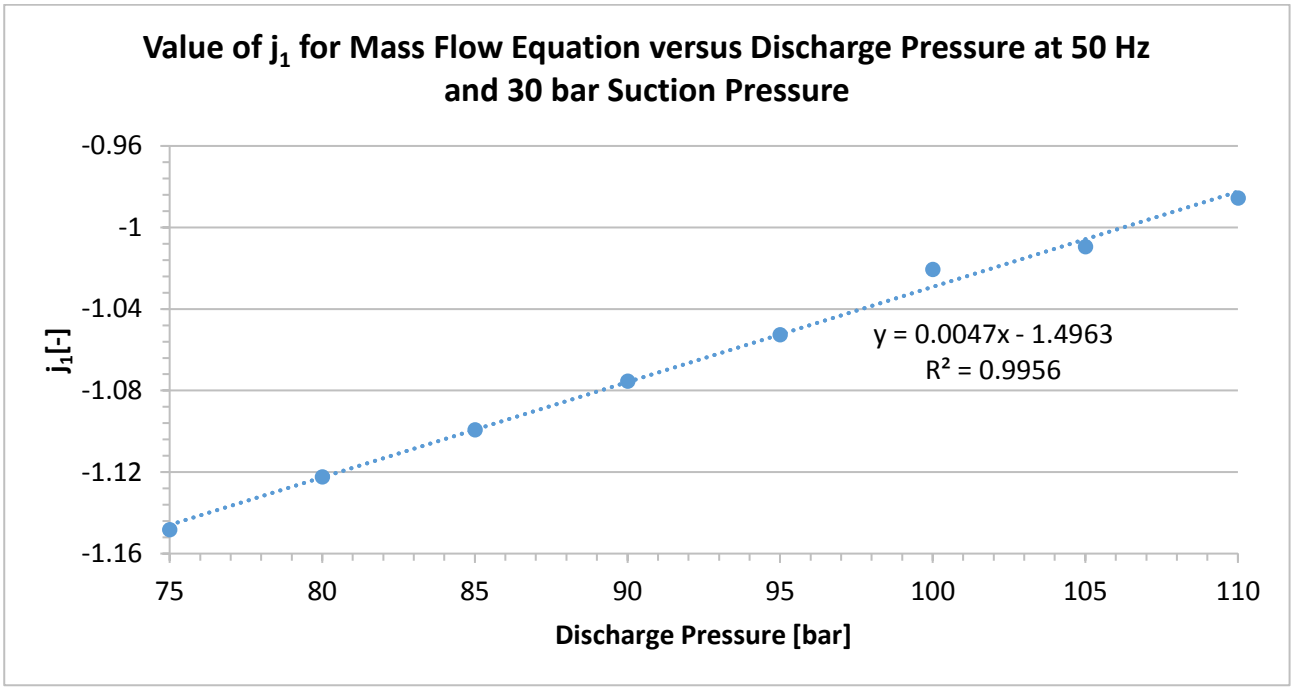

Figure 15: Plotting j_1 versus Discharge Pressure for $\dot{m}$ Equations (50 Hz and 30 bar Suction Pressure)

The objective of this step is evident in the plot above. Initially, the coefficients needed for the prediction equations are fixed. With the least-squares line, the coefficients become a function of the discharge pressure.

At the current moment, the equation in Figure 15 is in the form;

With $p = 1$;

$$j_1(x_1) = \sum_{m=0}^{p} k_m(x_2) P_{out}^m \tag{63}$$

The above mentioned process is repeated for other values of discharge pressure in the operational range. These equations are;

The linear correlation found for 30 bar suction pressure also holds for the other suction pressures for both the discharge temperature and mass flow variant, thus $p = 1$. These equations, for both the mass flow and discharge temperature variations, are then in the form;

With $p = 1$ and $i = 0{,}1$

$$j_i(x_1) = \sum_{m=0}^{p} k_m(x_2) P_{out}^m \tag{64}$$

The equations in (64) can then be combined with the respective equations for discharge temperature and mass flow, (46) and (47), to form;

With $p = 1$

$$T_{out} = \sum_{i=0}^{1} j_i(x_1) T_{in}^i$$

$$T_{out} = \sum_{i=0}^{1} \left(\sum_{m=0}^{p} k_m(x_2) P_{out}^m \right) T_{in}^i \tag{65}$$

$$\dot{m} = \sum_{i=0}^{n} j_i(x_1) T_{in}^i$$

$$\dot{m} = \sum_{i=0}^{1} \left(\sum_{m=0}^{p} k_m(x_2) P_{out}^m \right) T_{in}^i \tag{66}$$

Referring to Figure 10, after completing this step for the lowest suction pressure, the suction pressure is increased and the first and second correlation step is repeated. Note that this includes repeating the formulation of the equations for discharge temperature or mass flow versus suction temperature.

After reaching the maximum suction pressure, see Figure 10, the list of equations are evaluated. For a complete list of these equations, see Appendix D.

The completion of this step, and combining all of the equations in Appendix D, converts (49) to;

For $l = 20{,}40$ and with $p = 1$;

$$T_{out_j} = \sum_{i=0}^{1} \left(\sum_{m=0}^{p} k_{i,m}(x_2) P_{out}^m \right) T_{in}^i \tag{67}$$

$$\dot{m} = \sum_{i=0}^{1} \left(\sum_{m=0}^{p} k_{i,m}(x_2) P_{out}^m \right) T_{in}^i \tag{68}$$

Note that $l = 20{,}40$ since the suction pressure ranges from 20 to 40 bar. The denotation in the subscripts for $k(x_2)$ has changed to accommodate all equations coefficients in the outer summation equation.

In this section, for this specific compressor, it was noted that a polynomial of degree 1 delivers sufficiently accurate correlations. In other applications, this may not be the case. Thus, the equations in (67) and (68) are reported as discussed in Chapter 3.

To summarise the section above, equations are formulated, (67) and (68), that can be used to determine the discharge temperature and mass flow at varying suction pressures whilst the discharge pressure and suction temperature are known, constant values.

4.2.3 The Third Correlation

From Figure 10, the second correlation step stops when the maximum suction pressure has been reached. The third correlation step is to evaluate the coefficients from the range of equations formulated in the previous section.

The step objective is to establish a relationship between the coefficients in (67) and (68) and their associated suction pressure in equation form. The coefficient should thus become a function of the suction pressure.

Since both (67) and (68) have $p = 1$, the following statements can be made;

For $l = 20{,}40$

$$T_{out_l} = \sum_{i=0}^{1}\left(\sum_{m=0}^{1} k_{i,m}(x_2)P_{out}^{m}\right)T_{in}^{i} = \left(k_{1,1}(x_2)P_{out} + k_{1,0}(x_2)\right)T_{in} + \left(k_{0,1}(x_2)P_{out} + k_{0,0}(x_2)\right) \tag{69}$$

For $l = 20{,}40$

$$\dot{m}_l = \sum_{i=0}^{1}\left(\sum_{m=0}^{1} k_{m}(x_2)P_{out}^{m}\right)T_{in}^{i} = \left(k_{1,1}(x_2)P_{out} + k_{1,0}(x_2)\right)T_{in} + \left(k_{0,1}(x_2)P_{out} + k_{0,0}(x_2)\right) \tag{70}$$

Take note of the coefficient denotations declared above and the “branching out” in the headers in the table to follow;

Table IV: Sample of Data for Plotting Coefficients vs Suction Pressure

	Discharge Temperature Eq.					Mass Flow Eq.				
		$l_1(x_1)$		$l_0(x_1)$			$l_1(x_1)$		$l_0(x_1)$	
P_{in}[*bar*]	l	$k_{1,1}$	$k_{1,0}$	$k_{0,1}$	$k_{0,0}$	l	$k_{1,1}$	$k_{1,0}$	$k_{0,1}$	$k_{0.0}$
20	20	0.010	0.726	1.685	10.715	20	−0.002	−0.342	−0.498	117.665
25	25	0.007	0.831	1.370	3.314	25	−0.0007	−0.629	−0.521	155.382
30	30	0.006	0.922	1.225	−8.252	30	0.005	−1.496	−0.639	206.450
35	35	0.006	0.897	1.110	−16.801	35	0.006	−2.106	−0.746	262.863
40	40	0.006	0.869	1.015	−23.596	40	0.007	−2.713	−0.860	326.872

The table shows the coefficient values from (69) and (70) applicable to an operating frequency of 50 Hz. The full set of equations is given in Appendix D.

As mentioned, the objective of this step is to find a relationship between the suction pressure and the coefficient values above. To do this, the coefficient values will first be evaluated to decide upon the method of correlation.

There are changes present in every coefficient of all equations as the suction pressure varies, thus rendering the constant value method inefficient. The differences in specific coefficient values are also not negligible, thus removing the averages method as an option. The least squares method is applied again.

The $k_{1,1}$ -coefficient for the discharge temperature variant versus the discharge pressure is shown below. The correlation coefficient shows an accurate result for the polynomial function of the 2nd order. Plots similar to the one below are made for all of the coefficients given in the table above.

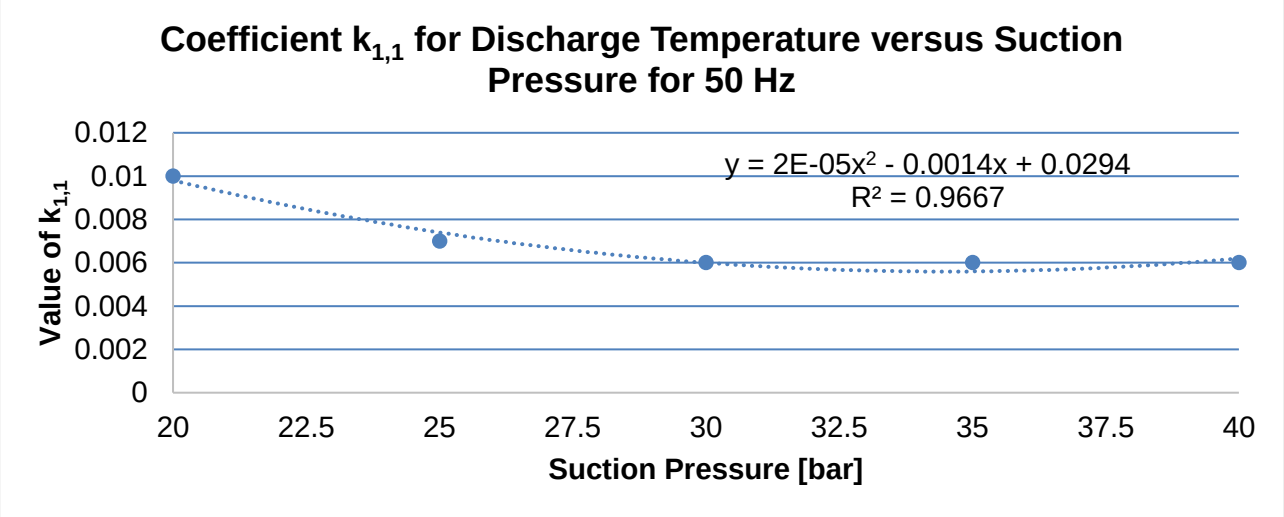

Figure 16: Plotting Coefficient $k_{1,1}$ for Discharge Temperature versus Suction Pressure

The plot above shows that the objective has been reached where a relationship has been established. The coefficients, referenced by fixed values per suction pressure before this step, is now described as a function thereof.

It is important to note at this stage that not all the functions resulting from this step is of the 2nd polynomial order, as shown below. In this case the functions will still be regarded as 2nd order polynomials, only with the n-th coefficient equal to zero.

Similar tables for 40 and 60 Hz are declared in Appendix E. Equations (69) and (70) are recalled to enable proper reference of the table below. The equation formulated in the Figure 16 is shown in bold to illustrate that all of the equation in the table below are generated in the same iterative process.

$$T_{out} = (k_{1,1}P_{out} + k_{1,0})T_{in} + (k_{0,1}P_{out} + k_{0,0})$$

$$\dot{m} = (k_{1,1}P_{out} + k_{1,0})T_{in} + (k_{0,1}P_{out} + k_{0,0})$$

Table V: Resulting Equations for 50 Hz after the Third Correlation Step

Equation	Coefficient	Equation
Discharge Temperature Equation	$k_{1,1}$	$= (\mathbf{2e^{-5} \cdot P_{in}^2}) + (\mathbf{-0,00138 \cdot P_{in}}) + \mathbf{0,0294}$
	$k_{1,0}$	$= (-0{,}001097 \cdot P_{in}^2) + (0{,}072909 \cdot P_{in}) - 0{,}296171$
	$k_{0,1}$	$= (0{,}001337 \cdot P_{in}^2) + (-0{,}112229 \cdot P_{in}) + 3{,}377771$
	$k_{0,0}$	$= (-1{,}7747 \cdot P_{in}) + 46{,}318$
Mass Flow Equation	$k_{1,1}$	$= (-0{,}000012 \cdot P_{in}^2) + (0{,}001243 \cdot P_{in}) - 0{,}02240$
	$k_{1,0}$	$= (-0{,}001095 \cdot P_{in}^2) + (-0{,}058631 \cdot P_{in}) + 1{,}341488$
	$k_{0,1}$	$= (-0{,}000490 \cdot P_{in}^2) + (0{,}0104 \cdot P_{in}) - 0{,}49964$
	$k_{0,0}$	$= (0{,}165505 \cdot P_{in}^2) + (0{,}587575 \cdot P_{in}) + 38{,}989$

At the current moment, the equations for both variants in the table above is in the form;

Thus, for $m = 0{,}1$ $i = 0{,}1$ and $s = 0{,}2$

$$k_{i,m}(x_2) = \sum_{t=0}^{s} r_t(Hz) P_{in}^t \tag{71}$$

With r_t a coefficient denotation as argued and declared in Chapter 3. By combining the equations in (71) with both (69) and (70), the following equation form is obtained;

With $s = 2$;

$$T_{out} = \sum_{i=0}^{1}\left(\sum_{m=0}^{1} k_{i,m}(x_2) P_{out}^m\right) T_{in}^i$$

$$T_{out} = \sum_{i=0}^{n}\left(\sum_{m=0}^{p}\left(\sum_{t=0}^{s} r_t(Hz) P_{in}^t\right) P_{out}^m\right) T_{in}^i \tag{72}$$

$$\dot{m} = \sum_{i=0}^{1}\left(\sum_{m=0}^{1} k_m(x_2) P_{out}^m\right) T_{in}^i$$

$$\dot{m} = \sum_{i=0}^{1}\left(\sum_{m=0}^{1}\left(\sum_{t=0}^{s} r_t(Hz) P_{in}^t\right) P_{out}^m\right) T_{in}^i \tag{73}$$

The process described above is repeated for other operating frequencies in the applicable range. The maximum polynomial order found is $n = 2$, and as already stated, all equations will be treated as such.

The equations for the other operating frequencies are all given in Appendix E. By combining all of the equations in Appendix E converts (72) and (73) to;

For $v = 40{,}60$

$$T_{out_v} = \sum_{i=0}^{1}\left(\sum_{m=0}^{1}\left(\sum_{t=0}^{2} r_{i,m,t}(Hz)P_{in}^{t}\right)P_{out}^{m}\right)T_{in}^{i} \tag{74}$$

$$\dot{m}_v = \sum_{i=0}^{1}\left(\sum_{m=0}^{1}\left(\sum_{t=0}^{2} r_{i,m,t}(Hz)P_{in}^{t}\right)P_{out}^{m}\right)T_{in}^{i} \tag{75}$$

Note that v ranges from 40 to 60 due to the frequency operating within these limits. The denotation in the subscripts for $r(Hz)$ has changed to accommodate all equations' coefficients in the outer equations generated in previous correlations.

For this specific compressor, it was noted that a polynomial of degree 2 delivers sufficiently accurate correlations, which may not be the case in other applications. Thus, the equations in (74) and (75) are reported as discussed in Chapter 3.

To summarise the section, equations are formulated that can be used to determine the discharge temperature and the mass flow at varying operating frequencies whilst the discharge pressure and suction pressure and temperature is known and constant.

4.2.4 The Fourth Correlation

From Figure 10, the third correlation step ends as soon as the maximum frequency has been reached. The fourth step is to use the coefficients of these equations to find a relationship between the operating frequency and the coefficient values.

The next, and final step, is to establish a relationship between the coefficients in (74) and (75) and their associated operating frequency. These coefficients can be viewed in Appendix E. The objective is thus to convert the coefficients from fixed values to a function of the operating frequency.

To ensure proper reference for the table below, (74) and (75) is recalled and expanded. The current, expanded equation for discharge temperature and mass flow are thus in the form;

For $v = 40{,}60$

$$\begin{aligned} T_{out_v} = {} & \Big(\big(r_{1,1,2}P_{in}^{2} + r_{1,1,1}P_{in} + r_{1,1,0}\big)P_{out} \\ & + \big(r_{1,0,2}P_{in}^{2} + r_{1,0,1}P_{in} + r_{1,0,0}\big)\Big)T_{in} \\ & + \big(r_{0,1,2}P_{in}^{2} + r_{0,1,1}P_{in} + r_{0,1,0}\big)P_{out} \\ & + \big(r_{0,0,2}P_{in}^{2} + r_{0,0,1}P_{in} + r_{0,0,0}\big) \end{aligned} \tag{76}$$

For $v = 40{,}60$

$$\dot{m}_v = \Big(\big(r_{1,1,2}P_{in}^2 + r_{1,1,1}P_{in} + r_{1,1,0}\big)P_{out} + \big(r_{1,0,2}P_{in}^2 + r_{1,0,1}P_{in} + r_{1,0,0}\big)\Big)T_{in} + \big(r_{0,1,2}P_{in}^2 + r_{0,1,1}P_{in} + r_{0,1,0}\big)P_{out} + \big(r_{0,0,2}P_{in}^2 + r_{0,0,1}P_{in} + r_{0,0,0}\big) \quad (77)$$

Take note of the coefficient denotations declared above, since some of these coefficients are displayed in the table to follow;

Table VI: Sample of Data for Plotting Coefficients vs Frequency

	Discharge Temperature Eq.				Mass Flow Eq.			
Hz	v	$r_{1,1,2}$	$\boldsymbol{r_{1,1,1}}$	$\boldsymbol{r_{1,1,0}}$	v	$r_{1,1,2}$	$\boldsymbol{r_{1,1,1}}$	$\boldsymbol{r_{1,1,0}}$
40	40	0.000018	-0.001248	0.027385	**40**	-0.000011	0.001020	-0.018311
50	50	0.00002	-0.00138	0.02940	**50**	-0.000012	0.00124	-0.02240
60	60	0.000017	-0.001213	0.026825	**60**	-0.000013	0.001411	-0.026130

After completing this table for the entire coefficient range given in (76) and (77), the final set of coefficients is established. The full list of values for each coefficient can be found in the equations in Appendix E.

The objective of this step is to establish a relationship between the frequency and the coefficient values in equation form. It is therefore necessary to evaluate the differences in coefficient values to determine a formulation method that will lead to both simplistic and accurate equations.

The difference between the coefficient values as the frequency changes are also evaluated according to the relevant coefficient position in the equation. By examining (76) and (77), a difference in coefficient value will have a larger impact on the result of an equation when the coefficient is, for example $r_{1,1,2}$ then for when it is $r_{0,0,0}$ since the coefficient is processed with the input variables according to it's position.

In simpler terms, the difference in coefficient values are more forgiving with regards to accuracy when the coefficient has less input variables to be multiplied with during the use of the prediction equation. The coefficients in this correlation can therefor range from sensitive to tolerant for variations. Each coefficient is thus evaluated individually.

The desired method differed from one coefficient to another. For each coefficients' formulation method and result, see Appendix F for both the discharge temperature and mass flow equation.

The $r_{1,0,1}$-coefficient for the mass flow equation versus the operating frequency is displayed below as an example. The correlation coefficient shows an accurate result for the polynomial function when $n = 1$. Plots similar to the one below is made for all of the coefficients given in (76) and (77).

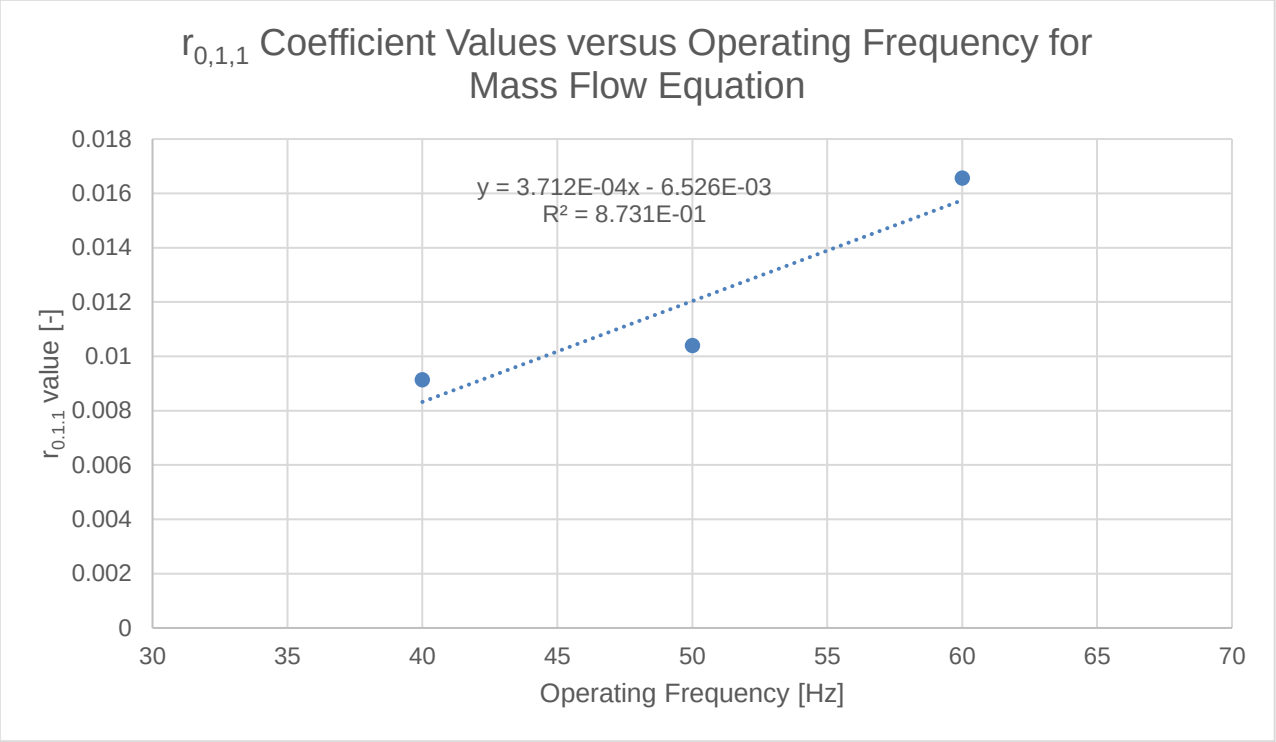

Figure 17: $r_{1,1,0}$ Coefficient values versus Operating Frequency for Mass Flow Equation

The plot above and the other formulated correlations indicates that the objective to formulate a function has been reached. The coefficients declared in (76) and (77), which were fixed values per operating frequency before this step, is now described as a function of the operating frequency.

It is important to note at this stage that a polynomial of degree two formulated for only three points will always deliver a fitted line with a coefficient of determination of one. This can lead to a false sense of accuracy, which is discussed in the chapter to follow. This false sense of accuracy can be avoided by decreasing the polynomial degree to one or even finding an average. This can also be avoided by increasing the number of points for which the curve is plotted.

None of these were needed since a straight line or average mostly delivered satisfying accuracies. Thus, the equations in (77) and (78) are now;

$$T_{Out} = \left(\left(r_{1,1,2}P_{in}^2 + r_{1,1,1}P_{in} + r_{1,1,0}\right)P_{out} + \left(r_{1,0,2}P_{in}^2 + r_{1,0,1}P_{in} + r_{1,0,0}\right)\right)T_{in} + \left(r_{0,1,2}P_{in}^2 + r_{0,1,1}P_{in} + r_{0,1,0}\right)P_{out} + \left(r_{0,0,2}P_{in}^2 + r_{0,0,1}P_{in} + r_{0,0,0}\right) \quad (78)$$

$$\dot{m} = \left(\left(r_{1,1,2}P_{in}^2 + r_{1,1,1}P_{in} + r_{1,1,0}\right)P_{out} + \left(r_{1,0,2}P_{in}^2 + r_{1,0,1}P_{in} + r_{1,0,0}\right)\right)T_{in} + \left(r_{0,1,2}P_{in}^2 + r_{0,1,1}P_{in} + r_{0,1,0}\right)P_{out} + \left(r_{0,0,2}P_{in}^2 + r_{0,0,1}P_{in} + r_{0,0,0}\right) \quad (79)$$

Since the operating frequency is now embedded into the equations. The table to follow deliver the equations for their appropriate coefficient denotation according to (78) and (79).

Table VII: Final Coefficient Equations for Discharge Temperature and Mass Flow Equations

Discharge Temperature Eq.		Mass Flow Eq.	
$r_{i,m,t}$	Equation/Formulation	$r_{i,m,t}$	Equation/Formulation
$r_{1,1,2}$=	1.83333e-5	$r_{1,1,2}$=	$-1e^{-7} \cdot Hz - 7e^{-6}$
$r_{1,1,1}$=	-0.00128	$r_{1,1,1}$=	$+1{,}955e^{-5} \cdot Hz + 2{,}472e^{-4}$
$r_{1,1,0}$=	0.02787	$r_{1,1,0}$=	$-3{,}91e^{-4} \cdot Hz - 2{,}733e^{-3}$
$r_{10,2}$=	-0.00104	$r_{10,2}$=	$-3{,}76e^{-5} \cdot Hz + 7{,}27e^{-4}$
$r_{1,0,1}$=	0.06739	$r_{1,0,1}$=	$-5{,}681e^{-4} \cdot Hz - 2.723e^{-2}$
$r_{1,0,0}$=	-0.17092	$r_{1,0,0}$=	$+2{,}015e^{-2} \cdot Hz + 3{,}037e^{-}1$
$r_{0,1,2}$=	0.00121	$r_{0,1,2}$=	$-1{,}35e^{-5} \cdot Hz + 1{,}583e^{-4}$
$r_{0,1,1}$=	-0.10292	$r_{0,1,1}$=	$-3.712e^{-4} \cdot Hz - 6.526e^{-3}$
$r_{0,1,0}$=	3.19947	$r_{0,1,0}$=	$-1{,}306e^{-2} \cdot Hz + 1{,}303e^{-1}$
$r_{0,0,2}$=	0	$r_{0,0,2}$=	$+3{,}954e^{-3} \cdot Hz - 2{,}954e^{-2}$
$r_{0,0,1}$=	-1.91663	$r_{0,0,1}$=	0.43268
$r_{0,0,0}$=	52.09667	$r_{0,0,0}$=	$+1.0523 \cdot Hz - 11.461$

The above table and equation was the coefficient and resulting equations for the discharge temperature equation. The mass flow variant's coefficient and resulting equations are given below.

The equations in the table above in combination with (78) and (79) are compiled and in the form;

$v = 0{,}1$

$$T_{out} = \sum_{i=0}^{n}\left(\sum_{m=0}^{p}\left(\sum_{t=0}^{s}\left(\sum_{w=0}^{v} a_{w,t,m,i} Hz^{w}\right) P_{in}^{t}\right) P_{out}^{m}\right) T_{in}^{i} \tag{80}$$

$$\dot{m} = \sum_{i=0}^{n}\left(\sum_{m=0}^{p}\left(\sum_{t=0}^{s}\left(\sum_{w=0}^{v} a_{w,t,m,i} Hz^{w}\right) P_{in}^{t}\right) P_{out}^{m}\right) T_{in}^{i} \tag{81}$$

With the coefficients $a_{w,t,m,i}$ being fixed value coefficients that are not determined by a function in this study.

The compiled equation form depicted in (80) and (81) are similar to (58) which was discussed in Chapter 3 as the desired end equation form when the methodology is followed.

To summarise the last section, the equations formulated can be used to determine the discharge temperature and mass flow whilst the operating frequency, suction and discharge pressure and suction temperature is known.

These equations can therefore be used to predict any of the six variables if the other four are known and within the operating range applicable to this study. The accuracy of these equations are yet to be verified through comparison with experimental data.

5. Results and Verification

The method followed to produce two different prediction equations for this specific compressor are illustrated in the previous chapter. The functions were created by isolating two variables and finding their internal relationship in equation form via the use of the least-squares method. These equations are in turn compiled to form the resulting equations with five variables in each.

The final equations, (79) and (80) are recalled for reference purposes;

$$T_{Out} = \left(\left(r_{1,1,2}P_{in}^2 + r_{1,1,1}P_{in} + r_{1,1,0}\right)P_{out} + \left(r_{1,0,2}P_{in}^2 + r_{1,0,1}P_{in} + r_{1,0,0}\right)\right)T_{in} + \left(r_{0,1,2}P_{in}^2 + r_{0,1,1}P_{in} + r_{0,1,0}\right)P_{out} + \left(r_{0,0,2}P_{in}^2 + r_{0,0,1}P_{in} + r_{0,0,0}\right) \quad (78)$$

$$\dot{m} = \left(\left(r_{1,1,2}P_{in}^2 + r_{1,1,1}P_{in} + r_{1,1,0}\right)P_{out} + \left(r_{1,0,2}P_{in}^2 + r_{1,0,1}P_{in} + r_{1,0,0}\right)\right)T_{in} + \left(r_{0,1,2}P_{in}^2 + r_{0,1,1}P_{in} + r_{0,1,0}\right)P_{out} + \left(r_{0,0,2}P_{in}^2 + r_{0,0,1}P_{in} + r_{0,0,0}\right) \quad (79)$$

The coefficient values and equations, where necessary, are given in Table VII: Final Coefficient Equations for Discharge Temperature and Mass Flow Equations. Thus far, the internal equations' accuracy was evaluated purely from their coefficient of determination. As discussed in 3.3.1 The Concept of Regression the coefficient of determination is an indication of how well the fitted curve fits the observed data. However, this does not deem the final, compiled equations accurate to the same degree.

To evaluate the final accuracy of the equations, a test method is followed that will compare the final equations' predicted answers to the experimental data.

5.1 Testing Method

A fixed, universal testing method is required to evaluate the prediction equations created. The testing and validation method will ensure that the function accuracies are not only repeatable when applied to this study but also when the methodology is in use during other studies.

A factor to keep in mind at this stage is that the methodology has the capability to use least-squares regression methods, averages or constant values. Each of these decisions have direct implications on the accuracy and simplicity of the function. If the evaluation indicates an inaccurate equation, the formulation can be changed by incorporating the more complex but also more accurate method.

This can be done by changing an average value to the more complex polynomial of degree one, or by increasing the degree of the applied polynomial. The accuracy of the equation can thus be improved by re-evaluating the decisions made during the formulation.

The testing method should ensure that the conclusions and results from the methodology is both accurate and reliable.

Thus, the testing method may not include any test data used in the mathematical formulation methodology. The test data should therefore constitute of randomly generated values, all within the operational limits of the compressor for which the methodology was applied. The number of randomised values and thus tests must ensure that the outcome of the evaluation is reliable.

A set of 30 tests to evaluate the prediction equations are deemed sufficient. Thus, the entire process of generating 30 randomised test sets are summarised below;

- Generate 30 random integers between $0 - 20$. These values will be used as the suction temperature, since $0 - 20\,°C$ is the expected operational range of the compressor, as mentioned in Chapter 3.
- Generate 30 random integers between $75 - 110$, excluding multiples of 5. These values will be used as the discharge pressure and the exclusions are due to the data used in the study being multiples of 5. The limited range is again due to operational limits as noted at the start of Chapter 4.
- Generate 30 random integers between $20 - 40$, again excluding multiples of 5. These values are to be used as the suction pressure and the exclusions are due to the formulation data consisting of values that are multiples of 5. The limitations are due to operational limits as noted in the previous chapter.
- Generate 30 random integers between $40 - 60$, this time excluding multiples of 10. These values will be used as the operational frequency values and the exclusions are due to the data used in the formulation of the equations consisting of values that are multiples of 10. The limitations are again due to operational ranges as stated in the previous chapter.
- Predict the discharge temperature and mass flow for each of these 30 sets with the use of the formulated equations. Use the same test variables to obtain actual experimental data. Compare the values for predicted and experimental, determining an error value as well as an average error and an absolute average error over the 30 test sets.

The only operational limit not addressed for the evaluation is the safe operating range for the discharge temperature. This problem will be addressed and corrected at a later stage, during testing since it is unknown at this stage whether or not the limit has been exceeded.

5.2 Verification Results

The testing method in the previous section delivered 30 random integers for four variables. By bringing these four variables together in random order, 30 independent test parameters are established. The compiled values generate a table similar to the one below.

Table VIII: Extraction of Randomised Values for Test and Evaluation

# Test	Suction Temperature $[°C]$	Discharge Pressure $[bar]$	Suction Pressure $[bar]$	Frequency $[Hz]$
1	10	87	39	41
2	7	76	36	59
⋮	⋮	⋮	⋮	⋮
29	8	101	26	52
30	10	107	39	58

Using (79), determine the predicted discharge temperature for all 30 of these tests. It may occur that the maximum allowable discharge temperature is exceeded.

This generally occurs when a relatively small suction pressure is inserted into the same test as a relatively high discharge pressure, also known as a test with a large pressure ratio. In this case, one or more of the input values can be altered until the discharge temperature is within the allowable range.

When all 30 of the tests are considered fully in-range and valid, (80) can be used to determine the predicted mass flow rate accordingly.

An extract of the prediction results are shown below, for the full test and validation table refer to Appendix F.

Table IX: Extract from Full Test and Evaluation Table

# Test	$T_{in}[°C]$	$P_{out}[bar]$	$P_{in}[bar]$	Frequency $[Hz]$	**Predicted $T_{out}[°C]$**	**Predicted $\dot{m}[\frac{g}{s}]$**
1	10	87	39	41	**81.0**	**175.93**
2	7	76	36	59	**73.5**	**246.62**
⋮	⋮	⋮	⋮	⋮	⋮	⋮
29	8	101	26	52	**150.7**	**108.14**
30	10	107	39	58	**102.8**	**242.92**

The values in the completed table for suction temperature, suction and discharge pressure and frequency is then in turn used to determine the experimental values. After obtaining all of the

experimental discharge temperature and mass flow values, the values are then compared as shown in the two figures to follow.

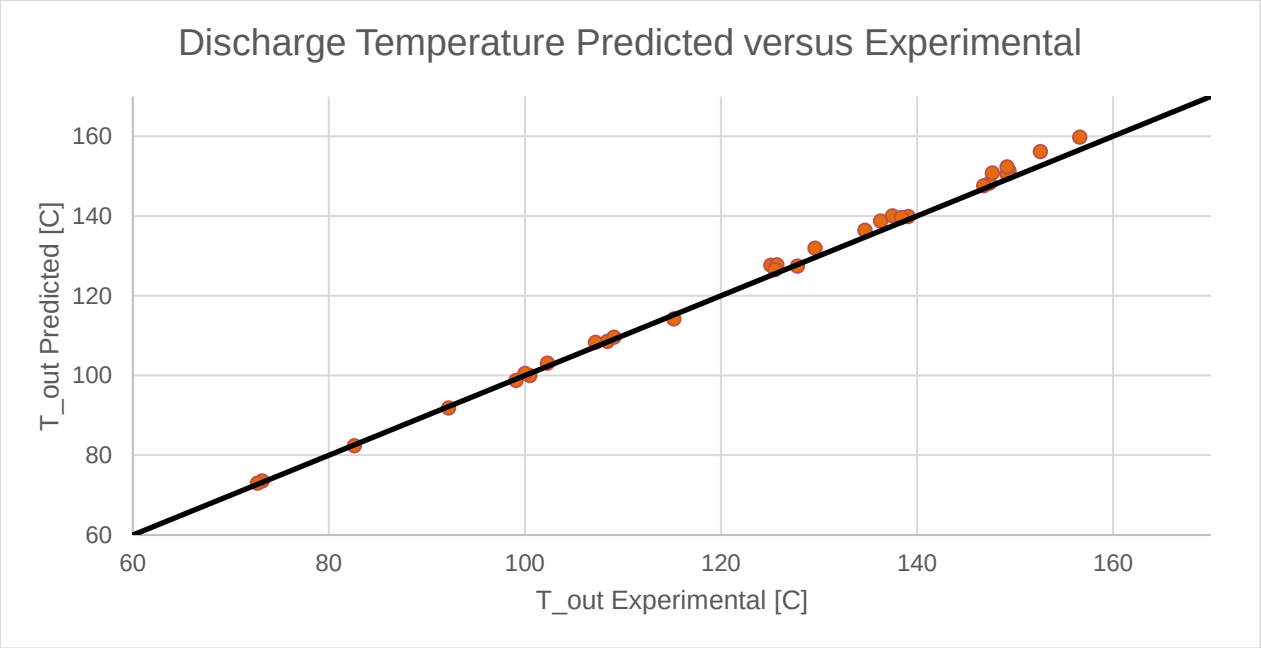

Figure 18: Discharge Temperature Predicted versus Experimental

In the plot above and below, the $x = y$ line shows the 100% accuracy line, since the predicted value will be equal to the experimental value when a 100% accuracy is achieved. Due to the large range in which the tests are set, the small inaccuracies may not be noted.

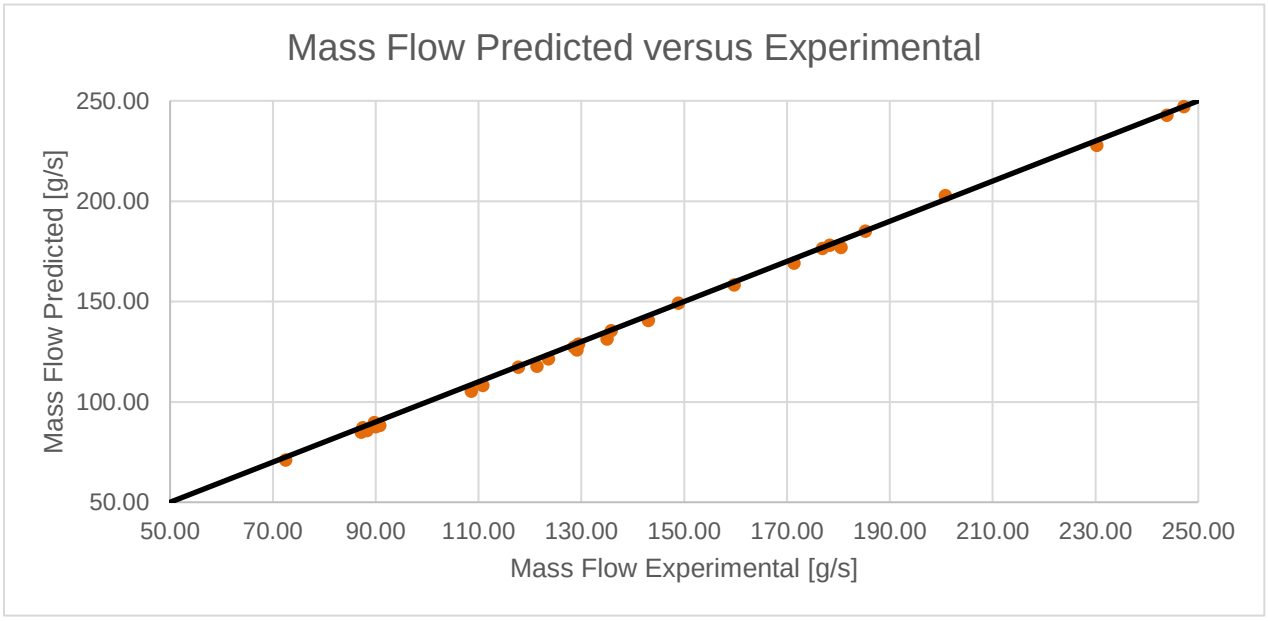

Figure 19: Mass Flow Predicted versus Experimental

The plots each show the predicted parameters versus the experimental parameter with the same input variable values. The errors are determined and tabulated. The table below is an extract from the table also given in Appendix F.

Table X: Extract from Comparison Table

# Test	Predicted $T_{out}[°C]$	Predicted $\dot{m}[\frac{g}{s}]$	Experimental $T_{out}[°C]$	Experimental $\dot{m}[\frac{g}{s}]$	Error $T_{out}[°C]$	Error $\dot{m}[\frac{g}{s}]$
1	81.0	175.93	82.6	176.94	-1.98%	0.57%
2	73.5	246.62	73.2	247.22	0.47%	0.24%
⋮	⋮	⋮	⋮	⋮	⋮	⋮
7	132,7	122,78	129,6	123,61	2,39%	0,68%
⋮	⋮	⋮	⋮	⋮	⋮	⋮
26	114,3	180,39	115,2	178,33	-0,75%	-1,15%
⋮	⋮	⋮	⋮	⋮	⋮	⋮
29	150.7	108.14	147.7	108.61	2.03%	0.43%
30	102.8	242.92	102.3	243.89	0.47%	0.40%
				Average	0.43%	0.06%
				Absolute Value Average	0.99%	0.43%
				Max	2.39%	-1.17%

The three accuracy indicators all evaluate the predicted equations, each with a different approach.

The average value delivers an indication of the accuracy over a large sample group. The tendency of some points to be over-predicted and some to be under-predicted normally in all practicality delivers a wider range of inaccuracies then expected when the absolute average value is evaluated. By evaluating the average values, the tendency of the equations to under- or over-predict over a large sample group can be identified.

The absolute value average delivers an indication of the overall accuracy. To determine this value, the absolute value from the errors are taken and averaged. The absolute error value would normally indicate the magnitude of inaccuracy, without considering the over- or under-prediction tendency.

The maximum value shows the most inaccurate value obtained throughout the tests. In a relatively large sample group this can indicate the limit of expected inaccuracy. In simpler terms, the equations will never predict a value with an error surpassing this indicator value.

5.3 Accuracy Evaluations

Before summarising the error values in the above table, another set of evaluations need to be done. As mentioned in 4.2.4 The Fourth Correlation formulating a polynomial of the 2nd degree for only 3 points can deliver a false sense of accuracy.

By means of experimental data, the false sense of accuracy is evaluated by using the mass flow prediction equation, only with 2nd order polynomials for certain coefficients. The mass flow equation is thus recalled for proper reference purposes and an updated table with the coefficient values and equations follow;

$$\dot{m} = \left(\left(r_{1,1,2}P_{in}^2 + r_{1,1,1}P_{in} + r_{1,1,0}\right)P_{out} + \left(r_{1,0,2}P_{in}^2 + r_{1,0,1}P_{in} + r_{1,0,0}\right)\right)T_{in} + \left(r_{0,1,2}P_{in}^2 + r_{0,1,1}P_{in} + r_{0,1,0}\right)P_{out} + \left(r_{0,0,2}P_{in}^2 + r_{0,0,1}P_{in} + r_{0,0,0}\right) \quad (79)$$

Table XI: Modified Mass Flow Equation

Mass Flow Eq.		
$r_{i,m,t}$	Equation/Formulation	Changed?
$r_{1,1,2}$=	$-1e^{-7} \cdot Hz - 7e^{-6}$	No
$r_{1,1,1}$=	$+1{,}955e^{-5} \cdot Hz + 2{,}472e^{-4}$	No
$r_{1,1,0}$=	$-3{,}91e^{-4} \cdot Hz - 2{,}733e^{-3}$	No
$r_{10,2}$=	$-3{,}76e^{-5} \cdot Hz + 7{,}27e^{-4}$	No
$r_{1,0,1}$=	$4{,}495e^{-5} \cdot Hz^2 - 5{,}064e^{-3} \cdot Hz + 8{,}216e^{-2}$	Yes – From $n = 1$
$r_{1,0,0}$=	$+2{,}015e^{-2} \cdot Hz + 3{,}037e^{-1}$	No
$r_{0,1,2}$=	$-1{,}35e^{-5} \cdot Hz + 1{,}583e^{-4}$	No
$r_{0,1,1}$=	$2{,}451e^{-5} \cdot Hz^2 - 2{,}08e^{-3} \cdot Hz + 5{,}312e^{-2}$	Yes – From $n = 1$
$r_{0,1,0}$=	$-1{,}306e^{-2} \cdot Hz + 1{,}303e^{-1}$	No
$r_{0,0,2}$=	$+3{,}954e^{-3} \cdot Hz - 2{,}954e^{-2}$	No
$r_{0,0,1}$=	$-2{,}323e^{-3} \cdot Hz^2 + 2{,}325e^{-1} \cdot Hz - 5{,}227$	Yes – From average
$r_{0,0,0}$=	$3{,}2503e^{-2} \cdot Hz^2 - 2{,}198 \cdot Hz + 67{,}63$	Yes – From $n = 1$

Only four equations are substituted with more complex, supposedly more accurate equations when only the coefficient of determination evaluated. This variant of the mass flow equation, noted as the modified mass flow equation in the table below, is then used to again predict the values which is compared to the experimental values. This table with the accuracies are shown below;

Table XII: Modified Mass Flow Equation Results

	Original Mass Flow Eq.			Modified Mass Flow Eq.	
# Test	**Predicted** $\dot{m}[\frac{g}{s}]$	**Error** $\dot{m}[\frac{g}{s}]$	**Experimental** $\dot{m}[\frac{g}{s}]$	**Error** $\dot{m}[\frac{g}{s}]$	**Predicted** $\dot{m}[\frac{g}{s}]$
1	175.93	0.57%	176.94	-0.22%	176.56
2	246.62	0.24%	247.22	-0.03%	247.14
⋮	⋮	⋮	⋮	⋮	⋮
29	108.14	0.43%	108.61	-3.03%	105.33
30	242.92	0.40%	243.89	-0.42%	242.88
		0.06%	Average	-1.28%	
		0.43%	Absolute Value Average	1.36%	
		-1.15%	Max	-3.03%	

The above table and resulting error averages indicate that the more complex equation did not result in a more accurate prediction. By changing a mere four equations of twelve, the average error was increased by more than 1% with an almost 2% deviation for the maximum error values. These values may be exaggerated by changing more of the equations or even changing other equations. .

This section aimed to evaluate the capability of the methodology to be versatile in its application, enabling the compressor to be characterised with equations both simple and accurate.

5.4 Results Summary

Firstly, the methodology showed versatility with its ability to adapt to experimental data. The decisions made whilst formulating the equation have an influence on both the complexity of the equations as well as the accuracy. As discussed in the section above, it can be proved that the errors obtained can differ, depending on the formulation choice made during each correlation phase.

As discussed earlier, these accuracies are between the experimental and predicted values. Comparison between the actual mass flows and discharge temperature will contribute around 3% and 5% inaccuracy respectively.

From the actual comparison table and the preceding plots, it can be observed that the discharge temperature equation tends to predict values that are on average 0.43% above the actual values. The absolute error average of 0.99% shows a low measure of inaccuracy.

The mass flow equation tends to predict 0.06 % on average above the actual value. The absolute error value of 0.43% is combined with the plain average to state that over a large sample group, the mass flow prediction equation will be the more accurate equation since the tendency of over- and under-predicted value are minimal.

The maximum error values obtained show sufficient accuracy and stability of the predictions in all cases.

It should be noted that these accuracies are measured against the experimental data validated in the previous chapter. Comparison to test bench data will add the inaccuracy between the test bench data and the experimental data used.

Since the equations have now been evaluated, certain conclusions can be made with regards to the methodology’s applicability and versatility, as well as the resulting equations for this specific compressor as mentioned in earlier chapters.

6. Conclusion and Recommendations

This study succeeded in formulating a simplistic numerical methodology that can be followed in order to determine a multi-hertz, reciprocating compressors' operating parameters both accurately and universally.

6.1 Methodology Conclusion

Other methodologies and approaches were studied, after which they were evaluated on their applicability to other compressors, their complexity and accuracy. It was found that the magnitude of analytical models are too complex with too much assumptions or unknowns to use for the characterisation of this specific compressor.

The governing equations for thermodynamics and physics was discussed and applied to the components within a vapour compression cycle. Thermodynamic properties were identified from these laws and their accompanying equations that have an influence, no matter how big or small, on the performance of a compressor. A total of six variables were identified; the discharge and suction pressures, the discharge and suction temperatures, the mass flow and the operating frequency.

A completely new, numerically based, methodology was created from following the above mentioned approach and displayed through the means of a logic diagram, Figure 10. The formulation of the equations inside the methodology was mathematically argued largely with the use of the least-squares method but other statistical methods were also evaluated that may simplify the resulting equations without sacrificing accuracy. The methodology uses the identified variables for each of its' iterative internal formulation processes and ensures that every variables' influence to the resulting prediction is evaluated and embedded.

The six parameters mentioned are the operating frequency, mass flow rate, inlet, as well as the outlet temperatures and pressures. The methodology was applied twice, thus two equations were numerically derived and used to determine any two of the mentioned parameters if the other four are known.

A carbon dioxide multi-hertz reciprocating compressor was used to demonstrate the formulated methodology. A set of operational ranges was chosen from where the methodology demonstrated how numerical equations can be determined from experimental results. From these ranges and the logic diagram for the characterisation methodology, the experimental data was obtained.

Within this methodology, certain choices are made to the processing of the data that affect not only the simplicity and accuracy but also the applicability to other compressors. One of these choices are which statistical method to use with the formulating of equations. An example of where an average value instead of the least-squares method result in similar accuracy but increased simplicity is shown in the fourth correlation.

This illustrates the methodology's ability to adapt to variables with differing influences to the workings of a compressor. When a negligibly small influence is found, the average value is used to remove complexity but still consider the small influence. If it were to happen that, a constant value is identified then, with the use of the constant value, the variable is simply removed from the equations. This shows the ability of the methodology to evaluate a list of variables and ultimately only use the most critical variables when formulating equations.

In Chapter 5 and 4, it both mentioned and proven that a situation can occur where the more complex equation also delivers a more inaccurate result. As mentioned in the above paragraph, one of the abilities the methodology possesses is to adapt to experimental data with the use of method choices. Through re-evaluation and iteration, the final characterisation equations can be refined until an equation with sufficient accuracy is obtained.

The two working equations derived from the process were tested against 30 independent, experimental values.

6.2 Equation and Specific Compressor Conclusion

The average value determined in the fourth correlation for discharge temperature indicates that the operating frequency does not have a significant influence on the discharge temperature for the applied operational range. It does however, influence the discharge temperature to a small degree. This influence can be further evaluated by generating an internal equation using the least-squares method instead of just using the average, as was the case in the mass flow variant. As mentioned, this will increase the complexity of the final equations.

The accuracy evaluations show that the use of the least-squares method is not required since the discharge temperature equation deliver predictions with sufficient accuracy. From the actual comparison table and the preceding plots it can be observed that the discharge temperature equation tends to predict values that are on average 0.43% above the experimental values. The absolute error average of 0.99% shows a low magnitude of inaccuracy.

As specifically mentioned in the previous chapter, the use of straight-line equations during the fourth correlation was more accurate than the polynomial of 2^{nd} degree. This is due to having only three points from which the correlation was made, which delivers a false sense of accuracy. This was discussed and illustrated.

The mass flow equation tends to predict 0.06 % on average above the experimental value. The absolute error value of 0.43% is combined with the plain average to state that over a large sample group, the mass flow prediction equation will be the more accurate equation since the tendency of over- and under-predicted value are minimal and will even out.

6.3 Recommendations

The influence of the internal formulation choice during each correlation can be identified by having a set decision on the formulation method or polynomial degree without considering the data plotted and the differences in between values or the coefficient of determination.

The above mentioned influence can then be evaluated by comparing the range of resulting equations and their predictions with one another and to a set of independent and valid experimental values.

When considering this specific compressor, the operational limits applied in this study is well within the safe operating limits for the compressor. The limits applied in this study can be increased by expanding the operating frequency to 30 – 70 Hz or by increase the discharge pressure beyond 110 Bar to 140 Bar.

The resolution of data sets within the ranges can also be increased by doing more tests and evaluations. For example, testing 45 and 55 Hz values eliminates the problem mentioned of correlating between three points with a polynomial of degree two. Increasing the resolution can also aid in making a decision between which formulation method to follow.

Finally, the methodology can also be applied to other reciprocating and even other types of compressors with fitted variable speed drives to evaluate the universal characteristic of the formulated methodology.

Appendices

Appendix A

A.1 Derivation of Least-Squares Equation

Denote the residual equation given in (2) with the error-term, ϵ, and find the sum for all values of x;

$$\epsilon = \sum(y_i - \hat{y}_i) \quad \text{(A.1)}$$

With y_i and $\hat{y}_i$ the actual and predicted value when $= x_i$. The square of this equation is taken since it renders the error value a positive. This is a fundamental principle of the least-squares method;

$$\epsilon^2 = \sum(y_i - \hat{y}_i)^2 \quad \text{(A.2)}$$

Let $$\hat{y}_i = bx_i + a \quad \text{(A.3)}$$

By combining A.2 and A.3 and expanding;

$$\epsilon^2 = \sum(y_i - \hat{y}_i)^2$$

$$\epsilon^2 = \sum(y_i - bx_i + a)^2$$

$$\epsilon^2 = \sum(b^2x_i^2 + 2bax_i - 2bx_iy_i + b^2 - 2ay_i + y_i^2) \quad \text{(A.4)}$$

The plot yielded at A.4 is a function of the fitted lines slope (b) and the intercept (a). As the best values are approached, the function reaches a minimum. The point where the first derivative is 0 and where the error as a function of the slope and intercept is at a minimum is desired;

$$\frac{d\epsilon^2}{db} = 0 ; \frac{d\epsilon^2}{da} = 0$$

$$\frac{d\epsilon^2}{db} = 2b\sum x_i^2 + 2a\sum x_i - 2\sum x_iy_i = 0 \quad \text{(A.5)}$$

$$\frac{d\epsilon^2}{da} = 2b\sum x_i + 2\sum a - 2\sum y_i = 0 \quad \text{(A.6)}$$

Solving for A.5 and A.6 and denoting $\sum a = na$ with n the number of data points observed;

$$b = \frac{\sum x_iy_i - a\sum x_i}{\sum x_i^2} \quad \text{(A.7)}$$

$$a = \frac{\sum y_i}{n} - b\frac{\sum x_i}{n} \quad \text{(A.8)}$$

If neither the slope nor intercept are known, use A.7 and A.8 to solve A.5;

$$0 = b\sum x_i^2 + \sum x_i(\frac{\sum y_i}{n} - b\frac{\sum x_i}{n}) - \sum x_iy_i$$

$$b\left(n\sum x_i^2 - \sum x_i\sum x_i\right) = n\sum x_iy_i - \sum x_i\sum y_i$$

$$b = \frac{n\sum x_iy_i - \sum x_i\sum y_i}{\left(n\sum x_i^2 - \sum x_i\sum x_i\right)} \quad \text{(A.10)}$$

Appendix B

Equations at 40 Hz for constant discharge and suction pressure

P_{out}	P_{in} = 20 *bar*	
75 *bar*	$T_{out} = 1.524 \cdot T_{in} + 138.852$	$\dot{m} = -0.378 \cdot T_{in} + 62.266$
80 *bar*	$T_{out} = 1.566 \cdot T_{in} + 147.166$	$\dot{m} = -0.385 \cdot T_{in} + 60.331$
85 *bar*	$T_{out} = 1.623 \cdot T_{in} + 155.315$	$\dot{m} = -0.395 \cdot T_{in} + 58.419$
90 *bar*	$T_{out} = 1.663 \cdot T_{in} + 163.202$	$\dot{m} = -0.403 \cdot T_{in} + 56.441$
95 *bar*	*N/A*	*N/A*
100 *bar*	*N/A*	*N/A*
105 *bar*	*N/A*	*N/A*
110 *bar*	*N/A*	*N/A*

Data above 90 *bar* discharge pressure deliver a temperature out value greater than 160 C, which is beyond the limits of this study.

P_{out}	P_{in} = 25 *bar*	
75 *bar*	$T_{out} = 1.421 \cdot T_{in} + 107.385$	$\dot{m} = -0.552 \cdot T_{in} + 90.503$
80 *bar*	$T_{out} = 1.449 \cdot T_{in} + 114.760$	$\dot{m} = -0.541 \cdot T_{in} + 88.308$
85 *bar*	$T_{out} = 1.477 \cdot T_{in} + 121.878$	$\dot{m} = -0.525 \cdot T_{in} + 86.052$
90 *bar*	$T_{out} = 1.495 \cdot T_{in} + 128.884$	$\dot{m} = -0.516 \cdot T_{in} + 83.965$
95 *bar*	$T_{out} = 1.538 \cdot T_{in} + 135.424$	$\dot{m} = -0.515 \cdot T_{in} + 81.945$
100 *bar*	$T_{out} = 1.591 \cdot T_{in}141.827$	$\dot{m} = -0.529 \cdot T_{in} + 80.064$
105 *bar*	$T_{out} = 1.632 \cdot T_{in} + 148.200$	$\dot{m} = -0.542 \cdot T_{in} + 78.218$
110 *bar*	$T_{out} = 1.700 \cdot T_{in} + 154.400$	$\dot{m} = -0.579 \cdot T_{in} + 76.412$

P_{out}	P_{in} = 30 *bar*	
75 *bar*	$T_{out} = 1.392 \cdot T_{in} + 84.732$	$\dot{m} = -0.891 \cdot T_{in} + 123.206$
80 *bar*	$T_{out} = 1.422 \cdot T_{in} + 91.432$	$\dot{m} = -0.871 \cdot T_{in} + 120.551$
85 *bar*	$T_{out} = 1.451 \cdot T_{in} + 97.883$	$\dot{m} = -0.847 \cdot T_{in} + 117.879$
90 *bar*	$T_{out} = 1.479 \cdot T_{in} + 104.135$	$\dot{m} = -0.832 \cdot T_{in} + 115.343$
95 *bar*	$T_{out} = 1.502 \cdot T_{in} + 110.219$	$\dot{m} = -0.816 \cdot T_{in} + 112.932$
100 *bar*	$T_{out} = 1.535 \cdot T_{in} + 116.138$	$\dot{m} = -0.797 \cdot T_{in} + 110.532$
105 *bar*	$T_{out} = 1.565 \cdot T_{in} + 121.857$	$\dot{m} = -0.780 \cdot T_{in} + 108.183$
110 *bar*	$T_{out} = 1.595 \cdot T_{in} + 127.500$	$\dot{m} = -0.766 \cdot T_{in} + 105.916$

P_{out}	P_{in} = 35 *bar*	
75 *bar*	$T_{out} = 1.366 \cdot T_{in} + 67.008$	$\dot{m} = -1.290 \cdot T_{in} + 160.821$
80 *bar*	$T_{out} = 1.391 \cdot T_{in} + 73.229$	$\dot{m} = -1.262 \cdot T_{in} + 157.646$
85 *bar*	$T_{out} = 1.421 \cdot T_{in} + 79.144$	$\dot{m} = -1.229 \cdot T_{in} + 154.498$
90 *bar*	$T_{out} = 1.450 \cdot T_{in} + 84.843$	$\dot{m} = -1.203 \cdot T_{in} + 151.551$
95 *bar*	$T_{out} = 1.483 \cdot T_{in} + 90.354$	$\dot{m} = -1.194 \cdot T_{in} + 148.824$
100 *bar*	$T_{out} = 1.513 \cdot T_{in} + 95.720$	$\dot{m} = -1.164 \cdot T_{in} + 145.869$
105 *bar*	$T_{out} = 1.539 \cdot T_{in} + 100.994$	$\dot{m} = -1.146 \cdot T_{in} + 143.211$
110 *bar*	$T_{out} = 1.570 \cdot T_{in} + 106.065$	$\dot{m} = -1.129 \cdot T_{in} + 140.540$

P_{out}	P_{in} = 40 *bar*	
75 *bar*	$T_{out} = 1.313 \cdot T_{in} + 52.908$	$\dot{m} = -1.701 \cdot T_{in} + 203.921$
80 *bar*	$T_{out} = 1.358 \cdot T_{in} + 58.379$	$\dot{m} = -1.672 \cdot T_{in} + 200.404$
85 *bar*	$T_{out} = 1.387 \cdot T_{in} + 63.865$	$\dot{m} = -1.630 \cdot T_{in} + 196.654$
90 *bar*	$T_{out} = 1.418 \cdot T_{in} + 69.092$	$\dot{m} = -1.610 \cdot T_{in} + 193.427$
95 *bar*	$T_{out} = 1.445 \cdot T_{in} + 74.223$	$\dot{m} = -1.584 \cdot T_{in} + 190.129$
100 *bar*	$T_{out} = 1.472 \cdot T_{in} + 79.168$	$\dot{m} = -1.552 \cdot T_{in} + 186.706$
105 *bar*	$T_{out} = 1.505 \cdot T_{in} + 83.883$	$\dot{m} = -1.530 \cdot T_{in} + 183.665$
110 *bar*	$T_{out} = 1.538 \cdot T_{in} + 88.465$	$\dot{m} = -1.513 \cdot T_{in} + 180.714$

Equations at 50 Hz for constant discharge and suction pressure

P_{out}	P_{in} = 20 *bar*	
75 *bar*	$T_{out} = 1.506 \cdot T_{in} + 136.989$	$\dot{m} = -0.486 \cdot T_{in} + 80.307$
80 *bar*	$T_{out} = 1.553 \cdot T_{in} + 145.591$	$\dot{m} = -0.500 \cdot T_{in} + 77.806$
85 *bar*	$T_{out} = 1.604 \cdot T_{in} + 153.987$	$\dot{m} = -0.513 \cdot T_{in} + 75.286$
90 *bar*	$T_{out} = 1.662 \cdot T_{in} + 162.270$	$\dot{m} = -0.514 \cdot T_{in} + 72.843$
95 *bar*	*N/A*	*N/A*
100 *bar*	*N/A*	*N/A*
105 *bar*	*N/A*	*N/A*
110 *bar*	*N/A*	*N/A*

Data above 90 *bar* discharge pressure deliver a temperature out value greater than 160 C, which is beyond the limits of this study.

P_{out}	P_{in} = 25 *bar*	
75 *bar*	$T_{out} = 1.400 \cdot T_{in} + 105.433$	$\dot{m} = -0.718 \cdot T_{in} + 116.765$
80 *bar*	$T_{out} = 1.428 \cdot T_{in} + 112.869$	$\dot{m} = -0.694 \cdot T_{in} + 113.757$
85 *bar*	$T_{out} = 1.459 \cdot T_{in} + 120.056$	$\dot{m} = -0.679 \cdot T_{in} + 110.956$
90 *bar*	$T_{out} = 1.488 \cdot T_{in} + 127.062$	$\dot{m} = -0.664 \cdot T_{in} + 108.202$
95 *bar*	$T_{out} = 1.529 \cdot T_{in} + 133.839$	$\dot{m} = -0.668 \cdot T_{in} + 105.670$
100 *bar*	$T_{out} = 1.573 \cdot T_{in} + 140.473$	$\dot{m} = -0.675 \cdot T_{in} + 103.150$
105 *bar*	$T_{out} = 1.612 \cdot T_{in} + 147.031$	$\dot{m} = -0.694 \cdot T_{in} + 100.772$
110 *bar*	$T_{out} = 1.660 \cdot T_{in} + 153.510$	$\dot{m} = -0.761 \cdot T_{in} + 98.509$

P_{out}	P_{in} = 30 *bar*	
75 *bar*	$T_{out} = 1.367 \cdot T_{in} + 83.092$	$\dot{m} = -1.148 \cdot T_{in} + 158.864$
80 *bar*	$T_{out} = 1.397 \cdot T_{in} + 89.748$	$\dot{m} = -1.122 \cdot T_{in} + 155.376$
85 *bar*	$T_{out} = 1.425 \cdot T_{in} + 96.221$	$\dot{m} = -1.099 \cdot T_{in} + 152.050$
90 *bar*	$T_{out} = 1.456 \cdot T_{in} + 102.467$	$\dot{m} = -1.075 \cdot T_{in} + 148.743$
95 *bar*	$T_{out} = 1.484 \cdot T_{in} + 108.572$	$\dot{m} = -1.053 \cdot T_{in} + 145.566$
100 *bar*	$T_{out} = 1.515 \cdot T_{in} + 114.514$	$\dot{m} = -1.021 \cdot T_{in} + 142.401$
105 *bar*	$T_{out} = 1.543 \cdot T_{in} + 120.339$	$\dot{m} = -1.009 \cdot T_{in} + 139.445$
110 *bar*	$T_{out} = 1.575 \cdot T_{in} + 126.073$	$\dot{m} = -0.986 \cdot T_{in} + 136.509$

P_{out}	P_{in} = 35 *bar*	
75 *bar*	$T_{out} = 1.339 \cdot T_{in} + 65.794$	$\dot{m} = -1.660 \cdot T_{in} + 207.262$
80 *bar*	$T_{out} = 1.365 \cdot T_{in} + 71.910$	$\dot{m} = -1.618 \cdot T_{in} + 203.109$
85 *bar*	$T_{out} = 1.395 \cdot T_{in} + 77.787$	$\dot{m} = -1.592 \cdot T_{in} + 199.273$
90 *bar*	$T_{out} = 1.423 \cdot T_{in} + 83.508$	$\dot{m} = -1.563 \cdot T_{in} + 195.474$
95 *bar*	$T_{out} = 1.450 \cdot T_{in} + 89.043$	$\dot{m} = -1.534 \cdot T_{in} + 191.735$
100 *bar*	$T_{out} = 1.483 \cdot T_{in} + 94.354$	$\dot{m} = -1.501 \cdot T_{in} + 188.050$
105 *bar*	$T_{out} = 1.511 \cdot T_{in} + 99.611$	$\dot{m} = -1.468 \cdot T_{in} + 184.476$
110 *bar*	$T_{out} = 1.545 \cdot T_{in} + 104.693$	$\dot{m} = -1.448 \cdot T_{in} + 181.126$

P_{out}	P_{in} = 40 *bar*	
75 *bar*	$T_{out} = 1.300 \cdot T_{in} + 51.893$	$\dot{m} = -2.178 \cdot T_{in} + 262.641$
80 *bar*	$T_{out} = 1.332 \cdot T_{in} + 57.475$	$\dot{m} = -2.150 \cdot T_{in} + 258.215$
85 *bar*	$T_{out} = 1.358 \cdot T_{in} + 62.912$	$\dot{m} = -2.109 \cdot T_{in} + 253.705$
90 *bar*	$T_{out} = 1.386 \cdot T_{in} + 68.147$	$\dot{m} = -2.065 \cdot T_{in} + 249.160$
95 *bar*	$T_{out} = 1.414 \cdot T_{in} + 73.216$	$\dot{m} = -2.041 \cdot T_{in} + 245.010$
100 *bar*	$T_{out} = 1.439 \cdot T_{in} + 78.152$	$\dot{m} = -2.007 \cdot T_{in} + 240.866$
105 *bar*	$T_{out} = 1.475 \cdot T_{in} + 82.79$	$\dot{m} = -1.962 \cdot T_{in} + 236.562$
110 *bar*	$T_{out} = 1.504 \cdot T_{in} + 87.430$	$\dot{m} = -1.933 \cdot T_{in} + 232.619$

Equations at 60 Hz for constant discharge and suction pressure

P_{out}	P_{in} = 20 *bar*	
75 *bar*	$T_{out} = 1.493 \cdot T_{in} + 135.491$	$\dot{m} = -0.591 \cdot T_{in} + 98.422$
80 *bar*	$T_{out} = 1.539 \cdot T_{in} + 143.794$	$\dot{m} = -0.607 \cdot T_{in} + 95.321$
85 *bar*	$T_{out} = 1.585 \cdot T_{in} + 151.897$	$\dot{m} = -0.624 \cdot T_{in} + 92.261$
90 *bar*	$T_{out} = 1.635 \cdot T_{in} + 159.821$	$\dot{m} = -0.630 \cdot T_{in} + 89.247$
95 *bar*	*N/A*	*N/A*
100 *bar*	*N/A*	*N/A*
105 *bar*	*N/A*	*N/A*
110 *bar*	*N/A*	*N/A*

Data above 90 *bar* discharge pressure deliver a temperature out value greater than 160 C, which is beyond the limits of this study.

P_{out}	P_{in} = 25 *bar*	
75 *bar*	$T_{out} = 1.392 \cdot T_{in} + 104.762$	$\dot{m} = -0.874 \cdot T_{in} + 143.036$
80 *bar*	$T_{out} = 1.421 \cdot T_{in} + 112.026$	$\dot{m} = -0.849 \cdot T_{in} + 139.414$
85 *bar*	$T_{out} = 1.449 \cdot T_{in} + 119.060$	$\dot{m} = -0.830 \cdot T_{in} + 136.029$
90 *bar*	$T_{out} = 1.477 \cdot T_{in} + 125.900$	$\dot{m} = -0.807 \cdot T_{in} + 132.571$
95 *bar*	$T_{out} = 1.511 \cdot T_{in} + 132.575$	$\dot{m} = -0.822 \cdot T_{in} + 129.537$
100 *bar*	$T_{out} = 1.552 \cdot T_{in} + 138.975$	$\dot{m} = -0.833 \cdot T_{in} + 126.474$
105 *bar*	$T_{out} = 1.588 \cdot T_{in} + 145.324$	$\dot{m} = -0.847 \cdot T_{in} + 123.481$
110 *bar*	$T_{out} = 1.660 \cdot T_{in} + 151.510$	$\dot{m} = -0.909 \cdot T_{in} + 120.691$

P_{out}	P_{in} = 30 *bar*	
75 *bar*	$T_{out} = 1.363 \cdot T_{in} + 82.768$	$\dot{m} = -1.396 \cdot T_{in} + 194.565$
80 *bar*	$T_{out} = 1.390 \cdot T_{in} + 89.387$	$\dot{m} = -1.377 \cdot T_{in} + 190.463$
85 *bar*	$T_{out} = 1.417 \cdot T_{in} + 95.744$	$\dot{m} = -1.348 \cdot T_{in} + 186.352$
90 *bar*	$T_{out} = 1.444 \cdot T_{in} + 101.921$	$\dot{m} = -1.317 \cdot T_{in} + 182.354$
95 *bar*	$T_{out} = 1.476 \cdot T_{in} + 107.870$	$\dot{m} = -1.291 \cdot T_{in} + 178.414$
100 *bar*	$T_{out} = 1.502 \cdot T_{in} + 113.743$	$\dot{m} = -1.263 \cdot T_{in} + 174.640$
105 *bar*	$T_{out} = 1.530 \cdot T_{in} + 119.440$	$\dot{m} = -1.232 \cdot T_{in} + 170.865$
110 *bar*	$T_{out} = 1.561 \cdot T_{in} + 125.027$	$\dot{m} = -1.208 \cdot T_{in} + 167.333$

P_{out}	P_{in} = 35 *bar*	
75 *bar*	$T_{out} = 1.333 \cdot T_{in} + 65.718$	$\dot{m} = -2.009 \cdot T_{in} + 253.672$
80 *bar*	$T_{out} = 1.364 \cdot T_{in} + 71.727$	$\dot{m} = -1.977 \cdot T_{in} + 248.926$
85 *bar*	$T_{out} = 1.391 \cdot T_{in} + 77.556$	$\dot{m} = -1.951 \cdot T_{in} + 244.275$
90 *bar*	$T_{out} = 1.415 \cdot T_{in} + 83.234$	$\dot{m} = -1.912 \cdot T_{in} + 239.556$
95 *bar*	$T_{out} = 1.448 \cdot T_{in} + 88.6425$	$\dot{m} = -1.874 \cdot T_{in} + 234.973$
100 *bar*	$T_{out} = 1.472 \cdot T_{in} + 93.995$	$\dot{m} = -1.841 \cdot T_{in} + 230.492$
105 *bar*	$T_{out} = 1.500 \cdot T_{in} + 99.167$	$\dot{m} = -1.809 \cdot T_{in} + 226.215$
110 *bar*	$T_{out} = 1.538 \cdot T_{in} + 104.079$	$\dot{m} = -1.768 \cdot T_{in} + 221.871$

P_{out}	P_{in} = 40 *bar*	
75 *bar*	$T_{out} = 1.300 \cdot T_{in} + 51.833$	$\dot{m} = -2.681 \cdot T_{in} + 322.102$
80 *bar*	$T_{out} = 1.326 \cdot T_{in} + 57.451$	$\dot{m} = -2.634 \cdot T_{in} + 316.503$
85 *bar*	$T_{out} = 1.356 \cdot T_{in} + 62.798$	$\dot{m} = -2.588 \cdot T_{in} + 311.015$
90 *bar*	$T_{out} = 1.383 \cdot T_{in} + 68.022$	$\dot{m} = -2.538 \cdot T_{in} + 305.493$
95 *bar*	$T_{out} = 1.411 \cdot T_{in} + 73.014$	$\dot{m} = -2.500 \cdot T_{in} + 300.315$
100 *bar*	$T_{out} = 1.440 \cdot T_{in} + 77.827$	$\dot{m} = -2.454 \cdot T_{in} + 295.123$
105 *bar*	$T_{out} = 1.470 \cdot T_{in} + 82.513$	$\dot{m} = -2.403 \cdot T_{in} + 289.954$
110 *bar*	$T_{out} = 1.497 \cdot T_{in} + 87.145$	$\dot{m} = -2.368 \cdot T_{in} + 285.106$

Appendix C

Combined Plots for 40 Hz Operating Frequency

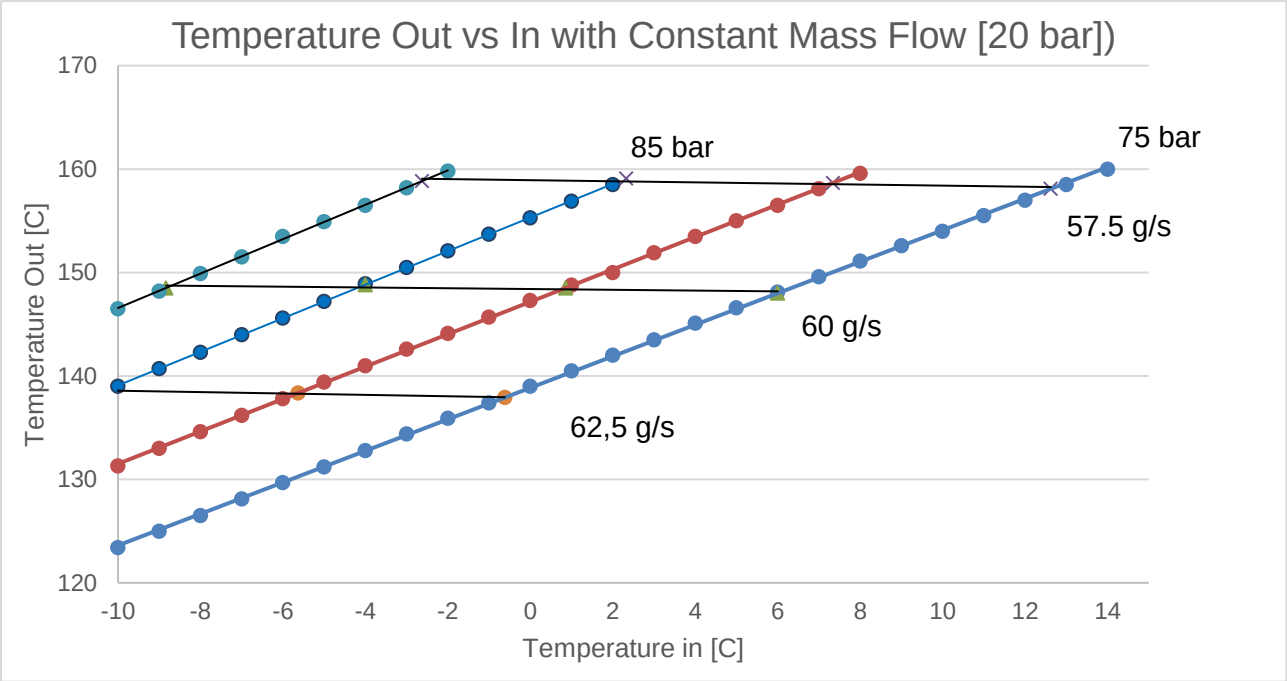

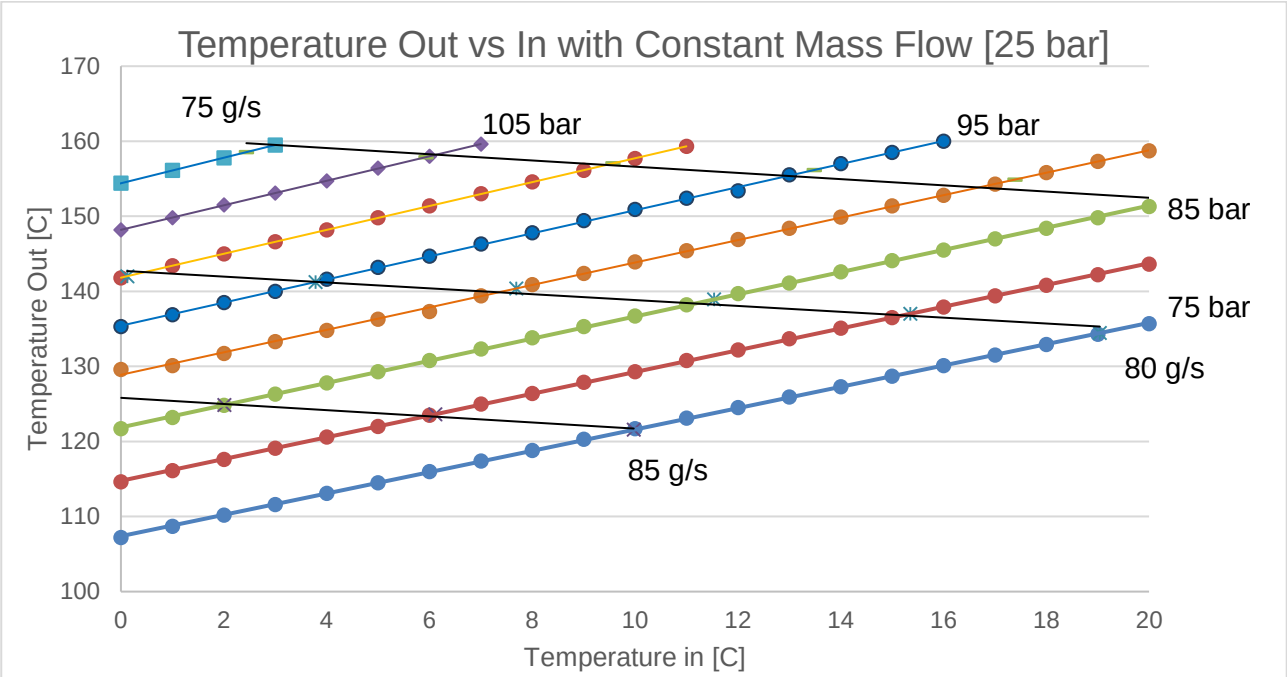

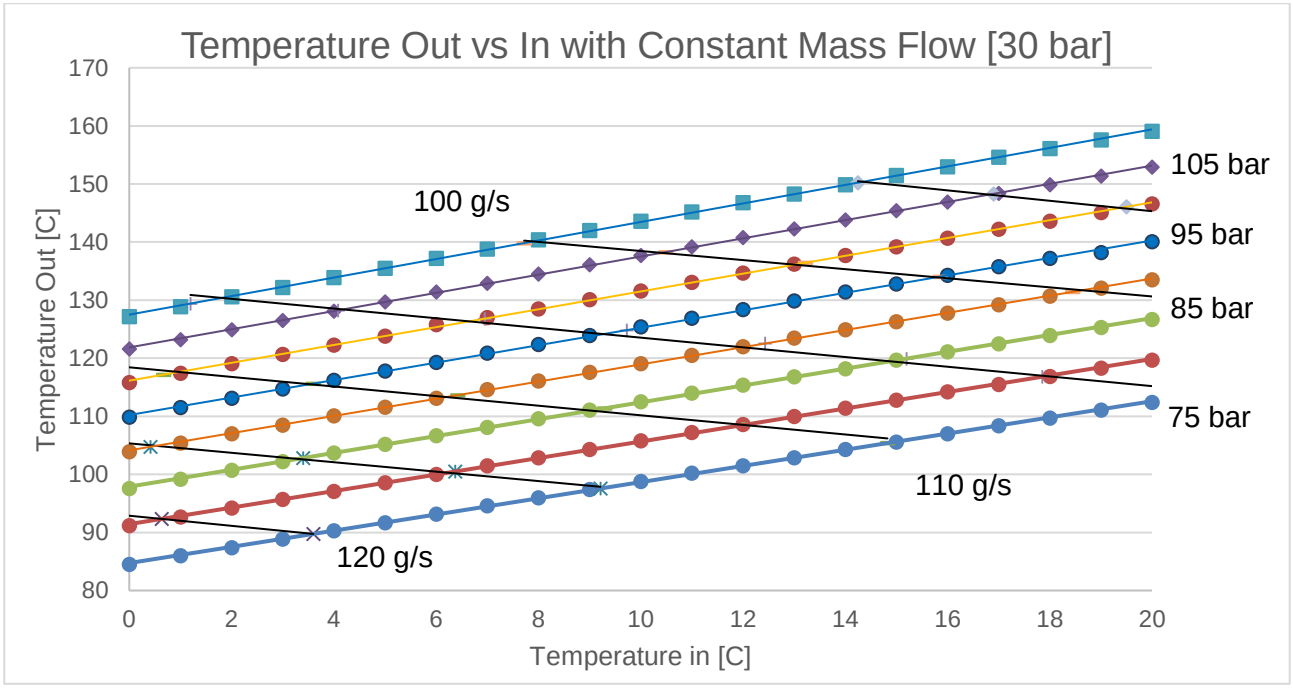
Temperature Out vs In with Constant Mass Flow [30 bar]
Temperature Out [C]
Temperature in [C]
100 g/s
110 g/s
120 g/s
105 bar
95 bar
85 bar
75 bar

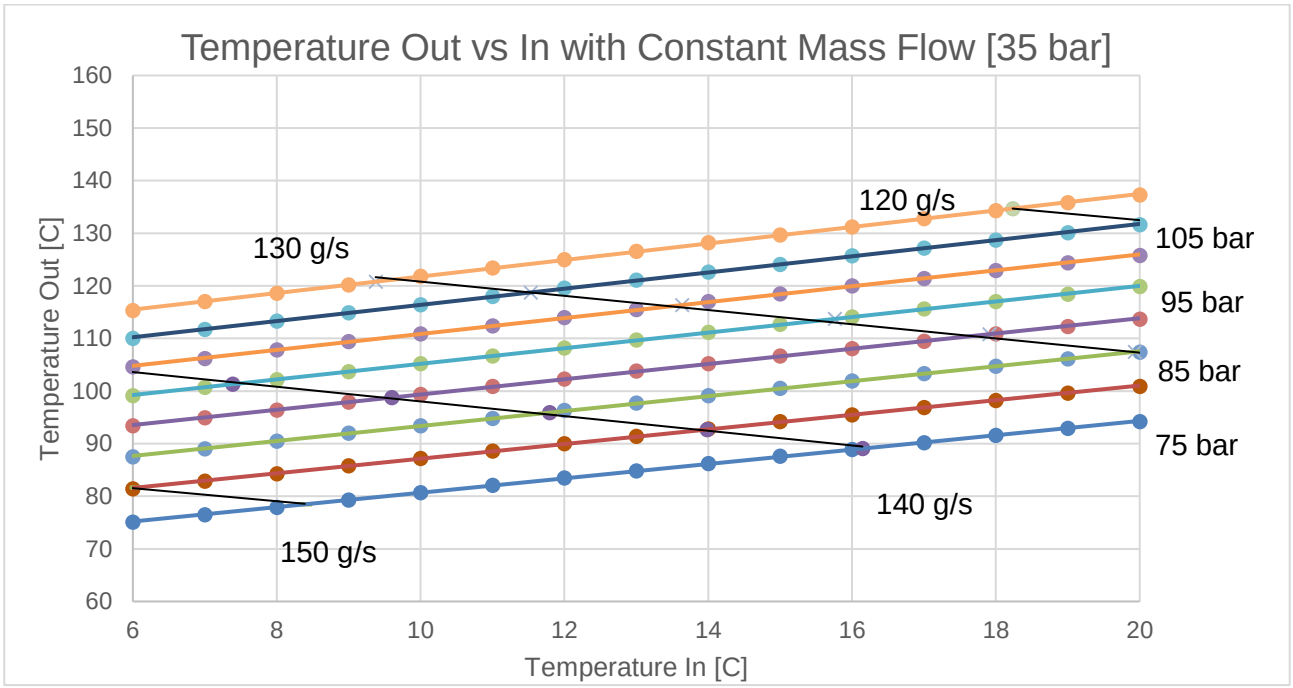
Temperature Out vs In with Constant Mass Flow [35 bar]
Temperature Out [C]
Temperature In [C]
130 g/s
120 g/s
140 g/s
150 g/s
105 bar
95 bar
85 bar
75 bar

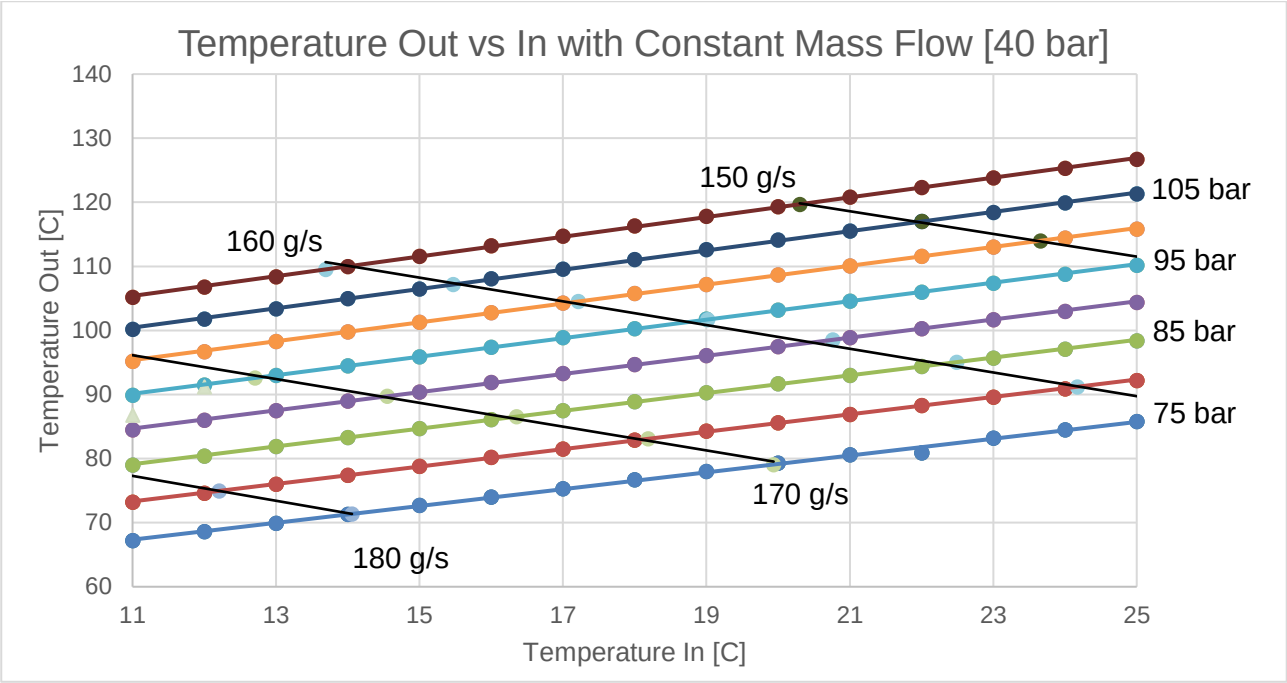

Combined Plots for 50 Hz Operating Frequency

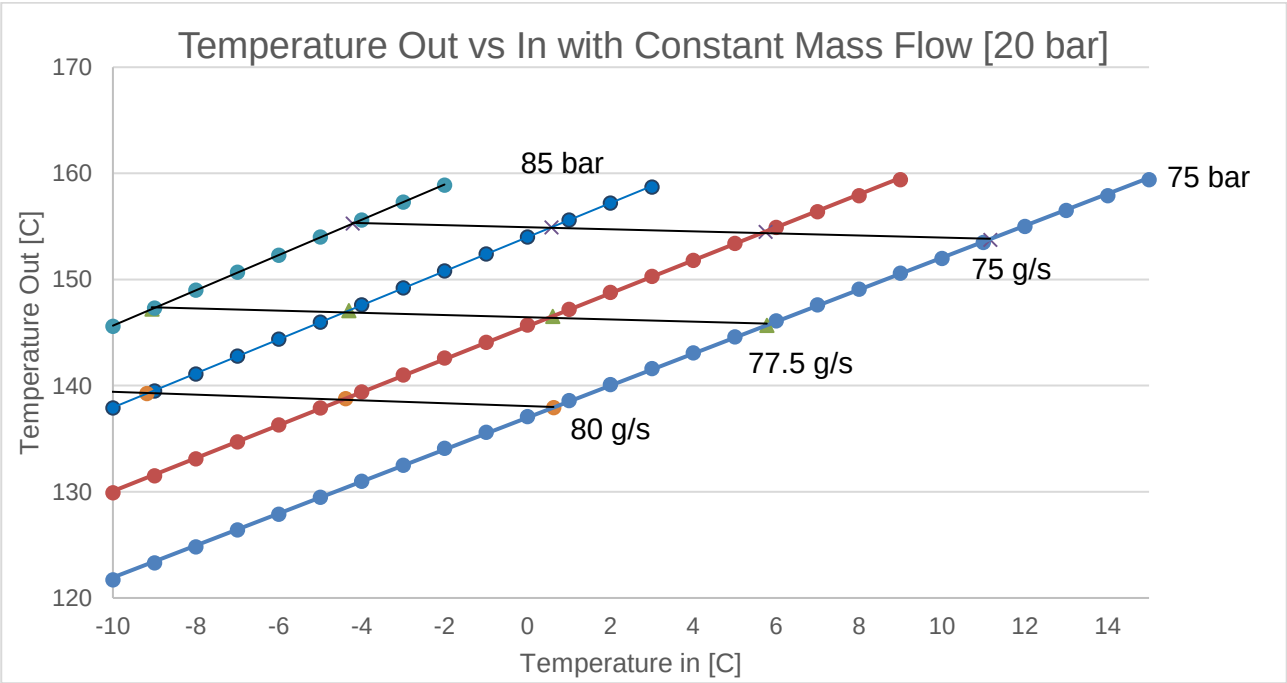

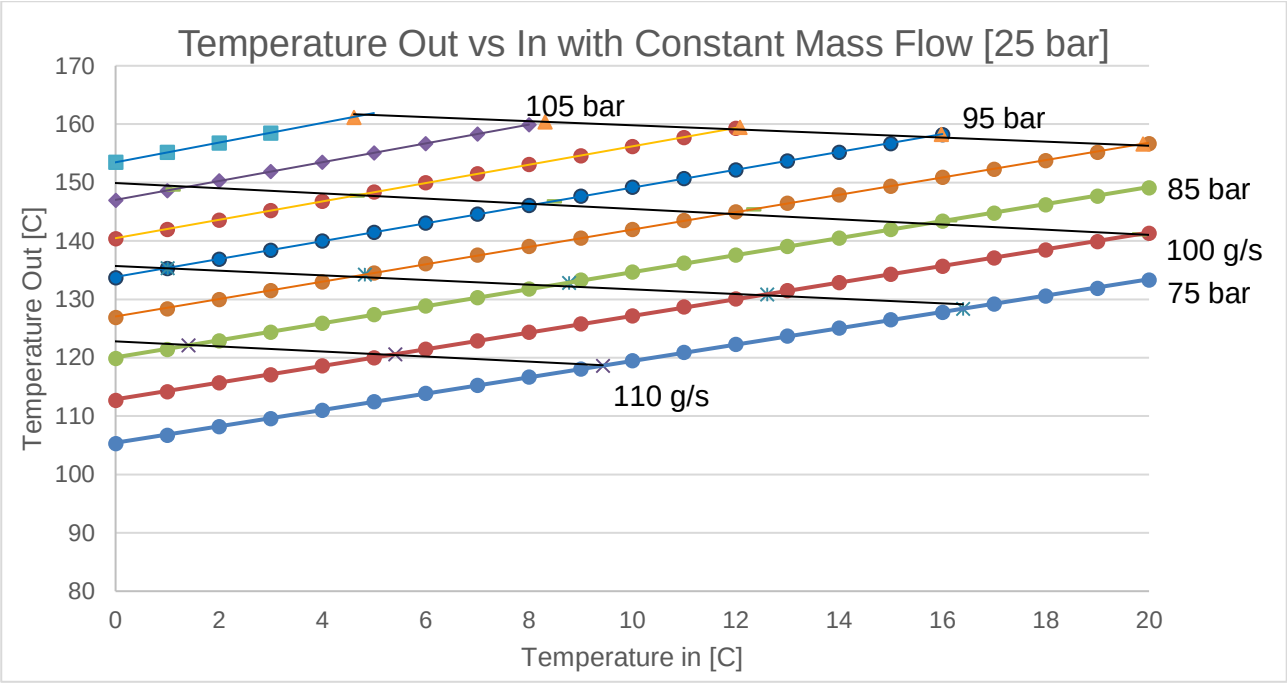
Temperature Out vs In with Constant Mass Flow [25 bar]
Temperature Out [C]
Temperature in [C]
105 bar
95 bar
85 bar
100 g/s
75 bar
110 g/s

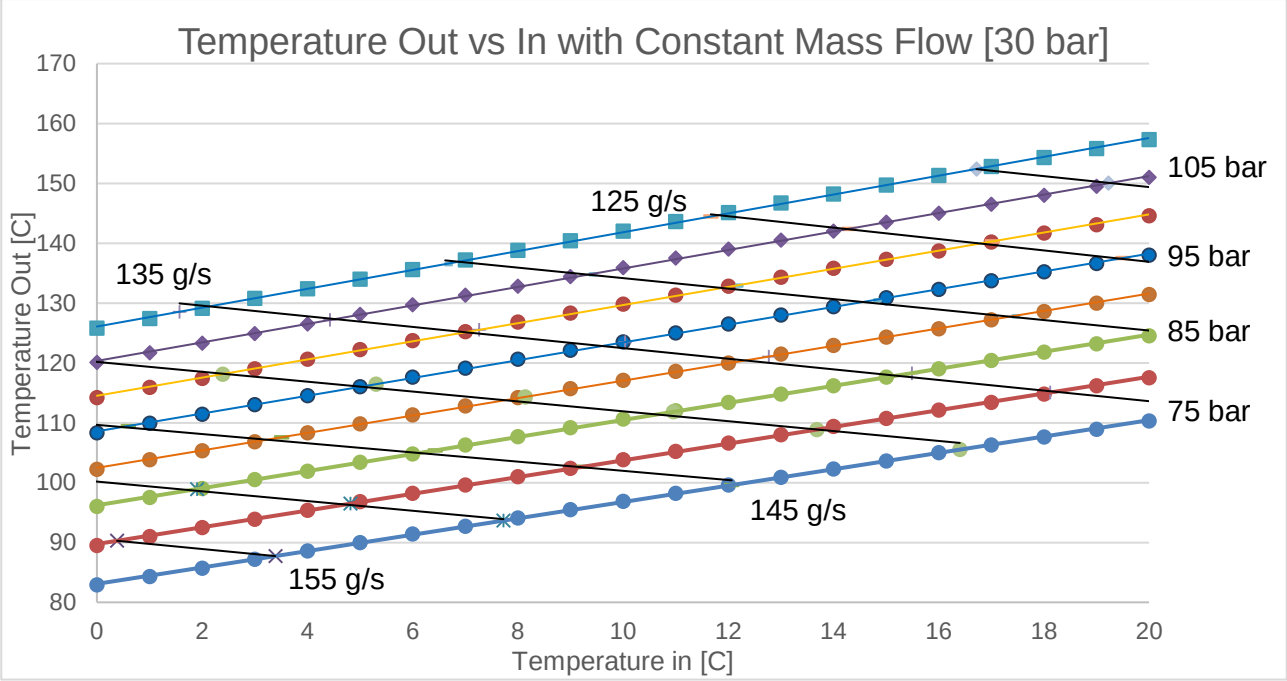
Temperature Out vs In with Constant Mass Flow [30 bar]
Temperature Out [C]
Temperature in [C]
105 bar
125 g/s
95 bar
135 g/s
85 bar
75 bar
145 g/s
155 g/s

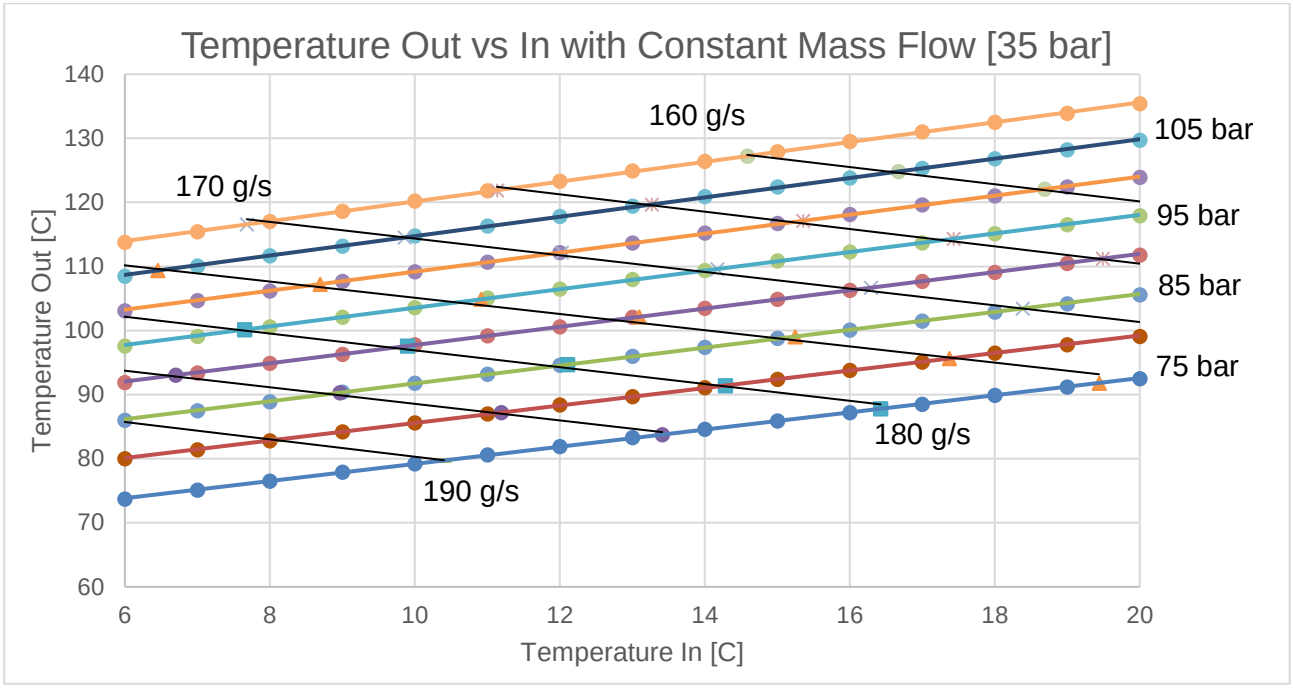
Temperature Out vs In with Constant Mass Flow [35 bar]
Temperature Out [C]
Temperature In [C]
160 g/s
170 g/s
180 g/s
190 g/s
105 bar
95 bar
85 bar
75 bar

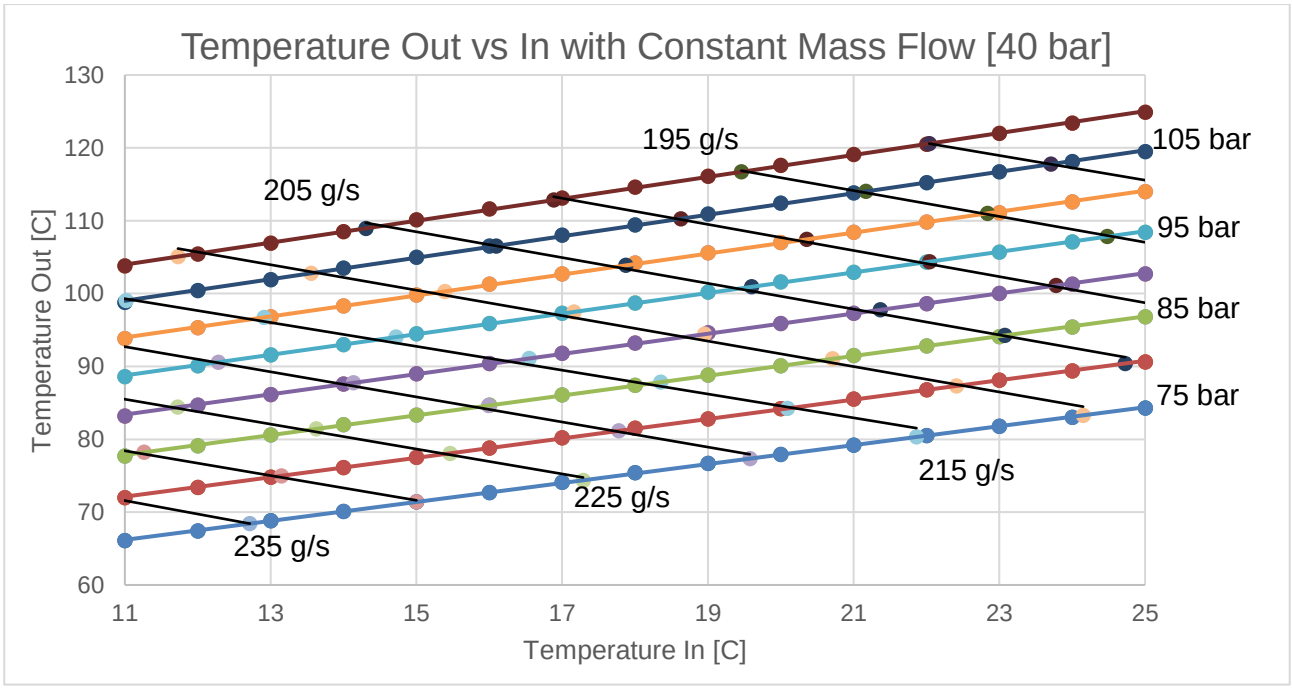
Temperature Out vs In with Constant Mass Flow [40 bar]
Temperature Out [C]
Temperature In [C]
195 g/s
205 g/s
215 g/s
225 g/s
235 g/s
105 bar
95 bar
85 bar
75 bar

Combined Plots for 60 Hz Operating Frequency

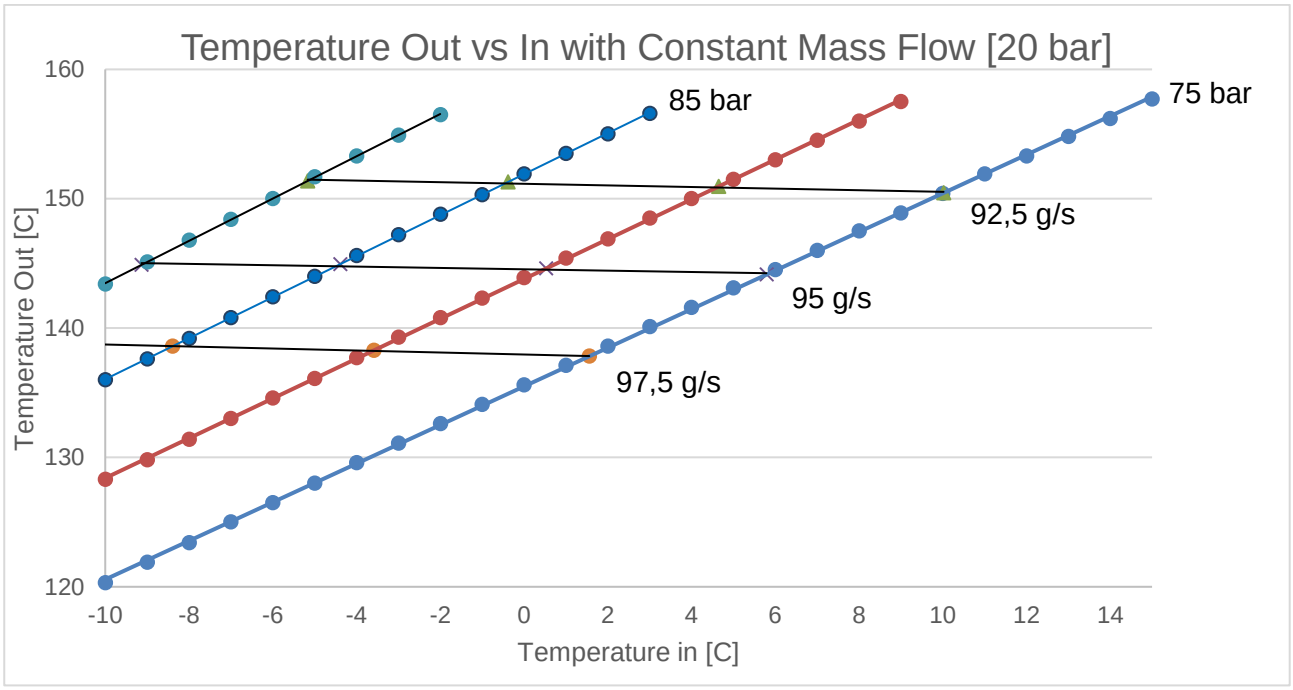

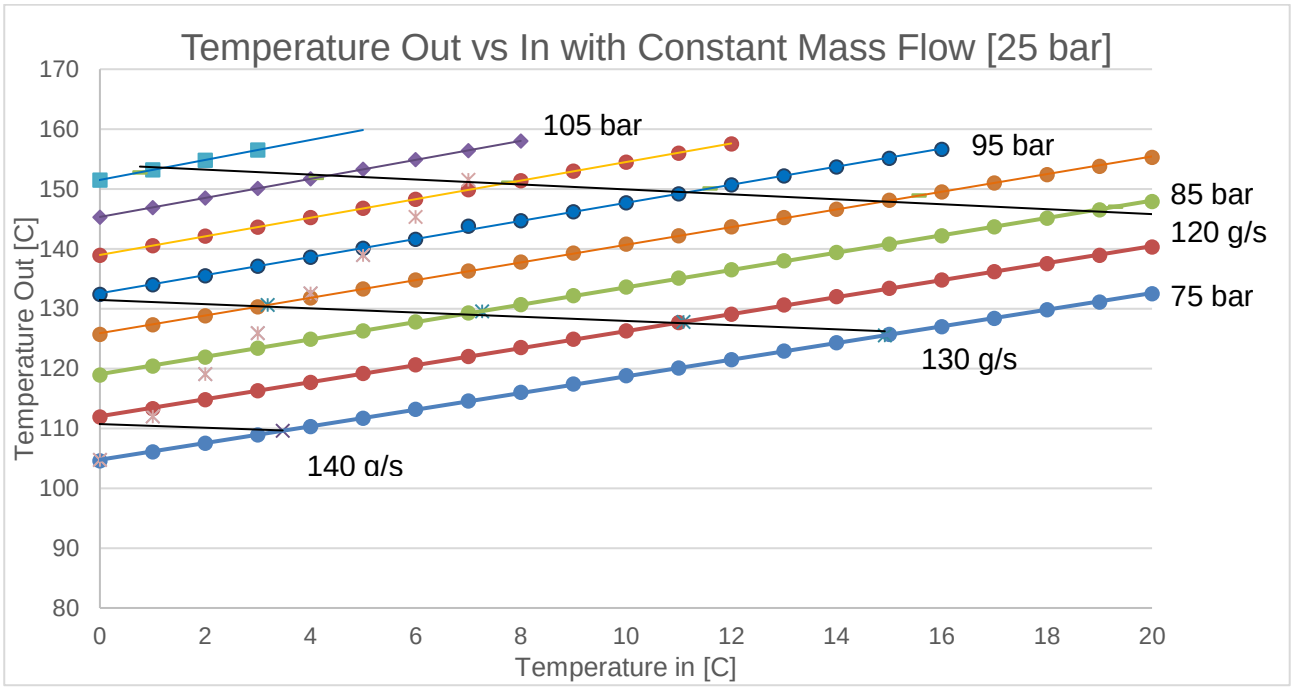

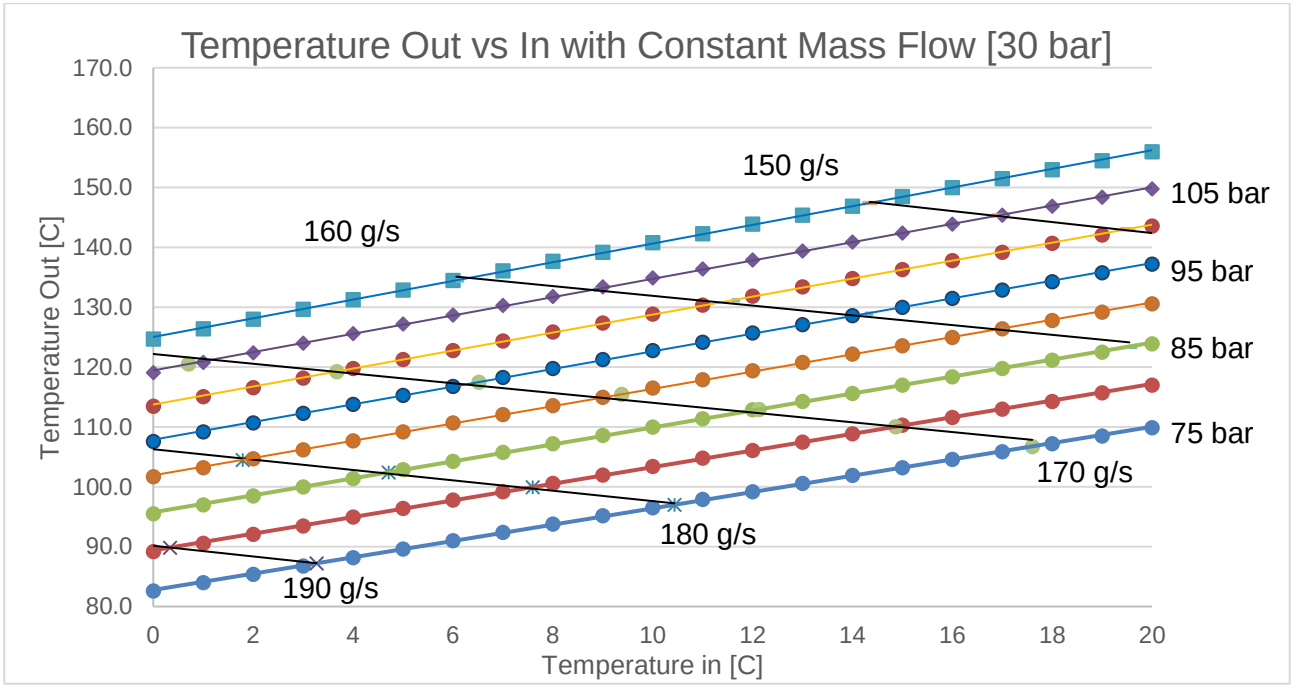
Temperature Out vs In with Constant Mass Flow [30 bar]
Temperature Out [C]
Temperature in [C]
150 g/s
160 g/s
170 g/s
180 g/s
190 g/s
105 bar
95 bar
85 bar
75 bar

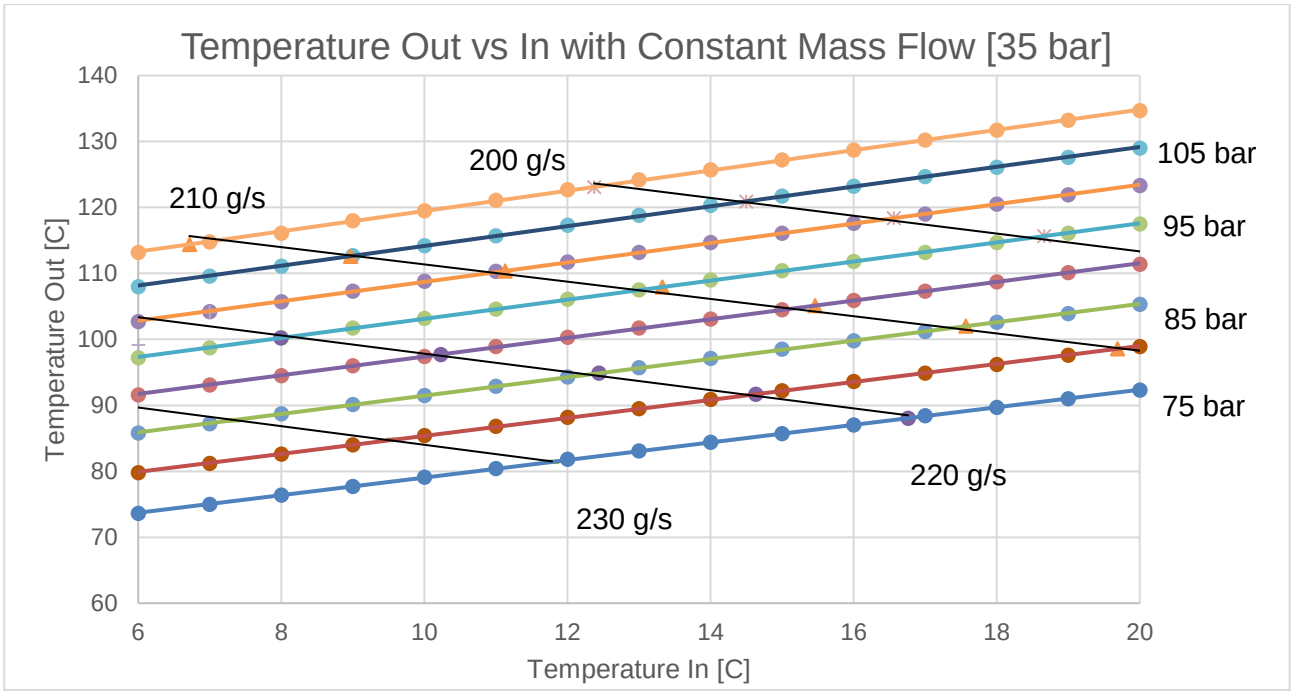
Temperature Out vs In with Constant Mass Flow [35 bar]
Temperature Out [C]
Temperature In [C]
200 g/s
210 g/s
220 g/s
230 g/s
105 bar
95 bar
85 bar
75 bar

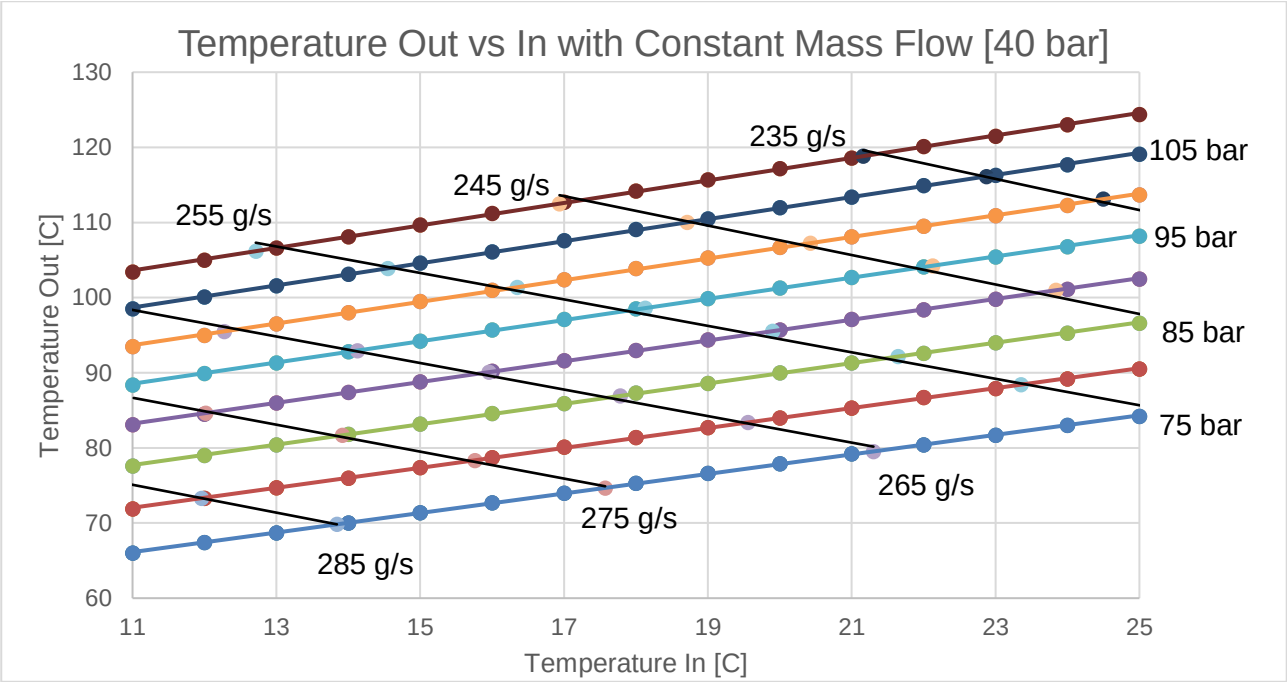
Temperature Out vs In with Constant Mass Flow [40 bar]
Temperature Out [C]
130
120
110
100
90
80
70
60
11
13
15
17
19
21
23
25
Temperature In [C]
255 g/s
245 g/s
235 g/s
265 g/s
275 g/s
285 g/s
105 bar
95 bar
85 bar
75 bar

Appendix D

Equations for 40 Hz per Suction Pressure

P_{in}[*bar*]	
20	$T_{out} = (0.095 \cdot P_{out} + 0.809) \cdot T_{in} + (1.624 \cdot P_{out} + 17.156)$ $\dot{m} = (-0.002 \cdot P_{out} - 0.249) \cdot T_{in} + (-0.388 \cdot P_{out} + 91.352)$
25	$T_{out} = (0.008 \cdot P_{out} + 0.822) \cdot T_{in} + (1.340 \cdot P_{out} + 7.689)$ $\dot{m} = (-0.0005 \cdot P_{out} - 0.491) \cdot T_{in} + (-0.403 \cdot P_{out} + 120.419)$
30	$T_{out} = (0.006 \cdot P_{out} + 0.963) \cdot T_{in} + (1.220 \cdot P_{out} - 6.101)$ $\dot{m} = (0.004 \cdot P_{out} - 1.155) \cdot T_{in} + (-0.494 \cdot P_{out} + 159.977)$
35	$T_{out} = (0.006 \cdot P_{out} + 0.921) \cdot T_{in} + (1.113 \cdot P_{out} - 15.784)$ $\dot{m} = (0.005 \cdot P_{out} - 1.623) \cdot T_{in} + (-0.578 \cdot P_{out} + 203.772)$
40	$T_{out} = (0.006 \cdot P_{out} + 0.858) \cdot T_{in} + (1.018 \cdot P_{out} - 22.895)$ $\dot{m} = (0.005 \cdot P_{out} - 2.103) \cdot T_{in} + (-0.665 \cdot P_{out} + 253.462)$

Equations for 50 Hz per Suction Pressure

P_{in}[*bar*]	
20	$T_{out} = (0.010 \cdot P_{out} + 0.726) \cdot T_{in} + (1.685 \cdot P_{out} + 10.715)$ $\dot{m} = (-0.002 \cdot P_{out} - 0.342) \cdot T_{in} + (-0.498 \cdot P_{out} + 117.665)$
25	$T_{out} = (0.007 \cdot P_{out} + 0.831) \cdot T_{in} + (1.370 \cdot P_{out} + 3.314)$ $\dot{m} = (-0.0007 \cdot P_{out} - 0.629) \cdot T_{in} + (-0.521 \cdot P_{out} + 155.382)$
30	$T_{out} = (0.006 \cdot P_{out} + 0.922) \cdot T_{in} + (1.225 \cdot P_{out} - 8.252)$ $\dot{m} = (0.005 \cdot P_{out} - 1.496) \cdot T_{in} + (-0.639 \cdot P_{out} + 206.450)$
35	$T_{out} = (0.006 \cdot P_{out} + 0.897) \cdot T_{in} + (1.110 \cdot P_{out} - 16.801)$ $\dot{m} = (0.006 \cdot P_{out} - 2.106) \cdot T_{in} + (-0.746 \cdot P_{out} + 262.863)$
40	$T_{out} = (0.006 \cdot P_{out} + 0.869) \cdot T_{in} + (1.015 \cdot P_{out} - 23.596)$ $\dot{m} = (0.007 \cdot P_{out} - 2.713) \cdot T_{in} + (-0.860 \cdot P_{out} + 326.872)$

Equations for 60 Hz per Suction Pressure

P_{in}[*bar*]	
20	$T_{out} = (0.009 \cdot P_{out} + 0.782) \cdot T_{in} + (1.621 \cdot P_{out} + 13.950)$ $\dot{m} = (-0.003 \cdot P_{out} - 0.393) \cdot T_{in} + (-0.612 \cdot P_{out} + 144.278)$
25	$T_{out} = (0.007 \cdot P_{out} + 0.834) \cdot T_{in} + (1.334 \cdot P_{out} + 5.402)$ $\dot{m} = (-0.0006 \cdot P_{out} - 0.788) \cdot T_{in} + (-0.638 \cdot P_{out} + 190.380)$
30	$T_{out} = (0.006 \cdot P_{out} + 0.938) \cdot T_{in} + (1.205 \cdot P_{out} - 6.959)$ $\dot{m} = (0.006 \cdot P_{out} - 1.815) \cdot T_{in} + (-0.780 \cdot P_{out} + 252.795)$
35	$T_{out} = (0.006 \cdot P_{out} + 0.906) \cdot T_{in} + (1.096 \cdot P_{out} - 15.896)$ $\dot{m} = (0.007 \cdot P_{out} - 2.531) \cdot T_{in} + (-0.910 \cdot P_{out} + 321.649)$
40	$T_{out} = (0.006 \cdot P_{out} + 0.838) \cdot T_{in} + (1.006 \cdot P_{out} - 22.995)$ $\dot{m} = (0.009 \cdot P_{out} - 3.354) \cdot T_{in} + (-1.059 \cdot P_{out} + 401.113)$

Appendix E

The equations of (70) and (71) are declared below to enable proper reference from this appendix.

$$T_{out} = \left(k_{1,1}(x_2)P_{out} + k_{1,0}(x_2)\right)T_{in} + \left(k_{0,1}(x_2)P_{out} + k_{0,0}(x_2)\right)$$

$$\dot{m} = \left(k_{1,1}(x_2)P_{out} + k_{1,0}(x_2)\right)T_{in} + \left(k_{0,1}(x_2)P_{out} + k_{0,0}(x_2)\right)$$

Substituted equations for 40 Hz

Equation	Coefficient	Internal Equation
Discharge Temperature Eq.	$k_{1,1}(x_2)$	$= \left(0{,}000018 \cdot P_{in}^2\right) + (- 0{,}001248 \cdot P_{in}) \ + \ 0{,}027385$
	$k_{1,0}(x_2)$	$= (-0{,}000955 \cdot P_{in}^2) \ + (0{,}061226 \cdot P_{in}) \ - \ 0{,}054832$
	$k_{0,1}(x_2)$	$= \left(0{,}001117 \cdot P_{in}^2\right) + (- 0{,}095809 \cdot P_{in}) \ + \ 3{,}075894$
	$k_{0,0}(x_2)$	$= (-2{,}0715 \cdot P_{in}) \ + \ 58{,}159$
Mass Flow Equations	$k_{1,1}(x_2)$	$= (-0{,}000011 \cdot P_{in}^2) \ + (0{,}001020 \cdot P_{in}) \ - \ 0{,}018311$
	$k_{1,0}(x_2)$	$= \left(-0{,}000806 \cdot P_{in}^2\right) + (- 0{,}048454 \cdot P_{in}) \ + \ 1{,}094856$
	$k_{0,1}(x_2)$	$= (-0{,}000395 \cdot P_{in}^2 \ ) \ + (0{,}009139 \cdot P_{in}) \ - \ 0{,}403780$
	$k_{0,0}(x_2)$	$= (0{,}129957 \cdot P_{in}^2) \ + (0{,}354042 \cdot P_{in}) \ + \ 31{,}715955$

Substituted equations for 50 Hz

Equation	Coefficient	Internal Equation
Discharge Temperature Eq.	$k_{1,1}(x_2)$	$= (2e^{-5} \cdot P_{in}^2) + (-0{,}00138 \cdot P_{in}) \ + \ 0{,}0294$
	$k_{1,0}(x_2)$	$= (-0{,}001097 \cdot P_{in}^2) \ + (0{,}072909 \cdot P_{in}) \ - 0{,}296171$
	$k_{0,1}(x_2)$	$= (0{,}001337 \cdot P_{in}^2) + (-0{,}112229 \cdot P_{in}) \ + \ 3{,}377771$
	$k_{0,0}(x_2)$	$= (-1{,}7747 \cdot P_{in}) \ + \ 46{,}318$
Mass Flow Equations	$k_{1,1}(x_2)$	$= (-0{,}000012 \cdot P_{in}^2) + (0{,}001243 \cdot P_{in}) \ - 0{,}02240$
	$k_{1,0}(x_2)$	$= (-0{,}001095 \cdot P_{in}^2) + (-0{,}058631 \cdot P_{in}) \ + 1{,}341488$
	$k_{0,1}(x_2)$	$= (-0{,}000490 \cdot P_{in}^2) + (0{,}0104 \cdot P_{in}) \ - \ 0{,}49964$
	$k_{0,0}(x_2)$	$= (0{,}165505 \cdot P_{in}^2) \ + (0{,}587575 \cdot P_{in}) \ + \ 38{,}989$

Substituted equations for 60 Hz

Equation	Coefficient	Internal Equation
Discharge Temperature Eq.	$k_{1,1}(x_2)$	$= \left(0{,}000017 \cdot P_{in}^2\right) + (-\,0{,}001213 \cdot P_{in}) \; + \; 0{,}026825$
	$k_{1,0}(x_2)$	$= (-0{,}001073 \cdot P_{in}^2) \; + (\,0{,}068028 \cdot P_{in}) \; - \; 0{,}161744$
	$k_{0,1}(x_2)$	$= \left(\,0{,}001189 \cdot P_{in}^2\right) + (-\,0{,}100734 \cdot P_{in}) \; + \; 3{,}144730$
	$k_{0,0}(x_2)$	$= (\,-1{,}9037 \; \cdot P_{in}) \; + \; 51{,}813$
Mass Flow Equations	$k_{1,1}(x_2)$	$= (-0{,}000013 \cdot P_{in}^2) \; + (0{,}001411 \cdot P_{in}) \; - \; 0{,}026130$
	$k_{1,0}(x_2)$	$= \left(-0{,}001558 \cdot P_{in}^2\right) + (\,-\,0{,}059817 \cdot P_{in}) \; + \; 1{,}497944$
	$k_{0,1}(x_2)$	$= (-0{,}000665 \cdot P_{in}^2) \; + (0{,}016563 \cdot P_{in}) \; - \; 0{,}665033$
	$k_{0,0}(x_2)$	$= (0{,}209039 \cdot P_{in}^2) \; + (0{,}356432 \cdot P_{in}) \; + \; 52{,}762594$

Appendix F

Discharge Temperature Equation Final Formulation

$$T_{Out} = \left((r_{1,1,2}P_{in}^2 + r_{1,1,1}P_{in} + r_{1,1,0})P_{out} + (r_{1,0,2}P_{in}^2 + r_{1,0,1}P_{in} + r_{1,0,0})\right)T_{in} + (r_{0,1,2}P_{in}^2 + r_{0,1,1}P_{in} + r_{0,1,0})P_{out} + (r_{0,0,2}P_{in}^2 + r_{0,0,1}P_{in} + r_{0,0,0})$$

(79)

Coefficient	Formulation Method	Result	
$r_{1,1,2}$	Average	$r_{1,1,2}$=	1.83333e-5
$r_{1,1,1}$	Average	$r_{1,1,1}$=	-0.00128
$r_{1,1,0}$	Average	$r_{1,1,0}$=	0.02787
$r_{10,2}$	Average	$r_{10,2}$=	-0.00104
$r_{1,0,1}$	Average	$r_{1,0,1}$=	0.06739
$r_{1,0,0}$	Average	$r_{1,0,0}$=	-0.17092
$r_{0,1,2}$	Average	$r_{0,1,2}$=	0.00121
$r_{0,1,1}$	Average	$r_{0,1,1}$=	-0.10292
$r_{0,1,0}$	Average	$r_{0,1,0}$=	3.19947
$r_{0,0,2}$	Average	$r_{0,0,2}$=	0
$r_{0,0,1}$	Average	$r_{0,0,1}$=	-1.91663
$r_{0,0,0}$	Average	$r_{0,0,0}$=	52.09667

Mass Flow Equation Final Formulation

$$\dot{m} = \left((r_{1,1,2}P_{in}^2 + r_{1,1,1}P_{in} + r_{1,1,0})P_{out} + (r_{1,0,2}P_{in}^2 + r_{1,0,1}P_{in} + r_{1,0,0})\right)T_{in} + (r_{0,1,2}P_{in}^2 + r_{0,1,1}P_{in} + r_{0,1,0})P_{out} + (r_{0,0,2}P_{in}^2 + r_{0,0,1}P_{in} + r_{0,0,0})$$

(80)

Coefficient	Formulation Method	Result	
$r_{1,1,2}$	Polynomial of $n = 1$	$r_{1,1,2}$=	$-1e^{-7} \cdot Hz - 7e^{-6}$
$r_{1,1,1}$	Polynomial of $n = 1$	$r_{1,1,1}$=	$+1{,}955e^{-5} \cdot Hz + 2{,}472e^{-4}$
$r_{1,1,0}$	Polynomial of $n = 1$	$r_{1,1,0}$=	$-3{,}91e^{-4} \cdot Hz - 2{,}733e^{-3}$
$r_{10,2}$	Polynomial of $n = 1$	$r_{10,2}$=	$-3{,}76e^{-5} \cdot Hz + 7{,}27e^{-4}$
$r_{1,0,1}$	Polynomial of $n = 1$	$r_{1,0,1}$=	$-5{,}681e^{-4} \cdot Hz - 2.723e^{-2}$
$r_{1,0,0}$	Polynomial of $n = 1$	$r_{1,0,0}$=	$+2{,}015e^{-2} \cdot Hz + 3{,}037e^{-}1$
$r_{0,1,2}$	Polynomial of $n = 1$	$r_{0,1,2}$=	$-1{,}35e^{-5} \cdot Hz + 1{,}583e^{-4}$
$r_{0,1,1}$	Polynomial of $n = 1$	$r_{0,1,1}$=	$-3.712e^{-4} \cdot Hz - 6.526e^{-3}$
$r_{0,1,0}$	Polynomial of $n = 1$	$r_{0,1,0}$=	$-1{,}306e^{-2} \cdot Hz + 1{,}303e^{-1}$
$r_{0,0,2}$	Polynomial of $n = 1$	$r_{0,0,2}$=	$+3{,}954e^{-3} \cdot Hz - 2{,}954e^{-2}$
$r_{0,0,1}$	Average	$r_{0,0,1}$=	0.43268
$r_{0,0,0}$	Polynomial of $n = 1$	$r_{0,0,0}$=	$+1.0523 \cdot Hz - 11.461$

Appendix G

Predicted values from (79) and (80) for a set of 30 tests

# Test	$T_{in}[°C]$	$P_{out}[bar]$	$P_{in}[bar]$	Frequency $[Hz]$	Predicted $T_{out}[°C]$	Predicted $\dot{m}[\frac{g}{s}]$
1	10	87	39	41	81,0	176,56
2	7	76	36	59	73,5	247,14
3	3	101	33	42	107,0	135,42
4	11	108	38	47	108,3	177,03
5	7	89	33	59	98,9	202,78
6	3	86	29	43	107,1	117,30
7	18	78	26	56	132,7	121,53
8	18	99	28	54	151,7	117,76
9	8	104	26	45	154,9	88,34
10	8	82	33	54	92,1	185,03
11	13	78	26	41	125,6	89,75
12	7	99	36	46	99,0	169,15
13	9	78	38	52	72,5	227,78
14	6	102	26	43	148,9	87,19
15	15	106	34	47	126,5	140,63
16	10	83	26	57	128,4	128,84
17	14	76	31	53	101,0	158,28
18	8	101	26	43	150,7	86,30
19	1	88	23	48	139,3	87,72
20	14	78	24	45	137,8	84,92
21	12	109	31	49	139,4	125,99
22	14	98	29	46	138,8	108,26
23	4	82	21	45	147,0	71,12
24	11	92	27	56	137,0	127,41
25	16	87	29	58	127,1	149,15
26	14	97	34	55	114,3	178,16
27	2	96	22	53	159,4	85,70
28	19	107	31	53	147,7	131,38
29	8	101	26	52	150,7	105,33
30	10	107	39	58	102,8	242,88

Comparison between Predicted and Experimental Values

# Test	Predicted $T_{out}[°C]$	Predicted $\dot{m}[\frac{g}{s}]$	Experimental $T_{out}[°C]$	Experimental $\dot{m}[\frac{g}{s}]$	Error $T_{out}[°C]$	Error $\dot{m}[\frac{g}{s}]$
1	81,0	175,93	82,6	176,94	-1,98%	0,57%
2	73,5	246,62	73,2	247,22	0,47%	0,24%
3	107,0	135,50	108,4	135,83	-1,33%	0,24%
4	108,3	180,65	109,1	180,56	-0,75%	-0,05%
5	98,9	202,12	99,1	200,83	-0,19%	-0,64%
6	107,1	117,80	107,2	117,78	-0,08%	-0,02%
7	132,7	122,78	129,6	123,61	2,39%	0,68%
8	151,7	120,64	149,4	121,39	1,54%	0,62%
9	154,9	90,31	152,6	90,83	1,50%	0,58%
10	92,1	186,66	92,2	185,28	-0,06%	-0,75%
11	125,6	89,21	125,1	89,72	0,40%	0,57%
12	99,0	171,51	100,5	171,39	-1,49%	-0,07%
13	72,5	229,71	72,7	230,28	-0,28%	0,25%
14	148,9	87,95	149,2	87,50	-0,19%	-0,51%
15	126,5	144,33	127,8	143,06	-1,04%	-0,89%
16	128,4	129,41	125,7	129,44	2,15%	0,03%
17	101,0	160,39	100	159,72	1,05%	-0,42%
18	150,7	87,09	149,2	87,50	1,00%	0,47%
19	139,3	89,54	137,5	90,00	1,32%	0,51%
20	137,8	86,47	136,3	87,22	1,10%	0,86%
21	139,4	129,88	139,1	129,17	0,24%	-0,55%
22	138,8	110,92	138,4	110,83	0,28%	-0,08%
23	147,0	72,33	147,4	72,50	-0,27%	0,23%
24	137,0	128,69	134,7	128,61	1,71%	-0,06%
25	127,1	149,20	125,5	148,89	1,30%	-0,21%
26	114,3	180,39	115,2	178,33	-0,75%	-1,15%
27	159,4	87,67	156,6	88,33	1,78%	0,75%
28	147,7	135,26	146,8	135,00	0,61%	-0,19%
29	150,7	108,14	147,7	108,61	2,03%	0,43%
30	102,8	242,92	102,3	243,89	0,47%	0,40%
				Average	0.43%	0.06%
				Absolute Value Average	0.99%	0.43%
				Max	2.39%	-1.15%

Works Cited

Barskii, I., Antipov, Y., Shatalov, I. & Tercjhov, D., 2011. Parameters of piston compressor of heat pumps in partial operation modes. *Chemical and Petroleum Engineering ,* Volume 47.

Bitzer , 2016. *Software: Bitzer.* [Online] Available at: https://www.bitzer.de/websoftware [Accessed 12 12 2016].

Borgnakke, C. & Sonntag, R. E., 2009. *Fundamentals of Thermodynamics.* 7th SI ed. Michigan: John Wiley & Sons .

Calm, J., 2008. The next generation of refrigerants - Historical reviews, considerations, and outlook. *International Journal of Refrigeration,* Issue 31, pp. 1123-1133.

Calm, J. M. & A, D. D., 1998. Trade-offs in refrigerant selections: past, present and future. *International Journal of Refrigeration,* 21(4), pp. 308-321.

Cecchinato, L., Corradi, M., Fornasieri, E. & Zamboni, L., 2005. Carbon dioxide as refrigerant for tap water heat pumps: A Comparison with the tradtional solution.. *International Journal of Refrigeration,* Issue 28, pp. 1250-1258.

Chua, K., Chou, S. & Yang, W., 2010. Advances in Heat Pump Sources: A Review. *Applied Energy,* Issue 87, pp. 3611-3624.

Duprez, M., Dumont, E. & Frere, M., 2007. Modelling of reciprocating and scroll compressors. *International Journal of Refrigeration,* 1(30), pp. 873-886.

Kim, M., Pettersen, J. & CW, B., 2004. Fundamental process and system design issues in CO2 vapor compression systems. *Progress in Energy and Combustion Science,* Issue 30, pp. 119-174.

Koury, R., Machado, L. & Ismail, K., 2001. Numerical simulation of a variable speed refrigeration system. *International Journal of Refrigeration,* I(24), pp. 192-200.

Lei, Z. & Zaheeruddin, M., 2005. Dynamic simulation and analysis of a water chiller refrigeration system. *Applied Thermal Engineering,* 1(25), pp. 2258-2271.

Linde-gas, 2018. *HCFC Refrigerants.* [Online] Available at: http://www.linde-gas.com/en/products_and_supply/refrigerants/hcfc_refrigerants/index.html [Accessed 19 02 2018].

Lorentzen, G., 1995. The use of natural refrigeration: a complete solution to CFC/HCFC predicament. *International Journal of Refrigeration,* 18(3), pp. 190-197.

Ma, Y., Liu, Z. & Tian, H., 2013. A review of transcritical carbon dioxide pump and refrigeration cycles. *Energy,* 55(4), pp. 156-172.

McGovern, J. & Harte, S., 1995. An exergy method for compressor performance analysis. *International Journal of Refrigeration,* Issue 18, pp. 421-433.

Navarro, E., Granryd, E., Urchueguia, J. & Corberan, J., 2007. A phenomenological model for analyzing reciprocating compressors. *International Journal of Refrigeration,* I(30), pp. 1254-1265.

Pearson, A., 2005. Carbon dioxide - New uses for an old refrigerant. *International Journal of Refrigeration,* Issue 28, pp. 1140-1148.

Perez-Segarra, C., Rigola, J., Soria, M. & Oliva, A., 2005. Detailed thermodynamic characterization of hermetic reciprocating compressors. *International Journal of Refrigeration,* Issue 28, pp. 579-593.

Rousseau, P., 2013. *Thermo-Fluid Systems Modelling I Course Notes.* 1st ed. Potchefstroom: North West University.

Shao, S., Shi, W., Li, X. & Chen, H., 2004. Performance representation of variable-speed compressor for inverter air conditioners based on experimental data. *International Journal of Refrigeration,* I(27), pp. 805-815.

Stouffs, P., Tazerout, M. & Wauters, P., 2001. Thermodynamic analysis of reciprocating compressors. *International Journal of Thermal Science,* Issue 40, pp. 52-66.

Swanepoel, J. et al., 2015. *Elementere Statistiese Metodes.* 5th red. Potchefstroom: AndCork Publishers.

Tassou, S. & Quresh, T., 1998. Comparative performance evaluation of positive displacement compressors in variable-speed refrigeration applications. *International Journal of Refrigeration,* 21(1), pp. 29-41.

Winandy, E., Saavedra, C. & Lebrun, J., 2002. Simplified modelling of an open-type reciprocating compressor. *International Journal of Thermal Sciences,* I(41), pp. 183-192.